DOE/NASA/0081-79/1
NASA CR-159651
AIRESEARCH 79-16182

ADVANCED ELECTRIC PROPULSION SYSTEM CONCEPT FOR ELECTRIC VEHICLES

A. E. Raynard and F. E. Forbes
AiResearch Manufacturing Company of California
The Garrett Corporation

(NASA-CR-159651) ADVANCED ELECTRIC PROPULSION SYSTEM CONCEPT FOR ELECTRIC VEHICLES (Garrett Corp., Torrance, Calif.) 157 p HC A08/MF A01 CSCL 13F
N80-17916
Unclas
G3/85 47174

August 1979

Prepared for
NATIONAL AERONAUTICS AND SPACE ADMINISTRATION
Lewis Research Center
Cleveland, Ohio 44135

for
U.S. DEPARTMENT OF ENERGY
Conservation and Solar Applications
Office of Transportation Programs

DOE/NASA/0081-79/1
NASA CR-159651
AIRESEARCH 79-16182

ADVANCED ELECTRIC PROPULSION SYSTEM CONCEPT FOR ELECTRIC VEHICLES

A. E. Raynard and F. E. Forbes
AiResearch Manufacturing Company of California
The Garrett Corporation
Torrance, California 90509

August 1979

Prepared for
National Aeronautics and Space Administration
Lewis Research Center
Cleveland, Ohio 44135
Under Contract DEN 3-81

for
U.S. DEPARTMENT OF ENERGY
Conservation and Solar Applications
Office of Transportation Programs
Washington, D.C. 20545
Under Interagency Agreement EC-77-A-31-1044

PREFACE

The Electric and Hybrid Vehicle Research, Development, and Demonstration Act of 1976 (Public Law 94-413) authorized a Federal program of research and development designed to promote electric and hybrid vehicle technologies. The Energy Research and Development Administration, now the Department of Energy (DOE), which was given the responsibility for implementing the act, established the Electric and Hybrid Vehicle Research, Development, and Demonstration Project within the Division of Transportation Energy Conservation to manage the activities required by Public Law 94-413.

The National Aeronautics and Space Administration under an interagency agreement (Number EC-77-A-31-1044) was requested by ERDA (DOE) to undertake research and development of propulsion systems for electric and hybrid vehicles. The Lewis Research Center was made the responsible NASA center for this project. The study presented in this report is an early part of the Lewis Research Center program for propulsion system research and development for electric vehicles.

TABLE OF CONTENTS

SUMMARY

The objective of this study was to evaluate a number of propulsion system concepts for electric vehicles and to prepare conceptual designs for the two most promising configurations. The program was divided into several tasks during which the various system configurations were evaluated and compared, design tradeoffs performed, and the two conceptual designs produced.

The objectives of Task I were to examine and compare 17 propulsion system configurations, weighing their relative merits to recommend several systems for more detailed evaluations in the following program tasks. The method adopted for this preliminary analysis was to compare all systems on a common basis of performance to determine the combinations of components and battery pack that would achieve the basic performance level. The 17 configurations included basic systems in which a controller varied the speed of a traction motor and other systems in which additional speed control was achieved by use of various transmissions. Some configurations also employed flywheel energy storage units with several different system arrangements.

The initial studies showed that for driving the required 161 km with successive cycles per SAE J227a, schedule D, the systems with a flywheel energy storage unit could achieve the range with the lowest battery weight. To meet the range of 209 km at a constant 72 km/hr, however, some of the basic systems (without a flywheel) required the lowest battery weight. Consequently, the five configurations selected for design tradeoff studies included both basic systems and flywheel systems.

In Task II, design tradeoffs were made on five candidate systems to find the optimum component characteristics for meeting all performance goals. Comparisons were made not only in range, but also in acceleration and cost. In addition, an evaluation was made of the anticipated performance when nickel-zinc batteries rather than the standard lead-acid batteries were used.

The two systems selected for the final conceptual design studies included a basic system and a system with a flywheel energy storage system. The principal features of the two systems are as follows:

<u>Basic System</u>--Brushless dc permanent-magnet motor, variable frequency inverter, traction continuously variable transmission

<u>Flywheel System</u>--Dc shunt motor, step voltage start and field control above base speed, continuously variable transmission, flywheel energy storage unit clutched to motor

The flywheel system can meet all the required performance goals, including acceleration from zero to 89 km/hr in 15 s, with either lead-acid or nickel-zinc batteries. The basic system can also meet all performance goals when the battery is fully charged. When the battery approaches 20 to 30 percent depth of discharge, however, the maximum acceleration capability of the basic system gradually degrades, although the remaining performance goals can still be achieved.

The flywheel system has an estimated life-cycle cost over a 10-year period of \$0.041/km when available lead-acid batteries are used. As a reference, when nickel-zinc batteries are used, the necessary battery weight is only half that of lead-acid batteries, which gives a much lighter vehicle weight. The high cost of the nickel-zinc batteries, however, results in a life-cycle cost of \$0.076/km. The basic system with available lead-acid batteries requires three battery changes in the 10-year life span of the vehicle, due to the more strenuous demands on the battery, and the life-cycle cost is \$0.06/km. For a basic system with lead-acid batteries that meet all the ISOA goals, the life-cycle cost would be \$0.043/km. The flywheel system would not be improved by use of a battery that meets ISOA goals, since the system power requirements are lower. All life-cycle costs include both the propulsion system and the battery. The life-cycle cost goal is \$0.05/km.

The following table summarizes the performance of the two final propulsion system configurations

Propulsion systems with lead-acid batteries	Basic system	Flywheel system
Vehicle test weight	1660 kg	1713 kg
Battery weight	671 kg	667 kg
Propulsion system weight	111 kg	159 kg
Range with J227a (D) cycle	161 km	186 km
Range at constant 72 km/hr	240 km	209 km
Maximum acceleration 0 to 72 km/hr	15 s	15 s
Maximum passing speed	105 km/hr	105 km/hr
Minimum life	10 yr	10 yr
Life-cycle cost (available lead-acid battery)	\$0.06/km	\$0.041/km
Life-cycle cost (ISOA goal battery)	\$0.043/km	\$0.041/km

Flywheel system with nickel-zinc batteries (reference)	
Vehicle test weight	1327 kg
Battery weight	370 kg
Life-cycle cost	\$0.076/km

INTRODUCTION

The program described in this report was initiated to identify and evaluate advanced propulsion system concepts for mid-size electric vehicles. Electric vehicles are of interest because their use will reduce petroleum consumption and pollution. Today about half of the petroleum consumed in the United States is used for transportation. The introduction of electric vehicles could significantly shift the transportation energy base to other sources such as coal, nuclear, and solar.

Background

In 1976 the Electric and Hybrid Vehicle Program was established within the Energy Research and Development Administration (ERDA), now the Department of Energy (DOE). In September Congress passed the Electric and Hybrid Vehicle Research, Development, and Demonstration Act of 1976 (Public Law 94-413). This act is intended to accelerate the integration of electric and hybrid vehicles into the nation's transportation system and to stimulate growth in the electric vehicle industry.

Program Objectives

The objectives of this program were to identify potentially attractive concepts for advanced propulsion systems that offer considerable performance improvement over existing propulsion systems with little or no potential cost penalty. The propulsion system design concepts were based on propulsion system components that could be developed by 1983.

Program Tasks

The program effort is discussed in this report in terms of the three principal tasks:

- Task I--Perform preliminary analysis of 17 candidate systems, weighing the relative advantages of the systems in terms of the performance goals and design features, to recommend 5 systems for further study.

- Task II--Perform design tradeoff studies of the five candidate systems, on the basis of cost and performance, to select the two best systems.

- Task III--Prepare conceptual designs of the two selected systems, documenting performance and life-cycle costs.

Task I, preliminary analysis.--The objectives of Task I were to examine and compare 17 propulsion system configurations, weighing their relative merits, to recommend five systems for more detailed evaluations in the following program task. The systems examined were specific variations of five basic concepts. For each of these basic concepts the specific variations yielded a total of

17 configurations. These configurations provide a comprehensive range of propulsion systems, encompassing a large percentage of systems currently being used or considered for electric vehicles.

The method of comparison of these systems was to use a computer program to simulate the operation of each propulsion system over a driving cycle in accordance with SAE J227a, schedule D. A primary performance goal is that the propulsion system be capable of propelling a four-passenger vehicle over a 161-km range, accomplished by successive J227a(D) cycles. The initial comparison thus became the battery weight needed by each system to accomplish the designated range. Further comparisons were then made on the relative complexity and cost of the components for a common basic performance level.

The characterization of the components used in the computer simulation was in the form of performance maps of power, speed, and efficiency. Component design was not done in Task I, but design criteria were applied in selection of performance parameters, so that the performance maps are representative of advanced state-of-the-art components, designed to optimize desirable characteristics. The established goal for the components was performance anticipating reasonable technological development by 1983.

In the integration of system components, consideration was also given to matching the component performance so as to secure the best system performance; however, in a preliminary analysis, it cannot be assumed that all systems are fully optimized. Therefore, some tolerance must be applied to the final standings, and small differences in performance may not have any great significance. What was sought were major trends.

The selection of five configurations for further study in Task II was made not only on the basis of the range and cost comparisons but also on the need for technological advancement and the relative advantages of similar systems.

Task II, design tradeoffs.--The objectives of Task II were to examine the candidate systems selected in Task I, and perform design tradeoffs to optimize performance and cost. Performance was evaluated not only for range but also for maximum acceleration, which determines peak power requirements. Machinery characteristics were examined to determine the best operating range, gear ratios, and peak power points.

The performance with nickel-zinc batteries was also evaluated. Nickel-zinc batteries provide a considerable increase in specific power and specific energy over that available with lead-acid batteries. The cost, however, is also much greater.

On the basis of the Task II studies, two of the five systems evaluated were selected for following conceptual design studies.

Task III, conceptual designs.--Component designs were made for the specific system applications, and system performance was evaluated for both performance and cost tradeoffs. Cost tradeoffs were carried beyond first cost of the propulsion system and batteries, and a life-cycle cost analysis was made. The final two systems were then measured against all the program performance and cost goals.

PROGRAM GOALS AND GUIDELINES

The program goals are established by the statement of work and are for application to a propulsion system suitable to power a four-passenger vehicle whose basic characteristics are also defined by the statement of work. Guidelines were given for certain calculations such as for vehicle weight, road load, and annual driving range. These basic goals and guidelines are presented in this section. Other guidelines and procedures were developed during the course of the program, and these guidelines and the resulting calculation procedures are discussed in subsequent sections.

Performance Goals

The primary performance goals as specified apply at the test weight of the vehicle, at an ambient temperaure of 27°C, and with a new battery pack:

(1) Minimum range with SAE J227a schedule D driving cycle . . . 161 km

(2) Minimum range at constant 72 km/hr. . . . . 209 km

(3) Maximum acceleration time for 0 to 89 km/hr . . . . 15 s

(4) Maximum merging time for 40 to 89 km/hr . . . . 10 s

(5) Minimum passing speed . . . . 105 km/hr

(6) Sustained speed on an uphill four percent grade . . . . . 89 km/hr

(7) Minimum ramp speed attainable from a stop on an uphill six percent grade. . . . . 65 km/hr

(8) Maximum electrical recharge energy on SAE J227a (D) cycle . . . . 0.16 kW-hr/km

Cost Goal

The goal for the maximum life cycle cost of the propulsion system and battery over the 10 year life is $0.05/km in 1976 dollars. Electricity cost is given as $0.04/kW-hr. Acquisition costs are based on production of 100,000 units per year.

Operating Conditions

The propulsion system must be able to operate in a range of ambient temperature within the following limits:

(1) Minimum ambient temperature . . . . -29°C

(2) Maximum ambient temperature . . . . 52°C

The propulsion system must have safety and reliability comparable to that of a 1977 compact car over a 10 year life. Minimum travel distance over the 10 year life is 160 900 km, which is assumed to be accumulated by an annual series of trips as follows: (1) 400 trips of 16.1 km, (2) 150 trips of 48.3 km, and (3) 30 trips of 80.5 km.

Battery Characteristic Goals

Battery characteristics are given for an improved state-of-the-art (ISOA) lead-acid battery and a nickel-zinc battery. The characteristics are goals established by the Department of Energy for battery development efforts for 1981.

		ISOA Lead-Acid	Nickel-Zinc
(1)	Specific energy	40 W-hr/kg	80 W-hr/kg
(2)	Specific power	100 W/kg	150 W/kg
(3)	Cycle life, 80 percent depth of discharge	800 cycles	500 cycles
(4)	Cost	\$50/kW-hr	\$75/kW-hr

Vehicle Characteristics

Engineering characteristics of the designated four-passenger vehicle are given as follows:

(1) Aerodynamic coefficient, C_DA . . . . 0.56 m^2

(2) Tire rolling radius. . . . . 29.2 cm

(3) Tire rolling resistance coefficient for vehicle velocity, V, in km/hr

$$C_R = 0.008 + 1 \times 10^{-5}\ V + 8 \times 10^{-8}\ V^2$$

(4) Vehicle test weight $W_T = W_G - 136$ kg

(5) Gross vehicle weight $W_G = W_S + W_{PL} + W_{PS} + W_B + W_F$

(6) Maximum design payload $W_{PL} = 272$ kg

(7) Fixed weight $W_F = 326$ kg

(8) Structure and chassis weight $W_S = 0.23\ W_G$

The propulsion system weight, W_{PS}, and the battery weight, W_B, are determined by the study program.

TECHNICAL APPROACH

The initial approach that was used to compare the various candidate systems employed a digital computer simulation of each vehicle system to calculate the power used to execute the SAE J227a schedule D cycle. An extrapolation was then made to predict total range for a fully charged battery. Successive adjustments were made to battery weight to find the battery weight necessary to achieve the desired 161-km range. Calculations were also made to ascertain the range that could be achieved at a constant 72 km/hr, and in some cases this requirement established the battery weight. The systems were then compared on the basis of weight, size, relative cost, and complexity to achieve the specified performance.

Propulsion System Configurations

The propulsion system configurations examined in the preliminary analysis are based on the five general concepts presented in fig. 1. The first three concepts are basic systems without an energy storage unit; the last two employ a flywheel as an energy storage unit. For each of these general concepts, specific variations were defined as shown in figs. 2 through 6, a total of 17 configurations. Group 1 includes two simple basic systems, and Group 2 uses a multiratio transmission with the same traction motors as in the first group. Group 3 uses various types of continuously variable transmission (CVT) with different traction motors. Group 4 uses two electrical machines as an electrical transmission with a flywheel energy storage unit. Group 5 uses a mechanical CVT with a flywheel energy storage unit.

These 17 configurations were defined in the initial statement of work, because they are representative of systems that are currently being used or considered for electric vehicles. There are many other possible variations, but the actual selections represent a range broad enough to assess trends and make meaningful comparisons. The 17 specific configurations are not completely defined in the diagrams. The multiratio transmission, for example, could be a three- or four-speed unit. In addition, the optimum speed range for such various components as motors, flywheels, and transmissions may require a gear ratio at the interface with the adjoining component, and this gearing can be considered an integral part of one component in the diagrams. Such items, however, must be defined for the computer simulation, and thus represent design decisions. For such design decisions that have a critical effect on performance, design tradeoffs were made as part of the Task II effort.

It is also implied, though not shown, that the controller includes both the power control electronics and the driving control logic. For those systems that regenerate back to the battery, the motor functions also as a generator. In addition, in those cases where there is not a transmission, reverse capability is obtained by running the motor in reverse rotation.

In all the preliminary comparisons, the battery was considered to be a lead-acid battery with performance approximately equivalent to the ISOA goals. In the design tradeoff activity, propulsion system performance also was evaluated using nickel-zinc batteries.

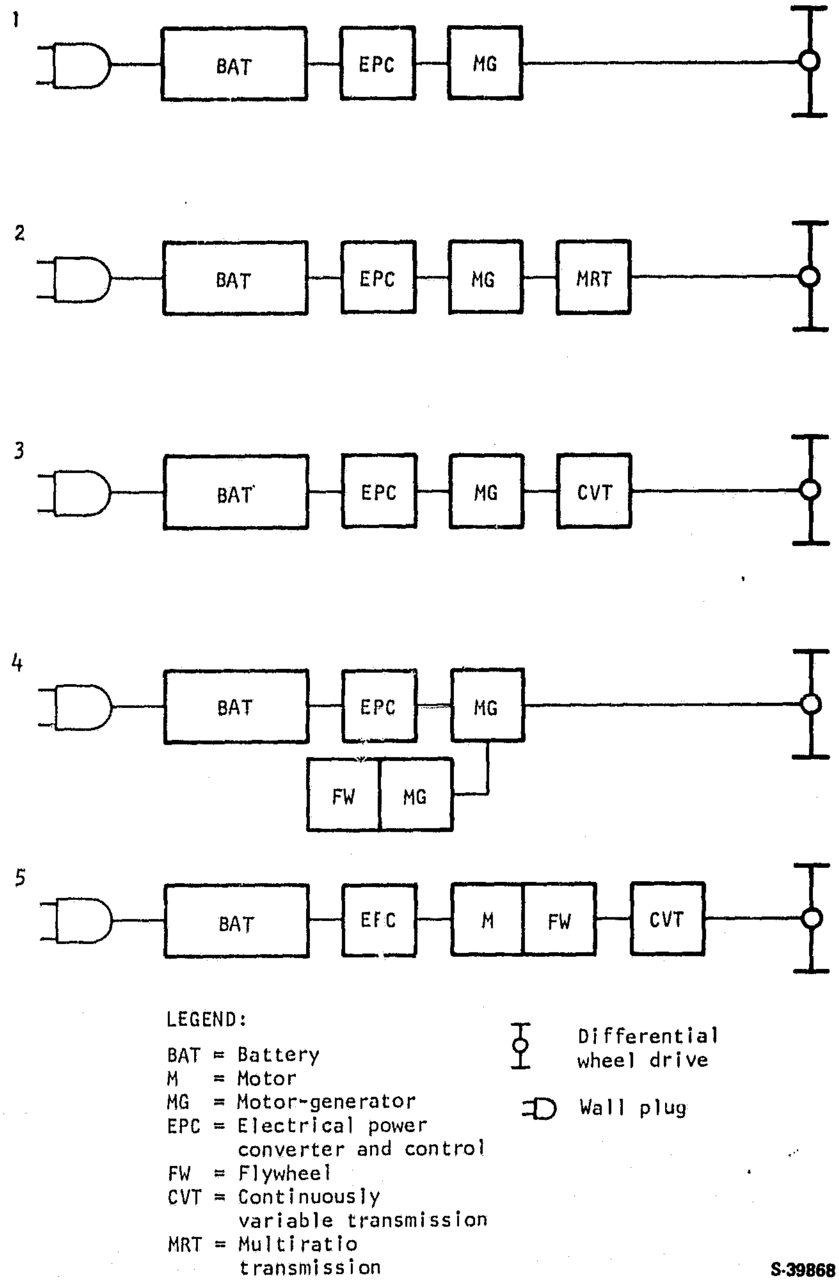

Figure 1.--General propulsion system configurations.

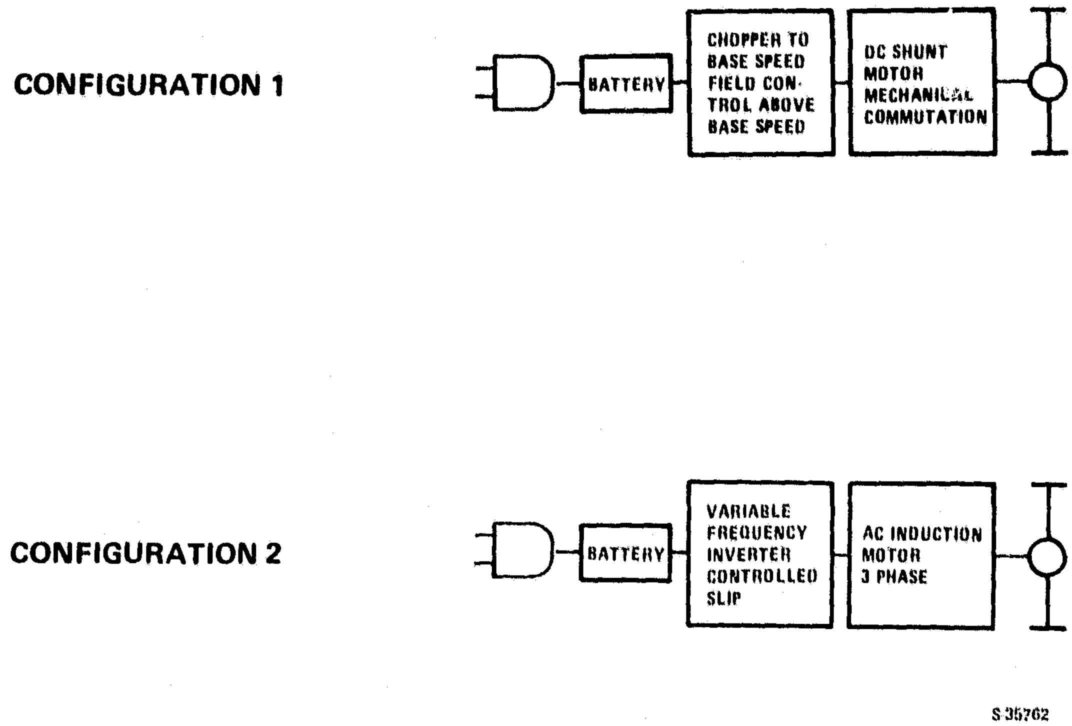

Figure 2.--Electric propulsion system configurations, group 1.

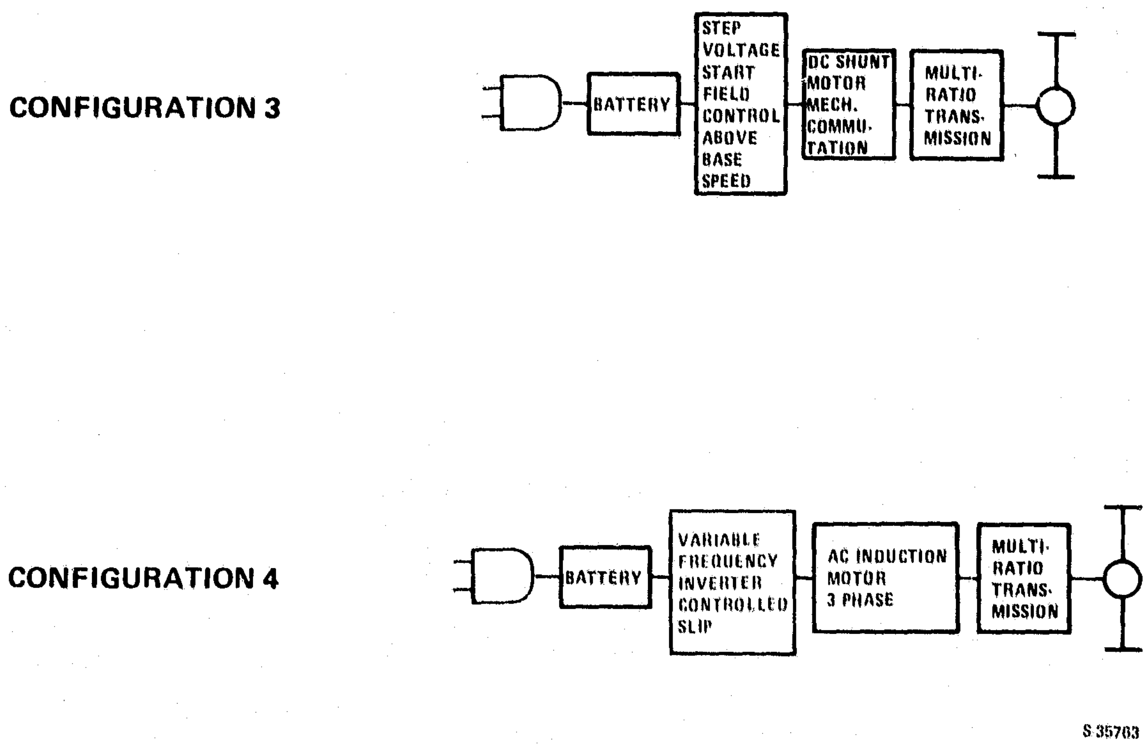

Figure 3.--Electric propulsion system configurations, group 2.

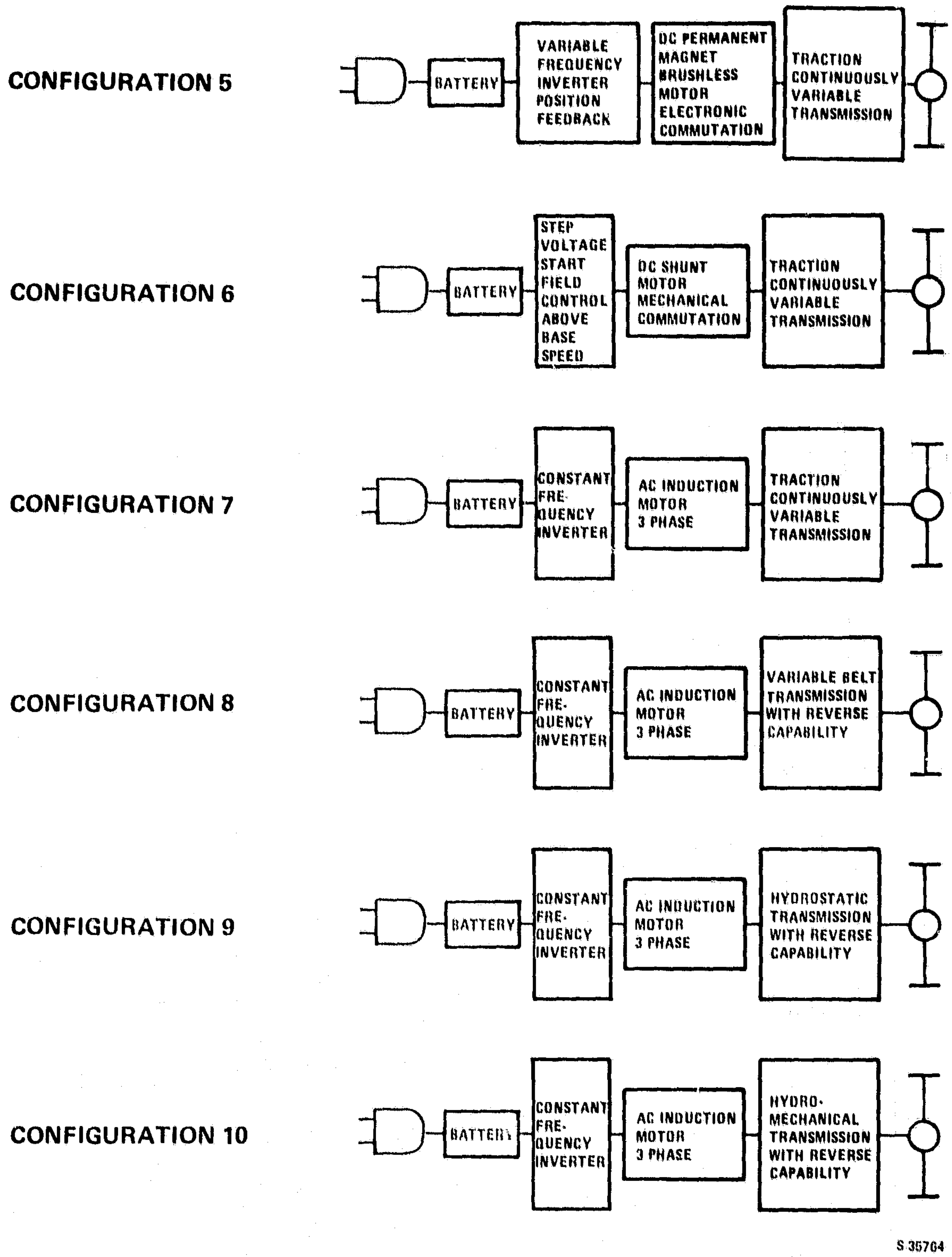

Figure 4.--Electric propulsion system configurations, group 3.

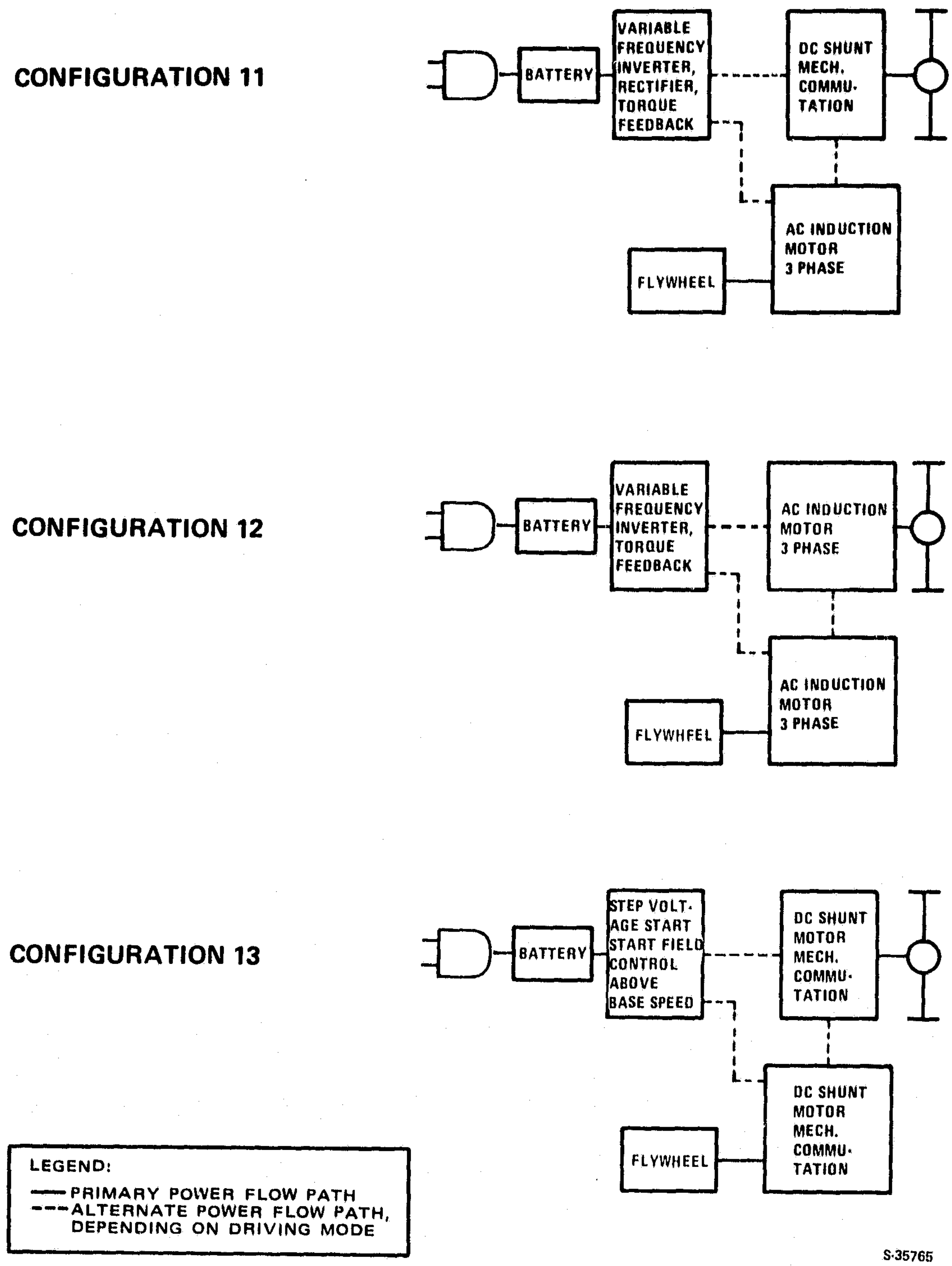

Figure 5.--Electric propulsion system configurations, group 4.

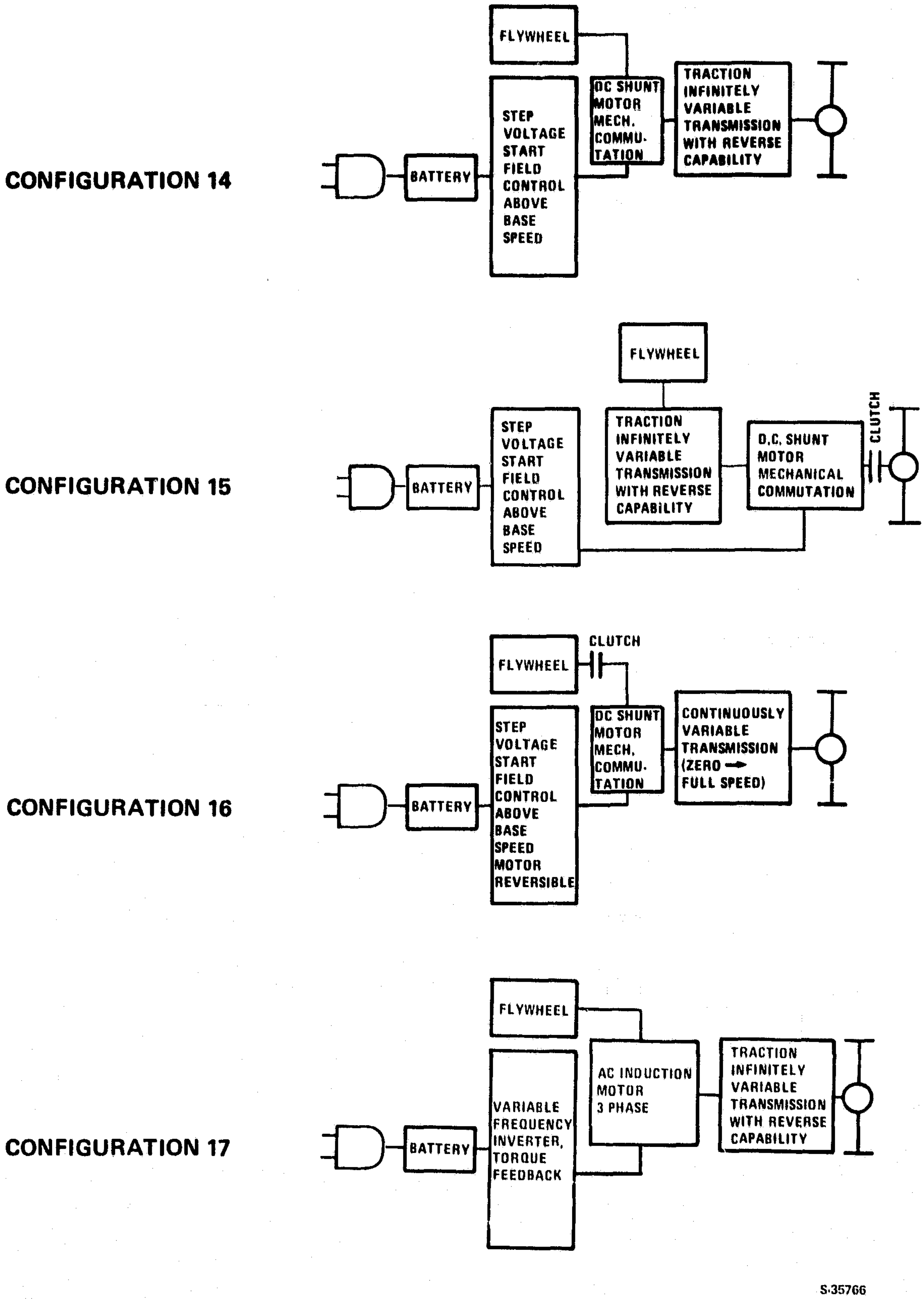

Figure 6.--Electric propulsion system configurations, group 5.

Vehicle Simulation

The digital computer program is constructed in modular form, which provides great flexibility in operation. Vehicle components are represented by performance maps that can be modified easily to represent changes in component design. The driving cycle is used in the form of vehicle velocity vs elapsed time, and can be modified easily to provide changes in acceleration.

The vehicle power required at any instant of time during the cycle is assumed to be matched ideally by the driver's exact positioning of the throttle or brake pedal, and by the controller's instantaneous response. With this procedure, the vehicle velocity and acceleration follow the specified driving cycle exactly at all times. The component models and driving cycle velocity profile are integrated into a performance simulation computer program according to the logic diagrams shown in figs. 7 and 8.

The computer program reads in vehicle characteristics such as vehicle gross weight, drag characteristics, tire rolling resistance, various gear and transmission ratios, and the specified driving cycle (vehicle velocity vs time). The road load is calculated at small time intervals by applying the appropriate equations. The power at the axle to meet road load also is the output of the differential. With the differential performance map, the input to the differential is calculated, and this in turn becomes the transmission output. This step-by-step procedure continues until battery drain is found. With successive time intervals, the battery drain can be found for an entire cycle. An extrapolation is then made to determine the number of cycles achievable with a given battery pack, when depleted to 100 percent depth of discharge.

The battery drain is found from a subroutine that was initially developed for the Near-Term Electric Vehicle* and has been adapted for this propulsion system simulation. The extrapolation from a single cycle was made to avoid the excessive amount of computation required if each variation of each configuration were run over 100 or more cycles. The extrapolation procedure had been previously evaluated for the Near-Term Electric Vehicle and was found to yield results within ten percent of those calculated for the full number of cycles.

If the calculated range is less than 161 km, the battery weight is increased, the cycle is repeated, and adjustments are made in battery weight until the 161-km range is achieved.

The simulation also has certain calculations not indicated on the flow charts. For example, the transmissions are regulated by a schedule of vehicle speed vs motor speed to maintain motor speed and efficiency within the optimum efficiency range. In general, motor speed is brought up to base speed at the lowest vehicle speed that the transmission range can allow. Under such circumstances motor inertia is a significant factor in power drain, and this inertia is entered into the calculations.

*The Near-Term Electric Vehicle Program was established by the Department of Energy in 1976 to study, design, and fabricate improved electric vehicles. Garrett/AiResearch has a contract to fabricate an electric vehicle, scheduled for delivery in 1979.

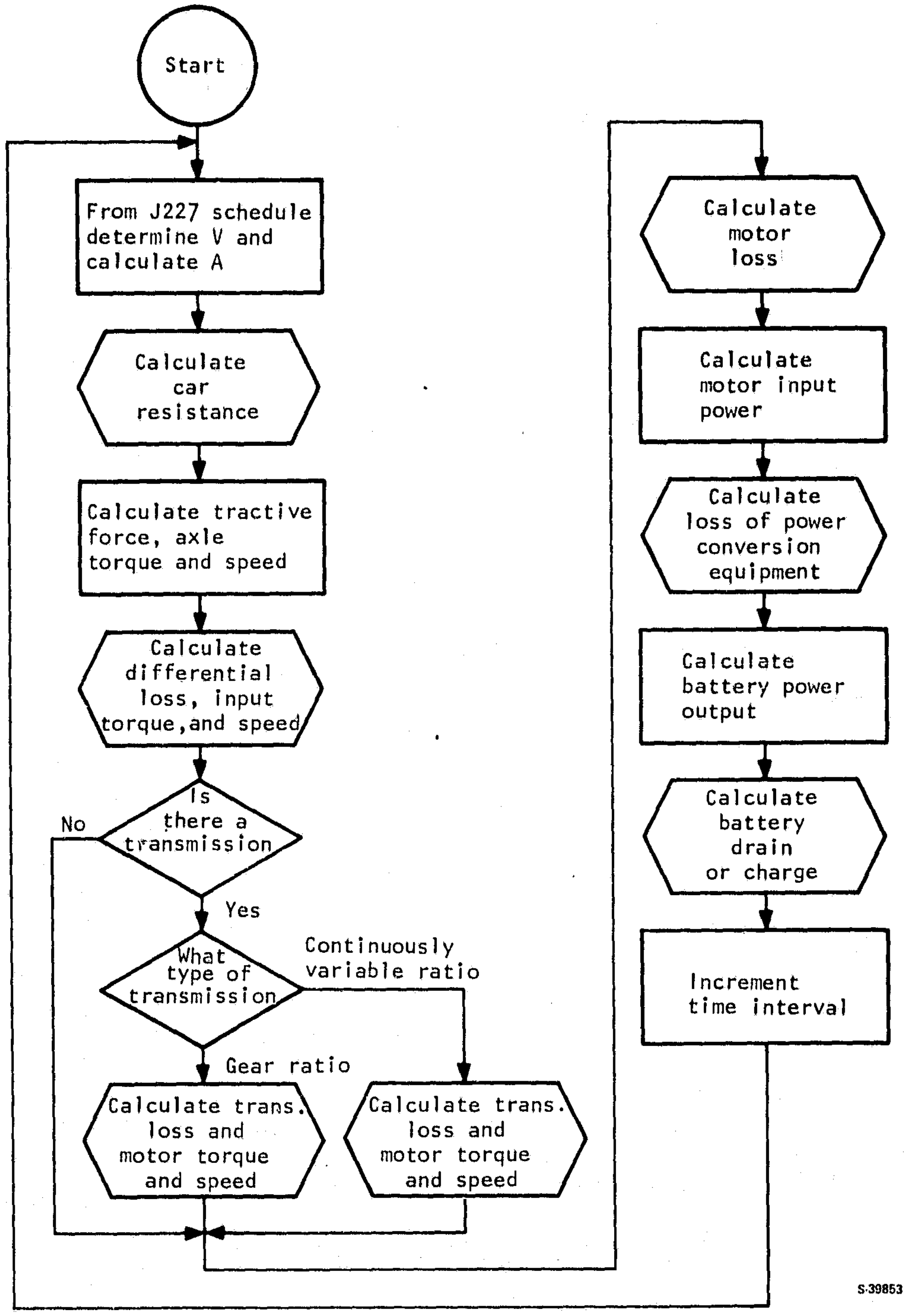

Figure 7.--Computer flow chart for configurations without a flywheel.

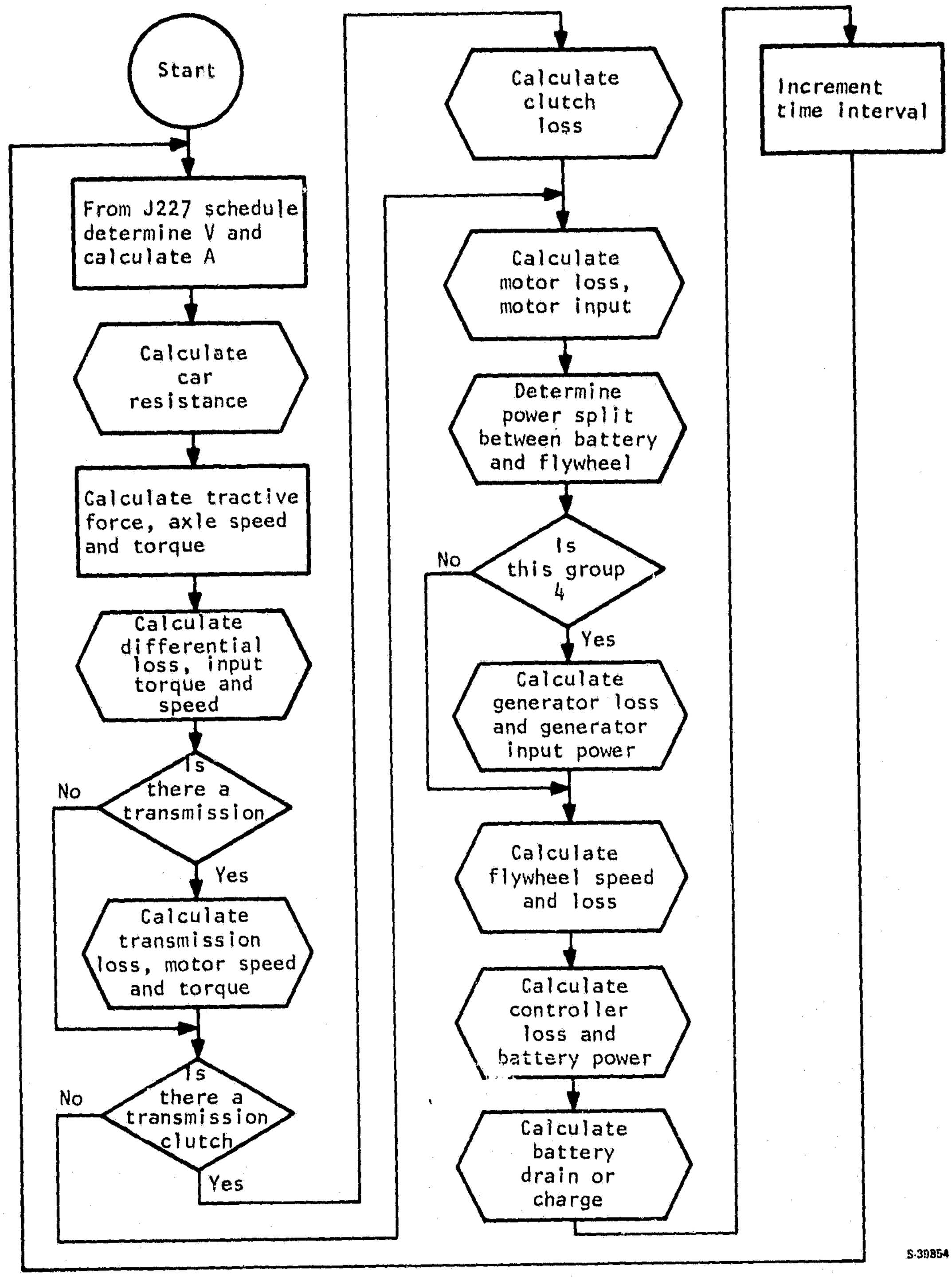

Figure 8.--Computer flow chart for configurations with a flywheel.

Driving Cycle

The required driving cycle is the SAE J227a schedule D, which is a cycle of 122 ± 2 sec that includes:

(1) Acceleration to 72 ± 1.5 km/hr in 28 ± 2 sec

(2) Cruise for 50 ± 2 sec

(3) Coast for 10 ± 1 sec

(4) Brake to a stop for 9 ± 1 sec

(5) Remain stopped for 25 ± 2 sec

Fig. 9 depicts the velocity-time profile of this cycle. The shaded areas are drawn to indicate that only the end points of each portion of the cycle are specified. Therefore, the shape of the acceleration portion of the curve can be deliberately varied by controlling the power applied. The speed at the end of the coast period depends on the vehicle drag and loss characteristics. The characteristics of the braking effort can also be varied: one such way is to vary the rate of regeneration to the battery or flywheel.

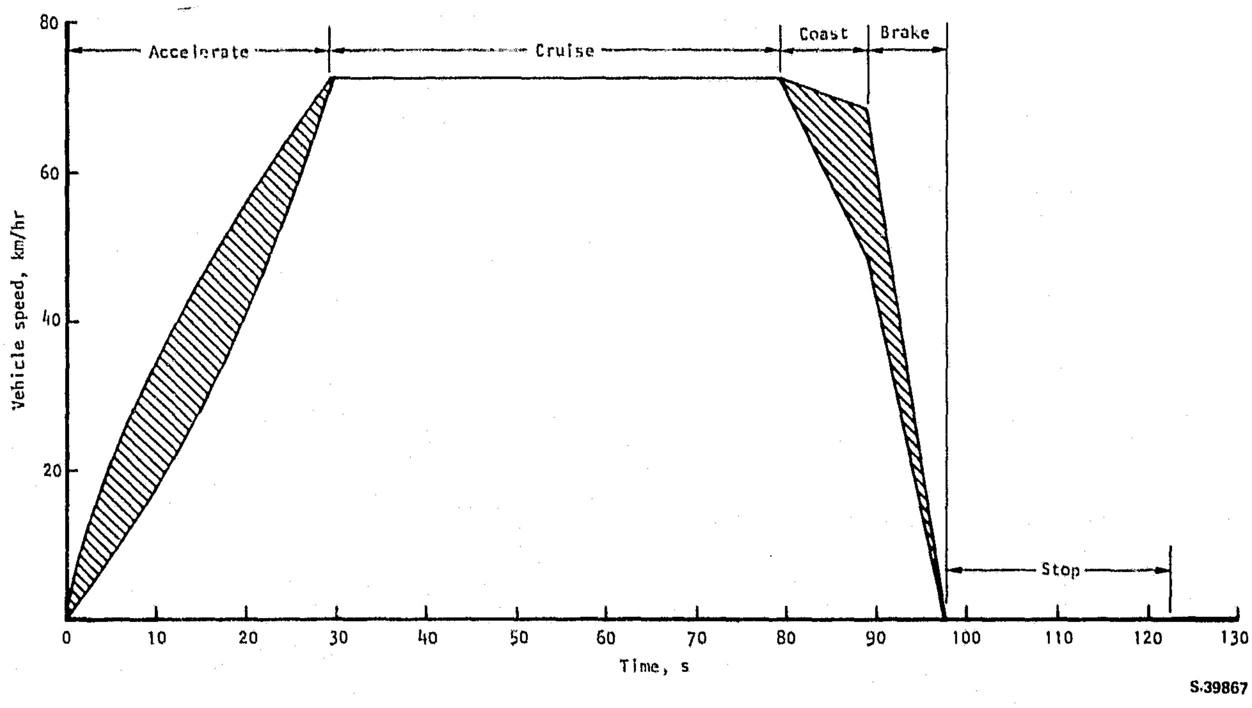

Figure 9.--SAE J227a schedule D cycle.

Previous studies (refs. 1 and 2) have shown that vehicle range is definitely affected by the acceleration profile adopted in the driving cycle. If acceleration is accomplished at approximately constant power, the total range is five to ten percent greater than if acceleration is simply constant. Absolutely constant power, however, requires very high acceleration at low speed (fig. 10), which may be beyond the capability of the electric motor, or beyond the ability of the tires to avoid slipping. Therefore, the acceleration schedule used for the driving cycle was nearly constant power, but lower at the beginning to stay within the capability of the traction motor.

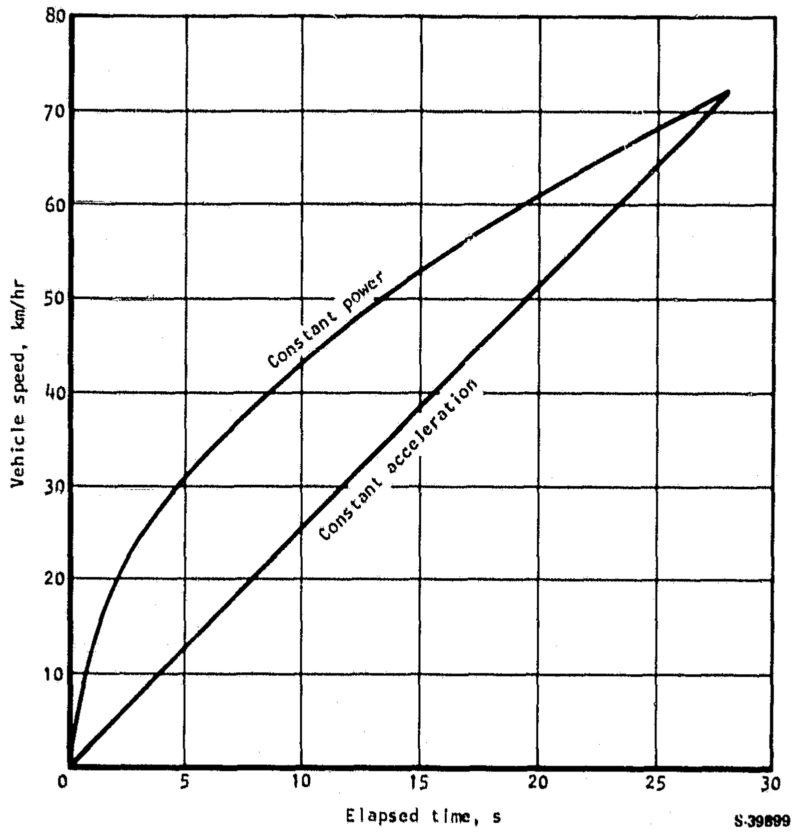

Figure 10.--Velocity schedules for J227a(D) driving cycle.

Comparison Criteria

The two basic goals of the advanced electric propulsion system were defined by the statement of work as the cost goal and the performance goal. The initial sorting of the various configurations was done on the basis of the battery weight required to meet the vehicle range goals, with a preliminary consideration of relative costs. Actual costs were considered in more detail during the design tradeoff activities, and life-cycle costs were calculated for the final designs.

The performance requirements of the advanced electric propulsion system program represent a considerable advance, particularly in range, beyond that specified in the Department of Energy Near-Term Electric Vehicle Programs that use the same type of batteries. Much of this increase in range was achieved by an increase in battery load, but an assessment was also made of the improved performance that can be obtained by advanced design of the power train components.

Component design was not done in the preliminary analysis, but design criteria were applied in selection of performance parameters. The component performance maps are representative of advanced state-of-the-art components that were designed to optimize the desirable characteristics. The criterion that was applied to the components was a performance that implies reasonable technology development that can be accomplished by 1983.

Baseline Calculation

To facilitate sizing of components, preliminary calculations were performed for a baseline vehicle in the form of the Garrett Near-Term Electric Vehicle, as shown schematically in fig. 11. By use of a computer simulation originally developed for the Near-Term Electric Vehicle Program, it was found that the range of 161 km with the SAE J227a schedule D cycle could be achieved with a battery load of 734 kg, and a gross vehicle weight of 1941 kg.

The calculated vehicle weight of 1941 kg was used for initial sizing calculations to determine motor power requirements. The battery weight of 734 kg was used to establish the basic battery voltage.

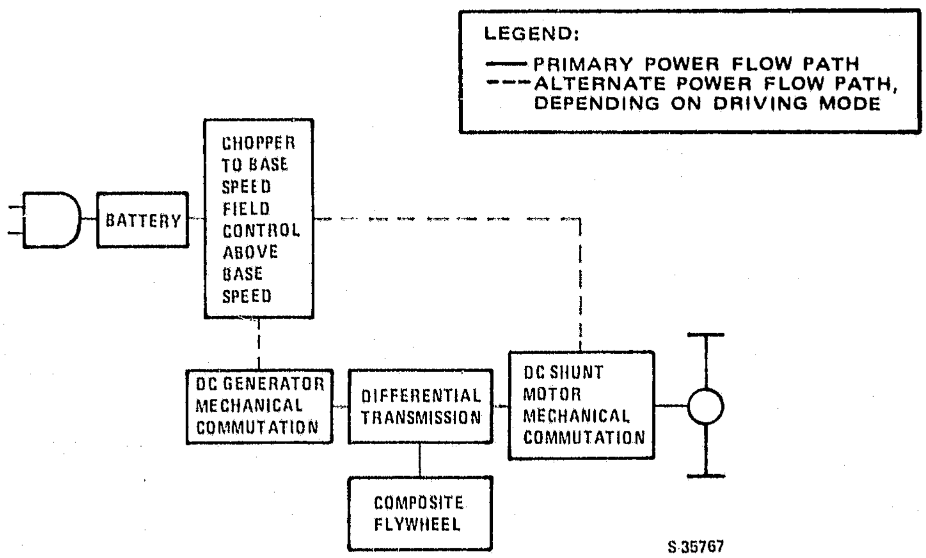

Figure 11.--Baseline system configuration.

Battery Interface and Voltage Selection

A battery load of 734 kg, as determined for the baseline system, can be achieved with 28 standard 6-V batteries. It was decided to maintain 168 V for all systems to provide a standard of comparison and to scale total energy capacity in proportion to total weight. It was assumed that a battery could be constructed with the exact proportion of energy capacity and weight needed for each particular application.

The ISOA battery performance is based on the primary characteristics given in the statement of work, and battery dynamic performance characteristics were based on data for the tubular, lead-acid battery developed by Eagle-Picher Industries for the Near-Term Electric Vehicle. Eagle-Picher has written a computer program to predict steady-state performance, such as capacity and voltage profiles. Inputs are current discharge rates, ambient temperatures, depth-of-discharge, and the age of the battery in terms of the charge-discharge cycles. A detailed discussion of battery performance data is presented subsequently under the title "Battery Characteristics"; at this point, the discussion is limited to the modeling procedure.

The battery program used for the propulsion system simulation, called the driving cycle dynamic program, is one developed for the Near-Term Electric Vehicle. It evolved from the program developed by Eagle-Picher and from the fractional-utilization method. When the vehicle negotiates a driving cycle, the current demanded from the battery will vary during the course of the cycle. If the cycle is divided into small time intervals, the current during each time interval may be considered as constant at the average value, and the battery depletion during the interval may be found from the steady-state performance program. The total depletion over an entire cycle may then be found by summation of the fractions of use for all time intervals.

The range of the vehicle can be evaluated by dividing the distance per driving cycle by the fraction of capacity used during the driving cycle. This calculated range depends on the assumption that the single cycle is representative of average battery depletion over the full range of operation. Previous experience has shown that the cycle that starts with battery depletion at 60 percent depth-of-discharge will yield a calculation of total range within 10 percent of the value found by running the total number of successive cycles.

The vehicle range requirements are considered to be limiting values, since the annual trip schedule does not include any trips at extreme range. Therefore, in the vehicle simulation and tradeoff studies, the maximum range was accomplished by using the battery to 100 percent depth of discharge. A level of 100 percent depth of discharge is a minimum power capability established by a battery manufacturer to indicate the practical limit for a particular battery, but does not represent total exhaustion of all energy; however, battery life, in terms of the number of charge and discharge cycles, is directly related to the depth of discharge of the cycles.

PERFORMANCE PARAMETERS

A number of the parameters affecting vehicle performance are given in the statement of work, and the vehicle weight and the operating road load are determined by a designated formula. Component power requirements are based on vehicle grade and acceleration limits, which are not completely defined. This section presents the procedures used to define the performance parameters.

Vehicle Weight

The vehicle weight is determined in the manner specified in the statement of work, using a procedure based on the following premises:

(1) There is a fixed weight for the passenger compartment, seats, instruments, heating and ventilation, body panels, and similar items. This fixed weight depends only on the selected payload and is independent of the amount of battery carried.

(2) The remaining structural and chassis weight is proportional to the gross vehicle weight, the weight of the vehicle with the maximum design payload aboard. This structural and chassis weight would include the structure, suspension, tires, wheels, and other components that must carry the maximum vehicle weight, which includes the fixed weight as well as the maximum payload, the propulsion system, and the battery.

(3) The propulsion system and battery weights are determined in the study program.

(4) Performance goals apply at the vehicle test weight.

The terms and relations are defined in table 1.

TABLE 1.--VEHICLE WEIGHT TERMS AND RELATIONS

Symbol	Definition	Evaluation
W_{PL}	Maximum design payload	272 kg
W_F	Fixed weight	326 kg
W_S	Structure and chassis weight	$W_S = 0.23\ W_G$
W_{P_S}	Propulsion weight	To be determined
W_B	Battery weight	To be determined
W_G	Gross vehicle weight	$W_G = W_S + W_{PL} + W_{PS} + W_B + W_F$
W_T	Vehicle test weight	$W_T = W_G - 136$ kg

Expressing the vehicle weight in terms of the various components, with the loads in kilograms, and using the relations in table 1:

$$W_T = 0.23\ W_G + 272 + W_{PS} + W_B + 326 - 136$$

Then:

$$0.77\ W_T = 493 + W_{PS} + W_B$$

For the baseline vehicle configuration

$$W_B = 734\ \text{kg}$$

$$W_T = 1941\ \text{kg}$$

This baseline vehicle weight was used in the preliminary sizing of the power train components.

Road Load

The road load is considered to consist of two components: the aerodynamic drag and the tire rolling resistance. These values are determined in the manner stipulated, using designated constants.

Aerodynamic drag.--The aerodynamic drag is calculated from the equation:

$$F_D = C_D\ A\ \rho\,(V^2/2)$$

Where:

C_D = Drag coefficient

A = Frontal area

ρ = Air density

V = Vehicle velocity

In consistent units:

$C_DA = 0.56\ m^2$ (given)

$\rho = 1.225\ kg/m^3$

For a vehicle speed of 89 km/hr, or a velocity of 24.7 m/s, the aerodynamic drag force is:

$$F_D = (0.56)\ (1.225)\ (24.7^2/2) = 209.3\ N$$

<u>Rolling resistance</u>.--The tire rolling resistance is found as:

$$F_R = C_R W_T g$$

Where:

$$C_R = \text{Rolling coefficient}$$

$$g = \text{Gravity constant } (9.81 \text{ m/s}^2)$$

When the velocity is expressed in km/hr, the coefficient is given as:

$$C_R = 0.008 + 1 \times 10^{-5} V + 8 \times 10^{-8} V^2$$

For a vehicle speed of 89 km/hr

$$C_R = 0.008 + 1 \times 10^{-5} (89) + 8 \times 10^{-8} (89)^2 = 0.0095$$

For a vehicle of 1941 kg the resistance force at 89 km/hr is then:

$$F_R = (0.0095)(1941)(9.81) = 180.9 \text{ N}$$

<u>Total road load</u>.--The total road load is the sum of the aerodynamic drag and rolling resistance

$$F_{RL} = F_D + F_R$$

At the vehicle speed of 89 km/hr

$$F_{RL} = 209.3 + 180.9 = 390.2 \text{ N}$$

Power Requirements

The power requirement at the axle to propel the vehicle may be conveniently divided into three categories: road load, grade, and acceleration.

<u>Road load</u>.--The road load conditions are used to find the steady-state power at a given speed. Thus, for a vehicle of 1941 kg weight, at a speed of 89 km/hr (24.7 m/s), the power is

$$P = F_{RL} V = (390.2)(24.7) = 9638 \text{ J/s} = 9.64 \text{ kW}$$

<u>Grade</u>.--As the vehicle negotiates a grade, the gravity component along the grade imposes an additional force on the vehicle, which may be written:

$$F_{GR} = W_T g \sin \emptyset$$

When the grade angle, $\emptyset$, is conventionally expressed by a percent, the relation is:

$$\text{Grade percent} = \tan \emptyset$$

For small angles the sine and the tangent are nearly equal, therefore, for a vehicle of 1941 kg on a four percent grade:

$$F_{GR} = (1941)(9.81)(0.04) = 761.7 \text{ N}$$

At 89 km/hr on a four-percent grade, the power for the grade required at the axle is

$$P = F_{GR}V = (761.7)(24.7) = 18814 \text{ J/s} = 18.81 \text{ kW}$$

Acceleration.--The performance goals include several conditions of acceleration, as follows:

(1) Driving Cycle: Acceleration from zero speed to 72 km/hr in 28 s.

(2) Maximum Acceleration: Acceleration from zero speed to 89 km/hr in 15 s.

(3) Merging: Acceleration from 40 km/hr to 89 km/hr in 10 s.

(4) Passing: Passing is at 105 km/hr, and it has been assumed that an acceleration maneuver is required from 89 km/hr to 105 km/hr in 8 s.

(5) Ramp Acceleration: A speed of 65 km/hr must be attained in 328 m from a stop. If this condition were at a constant acceleration, then

$$a = \frac{V^2 - V_o^2}{2x}$$

Using:

$$x = 328 \text{ m}$$

$$V_o = 0$$

$$V = 65 \text{ km/hr} = 18.1 \text{ m/s}$$

Then:

$$a = \frac{(18.1)^2}{2\ (328)} = 0.5 \text{ m/s}^2$$

(6) Braking Deceleration: During the driving cycle, in the coast segment, the speed will drop and then braking to zero speed will take 9 s. If the speed during coast drops to 60 km/hr the linear deceleration would be

$$a = \frac{0 - 60}{9}\ \frac{1000 \text{ m/km}}{3600 \text{ s/hr}} = -1.85 \text{ m/s}^2$$

Considering the case of maximum acceleration, from zero speed to 89 km/hr in 15 s, if we assume constant acceleration to 89 km/hr (24.7 m/s) then:

$$a = 24.7/15 = 1.65 \text{ m/s}^2$$

Using the baseline vehicle weight of 1941 kg, the acceleration force would be:

$$F_a = W_T a$$

Thus:

$$F_a = (1941)(1.65) = 3202.7 \text{ N}$$

The peak power would occur at maximum speed. Since:

$$P = F_a V$$

Thus:

$$P_{max} = (3202.7)(24.7) = 79\,107 \text{ J/sec} = 79.11 \text{ kW}$$

This level of power is required only at the end of the acceleration, when the vehicle reaches maximum speed. An alternative procedure is to apply a constant, reduced power, which results in variable acceleration, to reach the same terminal velocity in the required time. An approximation of the power required may be made by neglecting road load and then considering the power needed to accelerate the vehicle mass. The instantaneous power at time, t, and velocity, V, is then

$$P_a = W_T \frac{dV}{dt} V$$

Starting at zero velocity, and accelerating up to the velocity, V, the expression may be integrated directly:

$$V^2 = 2P_a t/W_T$$

For the conditions previously considered:

$$W_T = 1941 \text{ kg}$$

$$V = 24.7 \text{ m/s}$$

$$t = 15 \text{ s}$$

Then the power required for acceleration is:

$$P_a = (V^2)(W_T)/(2)(t)$$

$$= (24.7)^2 (1941)/(2)(15) = 39\,473 \text{ J/s} = 39.47 \text{ kw}$$

In practice, such a schedule cannot be followed exactly, since very high acceleration is required at low velocity to achieve constant power. Consequently, the acceleration schedule is empirically modified to achieve nearly constant power, with the road load included as well.

The acceleration schedule shown in fig. 12 achieves 89 km/hr in 15 s, and also establishes 40 km/hr to 89 km/hr in 10 s, as required for merging. The passing speed of 105 km/hr is reached by accelerating from 89 km/hr to 105 km/hr in 8 s.

The maximum power requirement is in the interval 40 km/hr to 89 km/hr. The final acceleration being:

$$a = 0.86 \text{ m/s}^2$$

The power for this acceleration at 89 km/hr (24.7 m/s) with a 1941-kg vehicle is:

$$P_a = (1941)(0.86)(24.7) = 41\ 231 \text{ J/s} = 41.23 \text{ kW}$$

Road load was previously found as 9.64 kW; thus total power at the axle is:

$$P_{max} = 41.23 + 9.64 = 50.87 \text{ kW}$$

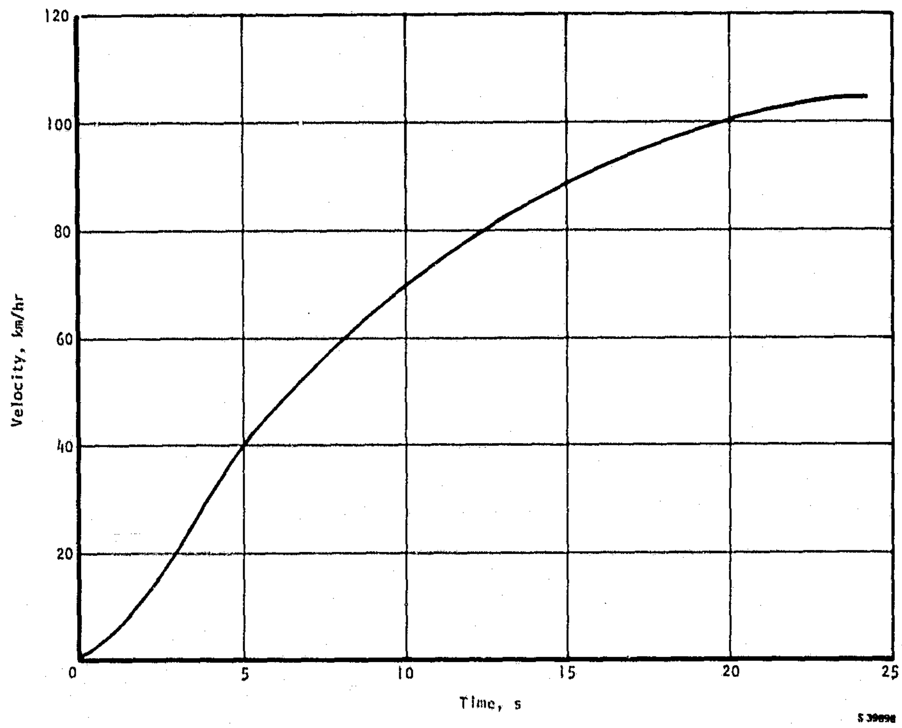

Figure 12.--Schedule for Maximum Acceleration

The power requirements needed to meet the various performance goals are listed in table 2 for the baseline vehicle. The baseline vehicle was the heaviest vehicle that was considered beyond the initial comparisons, and the final conceptual design is for a lighter vehicle.

The power levels listed in the table are the values required at the axle. The output of the traction motor must be higher to overcome the losses of the power train. For braking, on the other hand, the power required of the motor when used as a generator will be less than the axle power levels due to the retarding effect of the power train losses.

Initial Power Sizing

The initial power sizing of the power train components depends on two limits: (1) maximum sustained power, and (2) maximum power for acceleration. The maximum sustained power, which establishes the thermal limit of the electric motor and controller, is required for the specified case of a constant 89 km/hr on a four percent grade. For the baseline vehicle, the motor size required is approximately 30 kW.

Maximum power for acceleration is established by the acceleration profile used. As may be seen from the conditions shown in table 2, performance limits could be met for a vehicle as large as the baseline vehicle using a motor of approximately 60-kW size. Therefore, the traction motor requirement was set as

TABLE 2.--POWER REQUIREMENTS AT THE AXLE FOR A 1941-KG VEHICLE

Driving requirement	Required power, kW				
	Rolling	Aero	Grade	Accel	Total
Steady-state 72 km/hr	3.38	2.74	0	0	6.22
Acceleration, 0 to 89 km/hr, 15 s	5.17	4.47	0	Variable	50.87
Merging, 40 to 89 km/hr, 10 s	5.17	4.47	0	Variable	50.87
Passing, 89 to 105 km/hr, 8 s	5.51	8.39	0	Variable	45.38
Sustained four percent grade, 89 km/hr	5.17	4.47	18.81	0	28.45
Ramp, six percent grade, 65 km/hr	3.06	1.95	17.24	Variable	43.[illegible]
Driving cycle, 0 to 72 km/hr, 28 s	3.38	2.74	0	Variable	20.95
Braking, 60 km/hr to 0, 9 s	2.86	1.59	0	-59.86	-55.41

approximately 30 kW continuous power and 60-kW peak power, which is a reasonable range. The high power operating conditions do not occur in the J227a cycle, but the motor performance maps must reflect maximum capability to ensure a reasonable design.

These power levels were the guidelines for estimating component weights and preparing performance maps. The maps, however, were not plotted in terms of actual output power, but rather in percent of rated power. Therefore, they can be used to represent a family of units by designating some particular rated power within a limited range. A description of the component characteristics is included in the section "Power Train Characteristics."

Energy Management Criteria

When an energy storage device, such as a flywheel, is employed, it is necessary to establish criteria for the way in which the stored energy is used in conjunction with the battery. It is possible to operate periodically solely on one energy source or the other, or to split the energy demands. The philosophy that has been adopted for this study is to use the flywheel for high power requirements, and to recharge the flywheel from the battery at low power level.

The flywheel energy level was selected on the basis of preliminary calculations of the energy required to accelerate the baseline vehicle to 72 km/hr in 28 s. The required energy was approximately 180 W-hr, which included both the kinetic energy of the vehicle and the road load losses. A flywheel with a total of 250 W-hr would yield 188 W-hr when decelerated from full speed to half speed, and would be able to supply all the required energy to accelerate the vehicle. A larger flywheel would have less speed change, but would also add more to the vehicle cost, weight, and running losses.

The following criteria were established for the flywheel operation and charging procedures:

(1) The maximum flywheel energy is designated:

$$C_1 = 250 \text{ W-hr at } 36{,}000 \text{ rpm}$$

(2) Initially the flywheel is fully charged while the vehicle is at rest. To accelerate the vehicle, energy is taken from the flywheel. The kinetic energy of the vehicle increases as the kinetic energy of the flywheel decreases a like amount. Friction and windage losses in the system, however, will require additional withdrawal of flywheel energy until a level is reached at which recharge is initiated:

$$KE_{vehicle} + KE_{flywheel} = 0.96\ C_1$$

(3) Recharge will proceed at a regulated rate until the charge limit is reached:

$$KE_{vehicle} + KE_{flywheel} = C_1$$

(4) Recharge of the flywheel is accomplished by supplying power to the motor attached to the flywheel so that the total power from the controller does not exceed the limits shown in fig. 13.

(5) When the flywheel is charged up to the allowable limit and controller power is below 10 kw, the following energy management procedures apply:

(a) When the traction motor is attached to the flywheel (Group 5), the power to the traction motor is adjusted to supply sufficient power to maintain the flywheel speed while also meeting vehicle propulsion requirements, thus keeping the kinetic energy level at 1.0 C_1.

(b) When the flywheel is attached to a separate motor/generator (Group 4), no power is supplied to maintain the flywheel at the speed limit, and the speed is allowed to diminish while the controller only supplies power to the traction motor to meet vehicle propulsion requirements. Recharge is again initiated when the 0.96 C_1 limit is reached.

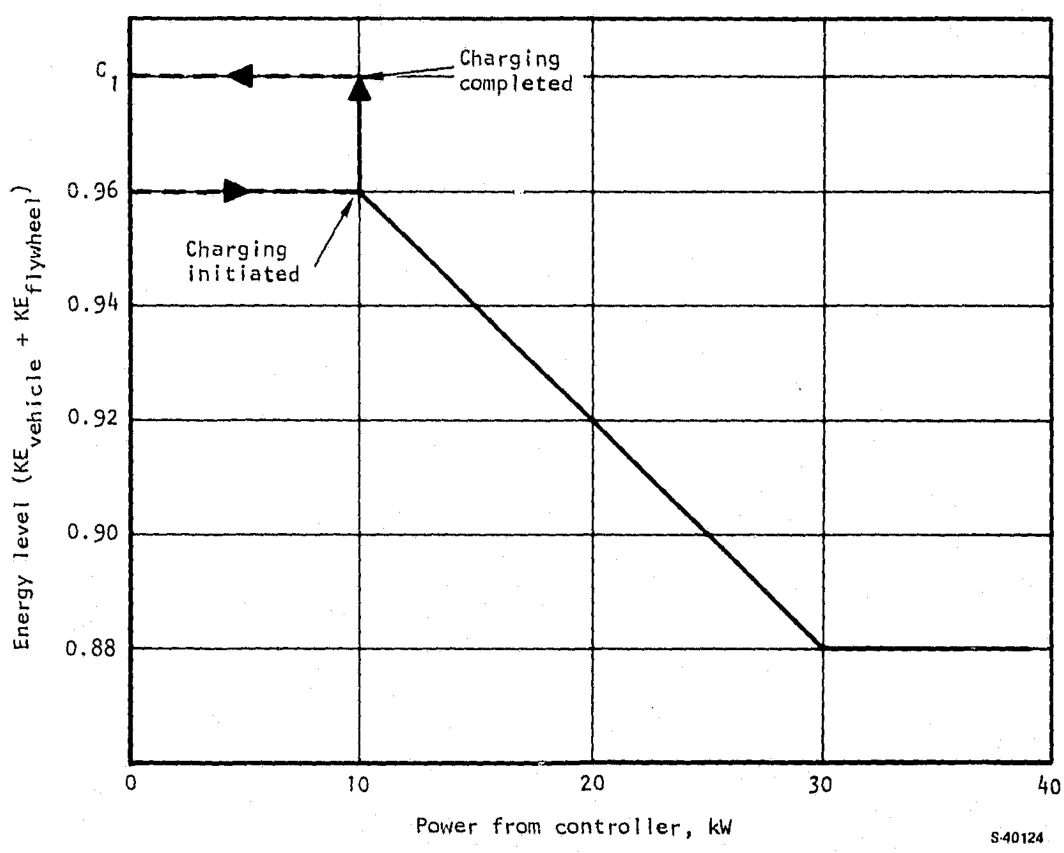

Figure 13.--Flywheel charging limits.

BATTERY CHARACTERISTICS

The propulsion battery is the heart of the electric vehicle, the sole source of energy to achieve the required performance; consequently, the discharge and charge characteristics of the battery are of vital importance in the simulation of vehicle performance. The battery characteristics as designated in the statement of work are limiting values, and are not sufficient to fully describe the dynamic performance of the battery. It was necessary to accumulate additional information to define a battery model with enough detail that representative discharge and range predictions could be presented.

Lead-Acid Battery

The designated battery for the initial comparisons of the propulsion systems is a lead-acid type, with performance defined as improved state-of-the-art (ISOA). The principal performance parameters as given in the statement of work are presented in table 3.

TABLE 3.--CHARACTERISTICS OF ISOA BATTERY

Specific energy (at a 3-hr discharge rate and an 8-hr charge rate, 27°F)	40 W-hr/kg
Specific power (peak power average for a period of 15 s)	100 W/kg
Cycle life (4- to 8-hr charge, 2- to 4-hr discharge	800 cycles to 80 percent depth of discharge

In the AiResearch Near-Term Electric Vehicle, the prototype batteries that are used have been developed by Eagle-Picher Industries with the design goal being ISOA performance characteristics. Therefore, the battery performance model used in the advanced propulsion system evaluations was based on the AiResearch model previously developed for the Near-Term Electric Vehicle, and uses data supplied by Eagle-Picher for their battery model, designated EP200AH.

The design of an ISOA battery involves more than meeting the specific energy and the specific power levels. The design may be optimized with regard to high power use or low power use, and there is a tradeoff between depth-of-discharge and total number of cycles. Since the Eagle-Picher EP200AH battery has been designed for the Near-Term Electric Vehicle, it has been optimized for a load-leveled application and maximum cycle life. There could be some penalty in total range when such a battery is used for a system that requires periods of high power consumption.

This effect of high power drain on range was not addressed in the initial comparisions, because the SAE J227a schedule D driving cycle requirements did not require high power drains; however, the battery model was later extended to evaluate the differentiation in performance due to battery drain capabilities for the final candidate configurations.

Battery Performance

The voltage of a battery cell depends on the potentials of the positive and negative plates with respect to the electrolyte solution. The potentials vary with the concentration of the electrolyte (at a fixed discharge rate and temperature), which in turn is a function of the discharge time. Hence, as the battery discharges, the voltage at the terminals falls gradually from its open-circuit value, until the end of the discharge is approached, when it begins to fall much more rapidly. Fig. 14 shows typical discharge curves for a lead-acid battery. These curves present the change in voltage, V, for various constant discharge currents, C, where the numbers indicate the time in hours to discharge. These relationships vary over the life of a battery, and are dependent on factors such as temperature.

For any given percent of capacity, S, the constant current discharge curves may be used to find the volt-ampere characteristics, as shown in fig. 15. These two figures, 14 and 15, contain the principal information needed for a battery operating model. A number of conditions are implied in the use of these curves, however, such as temperature level and definition of capacity. The definition of 100-percent depth-of-discharge for the Eagle-Picher EP200AH battery is defined as 1.67 V/cell at a discharge rate of 60 A. These values are somewhat different from the typical standard for golf-cart batteries of 1.75 V/cell at 80 A.

The most commonly used method of rating battery capacity is in terms of ampere-hours for a specified rate of discharge and end voltage. Fig. 16 shows the typical variations in the ampere-hour capacity of the EP200AH battery, as a function of discharge rate and environmental temperature (ref. 3). Thus, in operation, capacity improvement may be accomplished by the use of insulation to allow the battery temperature to increase, although there may be some effect on battery life.

Another commonly used battery-performance indication is the relation between energy density and power, shown for the EP200AH battery (ref. 3) in fig. 17.

The battery cycle life depends on a number of factors. If the battery has been operated and maintained properly, the cycle life becomes a function of environmental temperatures and depths of discharge (ref. 3), as shown in fig. 18. The recommendation is made, therefore, to limit the environmental temperature to 38°C, and the depth-of-discharge to 80 percent during normal operation.

The effect of the battery cycle life on the total range available over the life of the battery pack is examined in fig. 19 for the 25°C ambient temperature case (ref. 3). The curve shows maximum utilization of battery stored energy is achieved by regular cycling to a maximum of 50-percent depth of discharge.

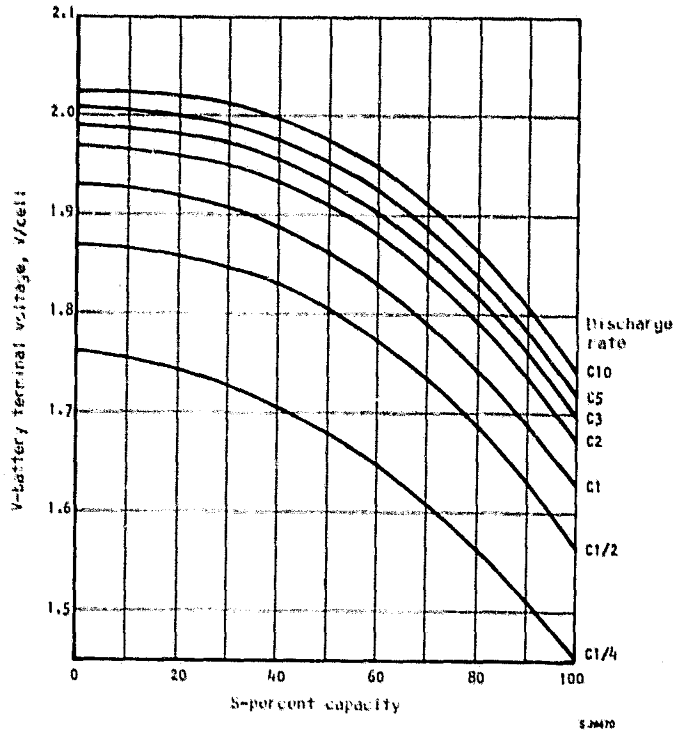

Figure 14.--Typical lead-acid battery current discharge characteristics.

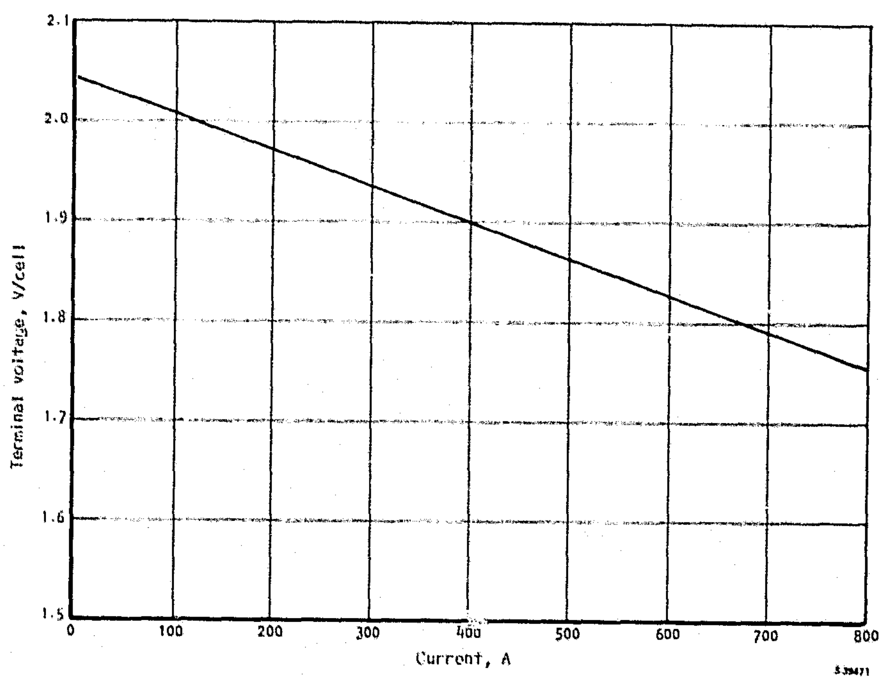

Figure 15.--Typical lead-acid battery volt-ampere characteristics at zero depth of discharge.

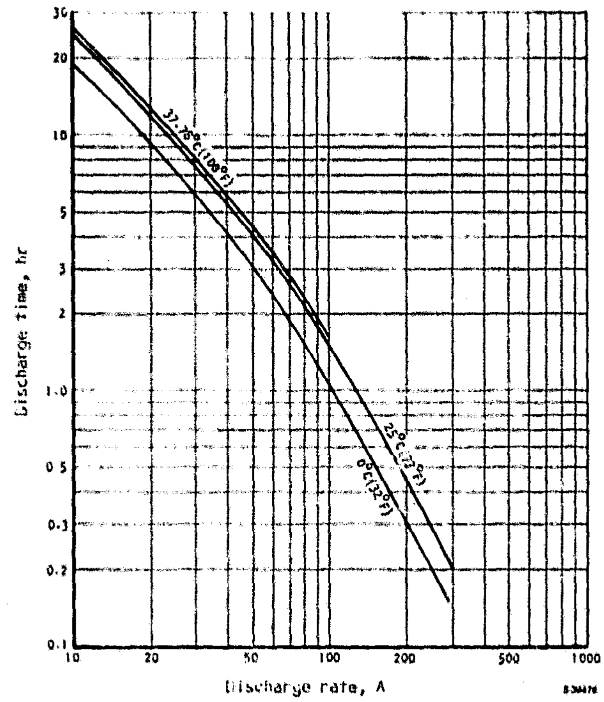

Figure 16.--EP200AH battery discharge time vs discharge rate at various environmental temperatures.

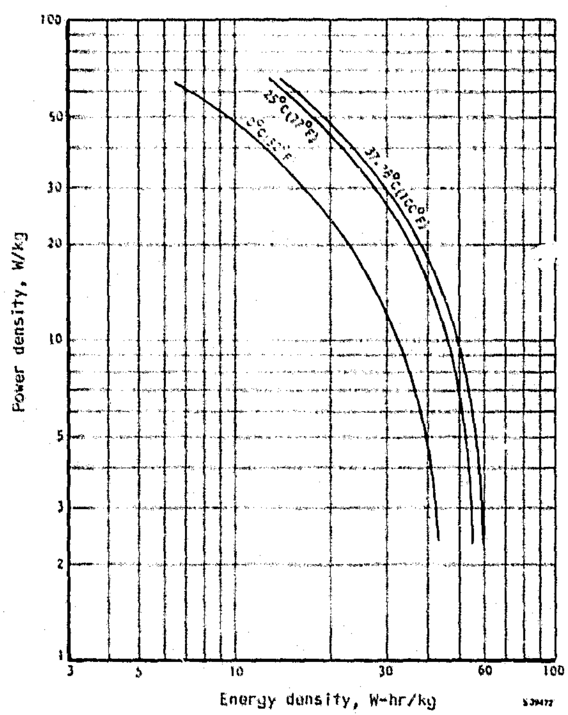

Figure 17.--EP200AH battery energy density vs power density at various environmental temperatures.

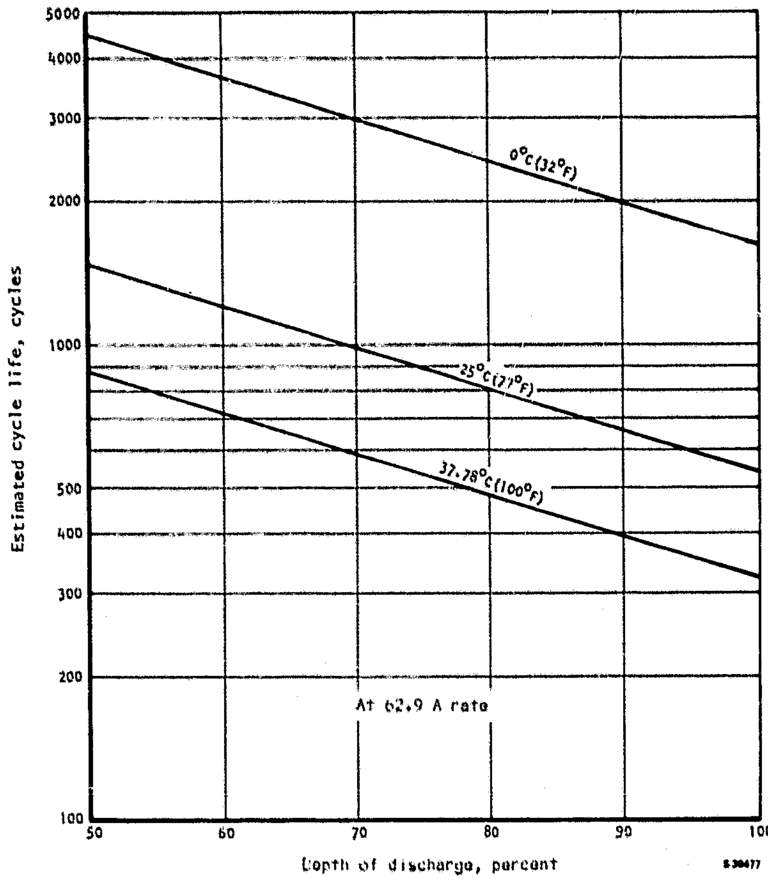

Figure 18.--Estimated cycle life vs depth of discharge for EP200AH battery at various environmental temperatures.

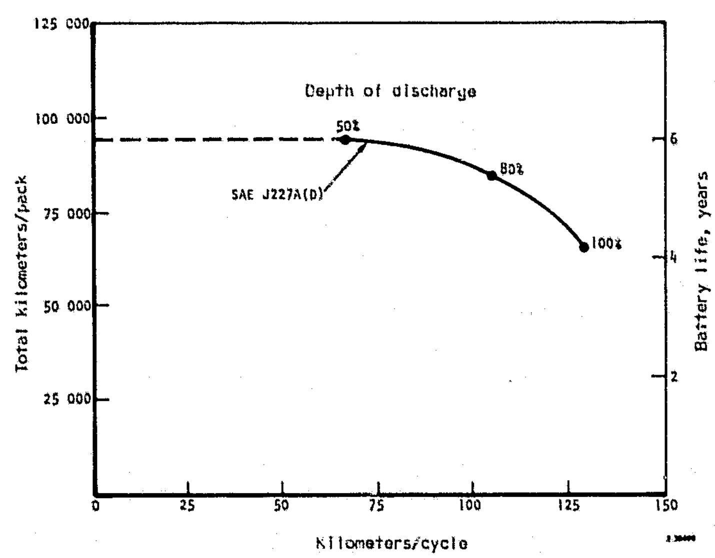

Figure 19.--Total battery pack life vs nominal use per charging cycle.

Battery Model

A series of digital computer simulation programs was developed to predict both the steady-state and the dynamic performance of the EP200AH battery for use in the Near Term Electric Vehicle program. These simulation programs have been adapted for use in the propulsion system study.

Steady-state performance.--Computer Program EP200 was developed by Eagle-Picher to predict the battery cycle life and its steady-state performance, such as capacity and voltage profile. Inputs are current-discharge rates (amperes), ambient temperatures, depths of discharge, and the age of the battery in terms of the charge-discharge cycles (ref. 3).

The program predicts (1) the theoretically available capacity, which is a function of discharge rate; (2) the actual capacity, which is the available capacity modified by the cycling and temperature effects; (3) the actual voltage profile, which is a function of the discharge rate and is modified by the temperature ature effect; (4) the discharge in watt-hours, which is the actual capacity multiplied by the average voltage; and (5) the expected cycle life, which is a function of depth-of-discharge and ambient temperature. It also predicts the electrolyte-concentration profile, the thermal-neutral-voltage profile, the thermal-neutral watt-hours, and the discharge temperature rise.

The program logic sequence is shown in fig. 20 and a typical printout is shown in table 4.

Driving cycle dynamic program.--The battery program used for the propulsion system simulation, as discussed in the section on technical approach, is one developed for the Near Term Electric Vehicle (ref. 3), and evolved from the steady-state performance program developed by Eagle-Picher, and from the fractional-utilization method. When the vehicle negotiates a driving cycle, the current demanded from the battery will vary during the course of the cycle. If the cycle is divided into small time intervals, the current during each time interval may be considered as constant at the average value, and the battery depletion during the interval may be found from the steady-state performance program. The total depletion over an entire cycle may then be found by summation of the fractions of utilization for all time intervals.

With the steady-state performance program, the battery capacity and its voltage profile can be calculated for any current-discharge demand at an ambient temperature. The fraction of capacity used, in any segment of time, is the ampere-hours used during that time divided by the ampere-hour capacity at that discharge rate, as determined by the steady-state program. By tracking the fraction of capacity used and that remaining, one can determine the battery voltage on the voltage profile. The program logic sequence is shown in fig. 21.

The range of the vehicle can be evaluated by dividing the travel-distance-per-driving-cycle by the fraction of capacity used during the drive cycle to avoid the necessity of repeating the cycle run hundreds of times. This calculated range depends on the assumption that the single cycle is representative of average battery depletion over the full range of operation. This assumption is justified by the results of another program described in the following section.

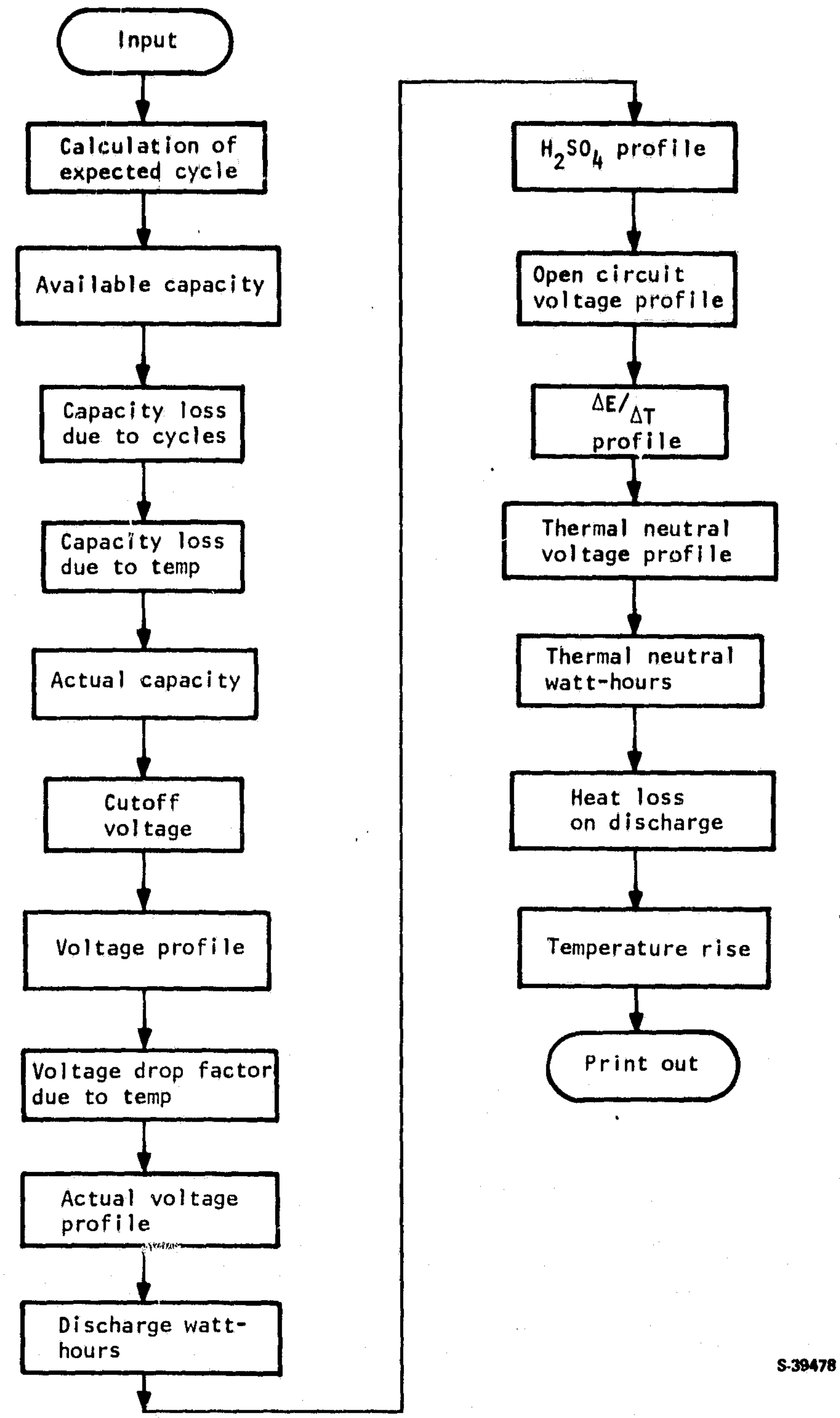

Figure 20.--Steady-state battery performance model, program logic sequence.

TABLE 4.--STEADY-STATE ANALYSIS OF EP200AH
TUBULAR LEAD-ACID BATTERY

SIMULATION OF CYCLE 200., AT 62.9 AMP RATE
BATTERY REGIME= 80.0 D.O.D. AT FAHRENHEIT 77.0

OPTIMUM CYCLES AT THIS REGIME IS 800.

AVAILABLE CAPACITY (AH)= 188.506

REDUCTION FOR CYCLES 1.000
REDUCTION FOR TEMP. 1.000

ACTUAL CAPACITY (AH)= 188.506

VOLTAGE REDUCTION (TEMP) 1.000

VOLTAGE PROFILE

PCT.DIS.	VOLT.
0.	2.030
10.	2.023
20.	2.013
30.	2.000
40.	1.982
50.	1.958
60.	1.926
70.	1.884
80.	1.827
90.	1.751
100.	1.650

DISCHARGE WATT HOURS 362.2

THERMAL NEUTRAL VOLTAGE AND PERCENT H2SO4 PROFILE

PCT.DIS.	PCT.H2SO4	VOLT.
0	42.1	2.1316
10	40.3	2.1038
20	38.5	2.0776
30	36.5	2.0532
40	34.5	2.0304
50	32.4	2.0092
60	30.2	1.9894
70	27.9	1.9709
80	25.4	1.9535
90	22.9	1.9367
100	20.2	1.9200

THERMAL NEUTRAL WATT HOURS 378.3

WATT HOURS LIBERATED ON DISCHARGE 16.1

DISCHARGE TEMPERATURE RISE 10.83 F

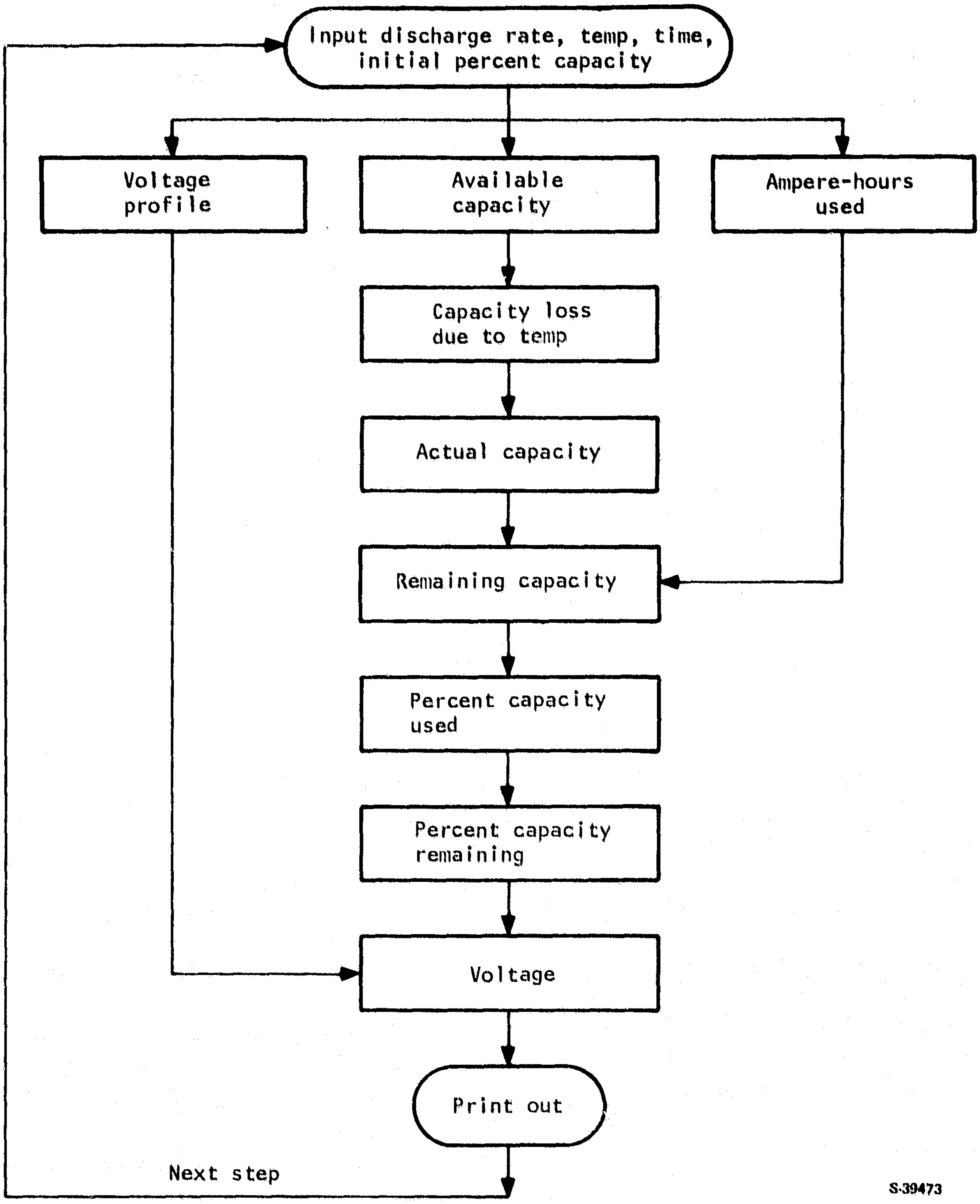

Figure 21.--Dynamic battery performance model, program logic sequence, using fractional-utilization procedure.

To utilize the driving cycle program for the advanced propulsion system study, a few modifications were required. First, the procedure used in the study is to vary the size of the battery pack to achieve the required range. This change in the battery pack is accomplished without a change in voltage, thus the additional capacity is added in parallel. However, the addition of capacity also results in a reduction of internal resistance. The effective internal resistance of the baseline battery pack, composed of 28 individual 6-V batteries, is 0.004 for each 6-V battery, or 0.112 total. The baseline volt-ampere characteristic is shown in fig. 22. This characteristic is used in the program, and is altered in accordance with changes in the battery pack weight above or below the baseline.

As shown, the program logic implies only battery discharge and does not have provision for charging. For those systems that charge the battery during regenerative braking, the charging current was treated simply as negative discharge. An additional factor in regeneration has been discovered during battery tests. It has been reported (ref. 4) that powerlimiting electrolyte concentration gradients are reduced, the battery also depolarizes, the ion concentration near the plates is increased, and new, more active, more optimally located sizes are formed. The net result is that regeneration can both conserve energy and increase battery effectiveness. Increases in total energy output can significantly exceed the regenerated input by as much as seven percent. To simulate this regeneration effect in the program, the calculated decrease in depth of discharge achieved during regeneration was enhanced by seven percent.

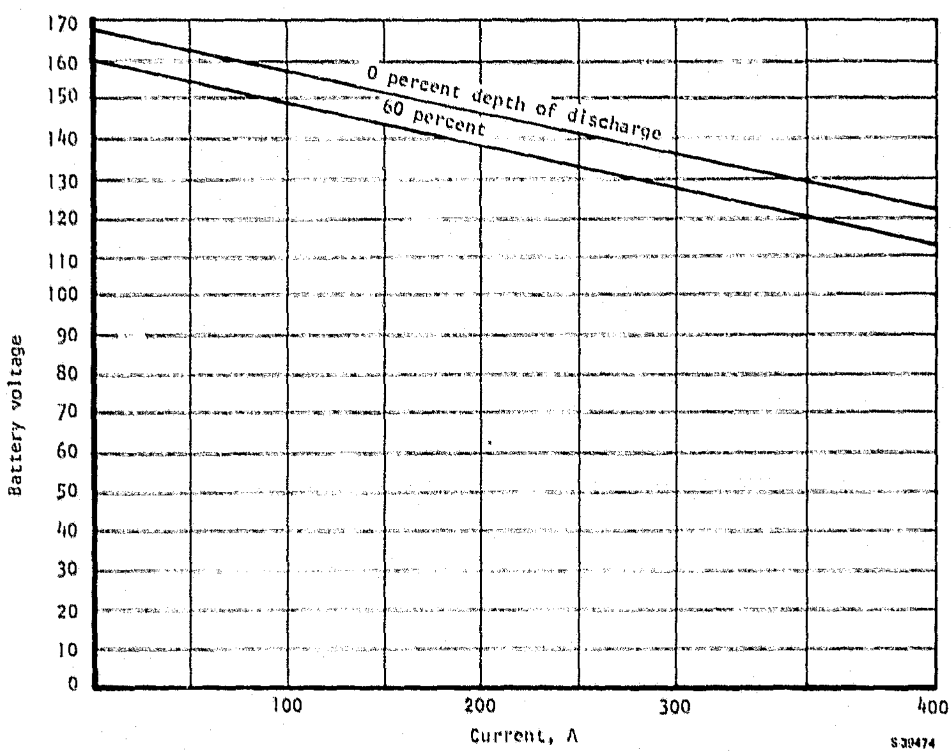

Figure 22.--Volt-ampere characteristic of battery pack.

Full mission range dynamic program.--The driving cycle program previously described makes an approximation to account for the effect on range and performance as the battery is continuously depleted. A second program, which can track battery performance over a full mission to the point of complete battery discharge, has been written, originally for use with the Near-Term Electric Vehicle.

The theory behind the fractional-utilization method previously described is that the fraction of capacity used in any segment of time is the energy used during that segment of time divided by the energy capacity at that power level or discharge rate. The drawback of this method is that it does not account for the variation in the energy capacity if the remaining portion is used at a different rate. As the battery load varies, the percent of capacity used can no longer reflect its true remaining capacity. For example, if a subsequent discharge rate is lower than that of the previous rate, the remaining capacity should be considered greater than that which would remain if the battery were subjected to the same discharge rate used previously, and vice versa. The fractional-utilization method also does not take into account the "recuperation effect" of the battery during periods of inactivity.

An approach aimed at correcting the deficiencies of the fractional-utilization method also employs the steady-state performance program. As with the previous program, the actual battery capacity and its voltage profile are calculated for any current-discharge demand and for any ambient temperature. In contrast to the previous procedure, where the capacity used and remaining is a function of the past history of the current demand only (accumulated fraction of capacity used), the battery capacity used and remaining is a function of the past history (accumulated ampere-hours used and average past discharge rate), and a function of its relationship to the present demand (rate of average discharge rate to instantaneous rate), as expressed in the following equation:

$$\text{Percent of capacity used} = Ah/Ah_t \times R_a \times Ah/AH_a \times (1 - R_a)$$

where Ah is the accumulated ampere-hour capacity used, Ah_t is the capacity based on the instantaneous discharge rate, R_a is the ratio of present discharge rate to average discharge rate or its inverse, whichever is smaller, and Ah_a is the capacity based on the past, average discharge rate. By knowing the voltage profile and the percent of capacity used, one can determine the battery voltage. When the battery voltage drops below a specified cut-off voltage, it is considered exhausted. The program logic sequence is shown in Fig. 23.

This program can be adapted to other batteries with known steady-state performances by replacing the steady-state performance program developed by Eagle-Picher with the Shepherd Equation and its associated constants. The validity of the program was shown by obtaining an exceptionally good match between the results calculated with this method and laboratory simulation tests conducted by JPL. The laboratory simulation results (ref. 5) using EV106 batteries on the J227a driving cycle, schedules B, C and D, are 369, 184, and 49 cycles, while the results calculated using the computer program are 361, 184, and 52 cycles, respectively.

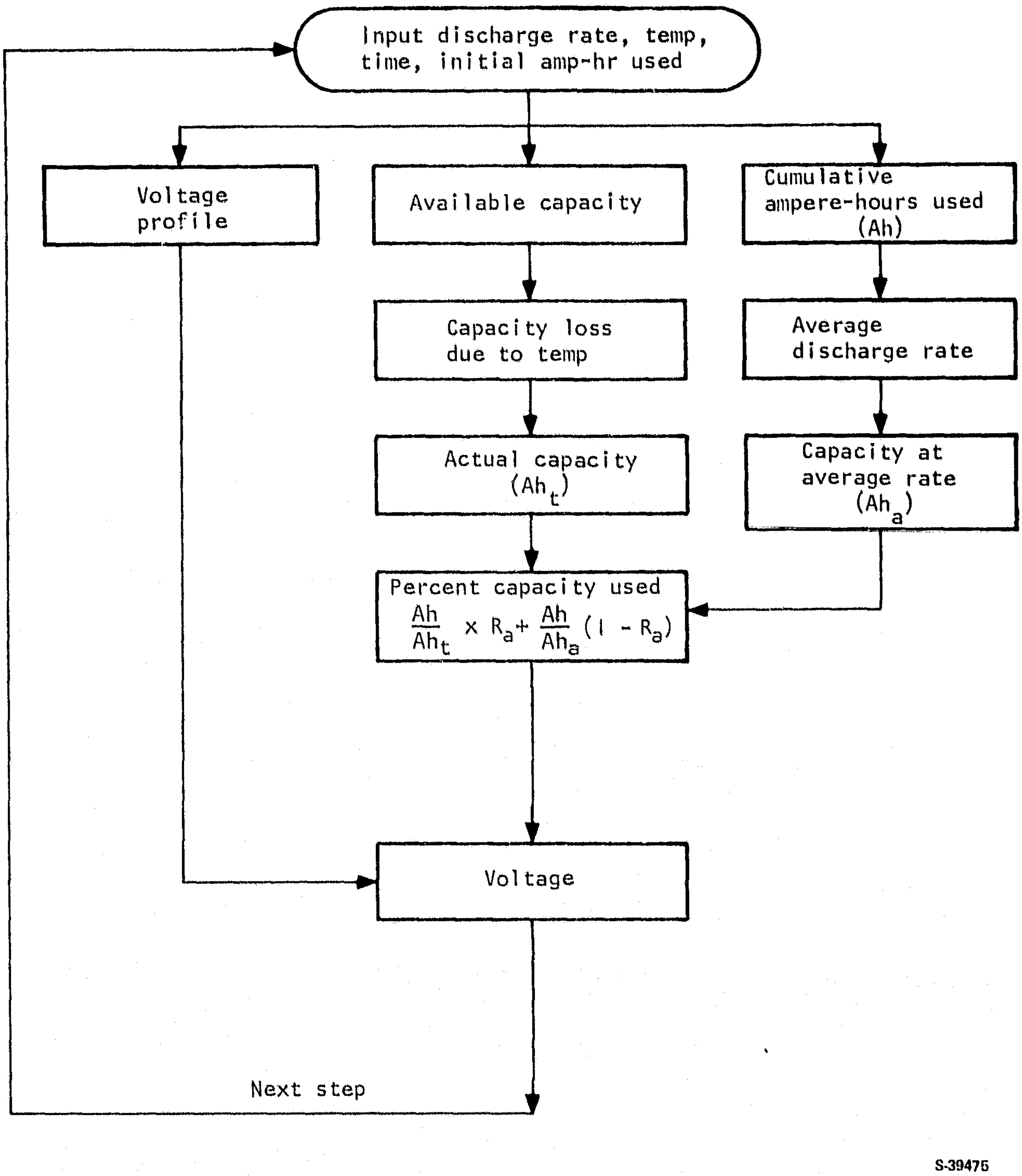

Figure 23.--Dynamic battery performance model for full mission range, program logic sequence.

Power and Energy Tradeoffs

In the previous discussion of the battery model, the ISOA characteristics were given in terms of both specific power and specific energy. The Eagle-Picher battery was selected as a model because it had been designed to meet the specific energy goals of 40 W-hr/kg. Although the performance was optimized to meet specific energy goals, however, it is not optimum in specific power.

In a system with an energy storage unit for load-leveling, or where operation does not require high power surges, the energy density criterion is most critical. On the other hand, systems that do not have an energy storage system require moderate power surges even when the J227a (D) cycle is executed, and a tradeoff can be made between specific power and specific energy to achieve maximum range.

Alternate battery types.--In the Near Term Electric Vehicle Program, the battery developed for the basic vehicle configuration (ref. 3) is made by Globe-Union Inc. and is designated EV2-13. The published information on discharge characteristics, combined in fig. 24 indicates an advantage of the EV2-13 over the EP200AH for operation in excess of 100 A. There is an apparent penalty in battery life, as shown in fig. 25, since the design goal (ref. 6) is 500 cycles at 70 percent depth of discharge for the EV2-13, which is lower than the predicted value for the EP200AH. The ISOA goal is 800 cycles at 80 percent depth of discharge.

The operating simulation with the EV2-13 battery can be made by use of the full mission range dynamic program previously described. This program requires characterization of the battery in terms of the constants of the Shepherd Equation (ref. 7).

Power limits.--The volt-ampere characteristics, such as shown in fig. 22, carry a definite implication as to the power limitation of the battery pack. The instantaneous power output, P, is found:

$$P = VI$$

where

V = Battery voltage
I = Discharge current

The voltage-current relationship has the form:

$$V = V_o - IR$$

where

V_o = No-load terminal voltage
R = Internal resistance of battery pack

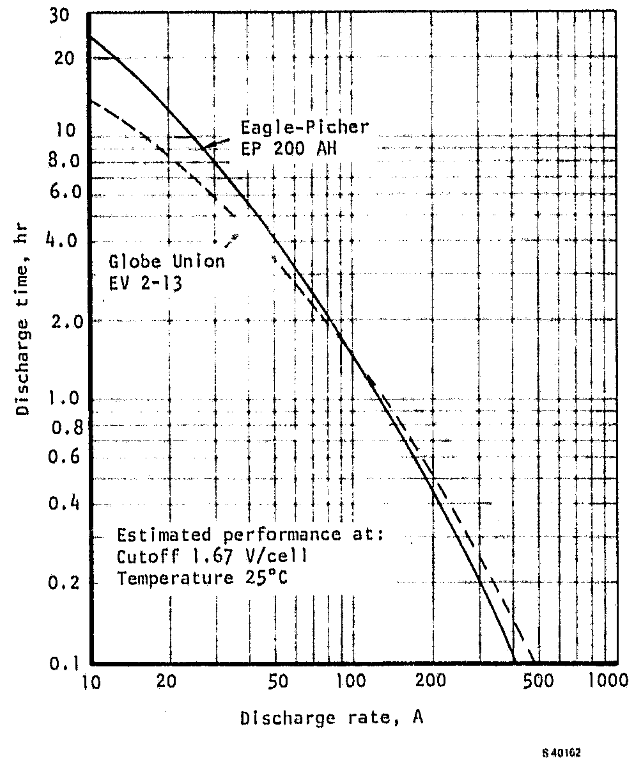

Figure 24.--Discharge time vs discharge rate for lead-acid batteries (at 25°C).

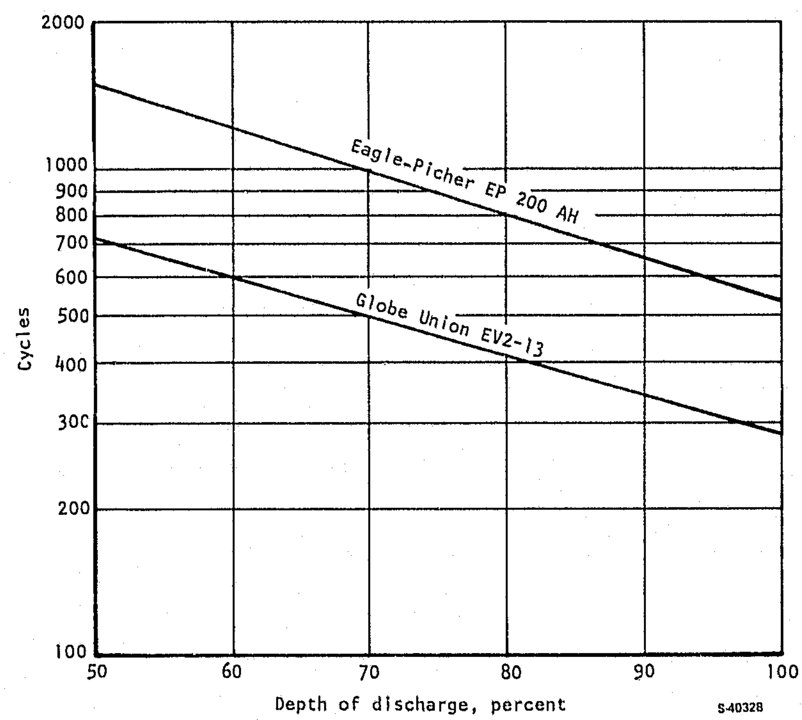

Figure 25.--Cycle life vs depth of discharge for lead-acid batteries.

The power equation may then be written

$$P = (V_o - IR)\ I = V_oI - I^2 R$$

It is apparent that the power is zero when the current is zero and also when the voltage is zero. Therefore, there is a maximum point that may be found by differentiating and setting the result to zero, thus:

$$\frac{dP}{dI} = V_o - 2IR = 0$$

$$I_{max} = V_o/2R$$

Using the values for the Eagle-Picher EP200AH battery, with 28 units:

$$V_o = 168\ V$$
$$R = 0.112$$

Then the operating conditions at maximum power are:

$$I = 168/(2)(0.112) = 750\ A$$
$$V = 168 - (750)(0.112) = 84\ V$$
$$P = (168)\ (750) - (750)^2(0.112) = 63\ 000\ W$$

The specific power for this battery pack of 733.5 kg is thus:

$$\text{Specific power} = 63\ 000/733.5 = 85.9\ W/kg$$

If the battery pack met the ISOA goal of 100 W/kg, the power would be:

$$P = (733.5)(100) = 73\ 350\ W$$

This battery power would be available to meet the maximum power requirement for acceleration when the battery is fully charged. As the battery is depleted, the maximum power capability is also eroded, because the voltage level drops as shown in fig. 22. Therefore, propulsion systems that do not have an energy storage system for peak power usage cannot maintain full performance capability throughout a complete vehicle mission, even though the range requirement can be met. This power limit also poses a considerable problem in design of the motor and controller, because these components must handle the maximum power at half the nominal battery voltage.

Nickel-Zinc Battery

The initial system comparisons were made with a battery pack of lead-acid batteries, while the final selected configurations were evaluated with both lead-acid and nickel-zinc batteries. The information used to make the evaluations with nickel-zinc batteries was derived in part from the statement of work, and in part from studies done for Argonne National Laboratory in 1976 (refs. 8 and 9).

Power and energy characteristics.--The stipulated characteristics of the nickel-zinc battery are presented in table 5.

TABLE 5.--CHARACTERISTICS OF NICKEL-ZINC BATTERY

Specific energy (at a 3-hr discharge rate and an 8-hr charge rate, 27°C)	80 W-hr/kg
Specific power (peak power average for a period of 15 s)	150 W/kg

Supplementary information was provided that defines the relationship between specific energy and specific power, as shown in fig. 26. Cycle life,as shown in fig. 27, is based on the stipulated goal of 500 cycles at 80 percent depth of discharge.

No contemporary reports were found that substantiate these battery characteristics for existing batteries. Therefore, the characteristics are regarded as design goals that could be achieved within the development period.

Battery performance.--The simulation of performance was made with the use of the full mission range dynamic program previously described, which requires characterization of tho battery in terms of the constants of the Shepherd Equation (ref. 7). These constants were derived from the nickel-zinc battery design that was described in ref. 9.

The battery design was a unit of four cells, each of 1.6 V, which gives a nominal battery voltage of 6.4 V. Capacity is 310 AH at 25°C, and energy density is 75 W-hr/kg. Projected performance is shown in figs. 28 and 29.

System Applications

When a battery is integrated into a propulsion system, consideration must be given to a number of performance characteristics that cannot be derived from the constant discharge curves. One area of concern is the effect on the battery of large current surges of short duration, whether in discharge or charge.

Chopper controls.--Choppers comprise one widely used technique for motor speed control in electric vehicles. There is comparatively little data available on battery response to the pulse discharges presented by these choppers in contrast with alternative constant current discharge.

It has been suggested that discharging a battery in successive pulses can yield a greater total of delivered energy from the battery than discharge at an equivalent average constant current. The basis for this increased capacity was thought to be that various recovery phenomena would operate during the off time between current pulses (see fig. 30), and battery capacity would

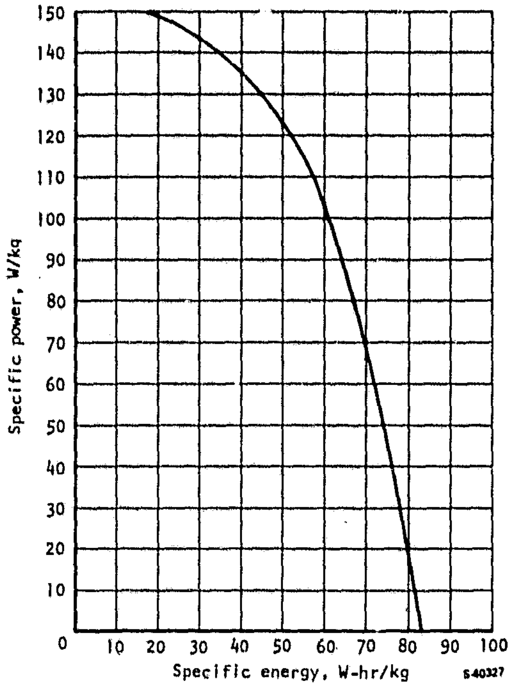

Figure 26.--Power and energy characteristics of nickel-zinc battery.

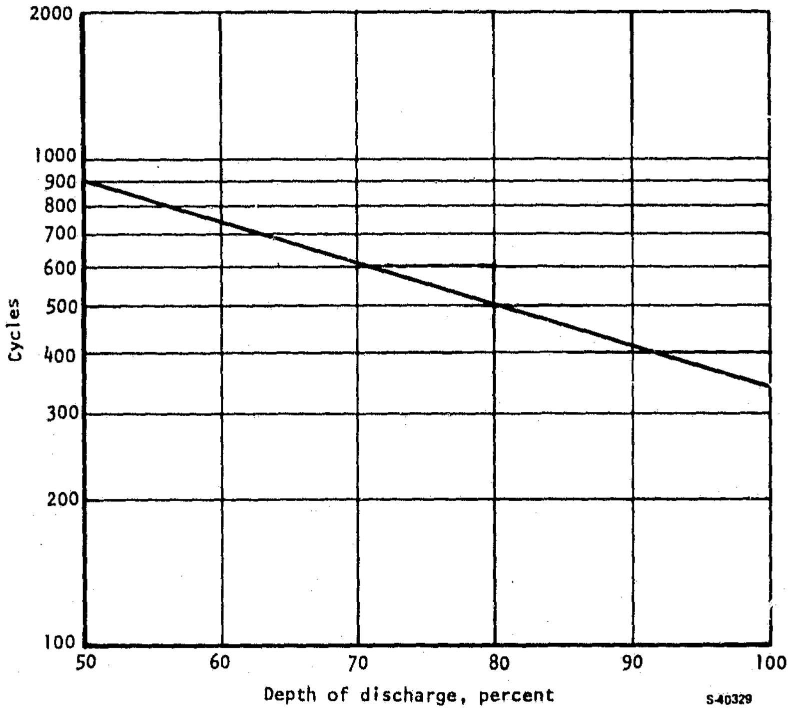

Figure 27.--Estimated cycle life vs depth of discharge for nickel-zinc battery.

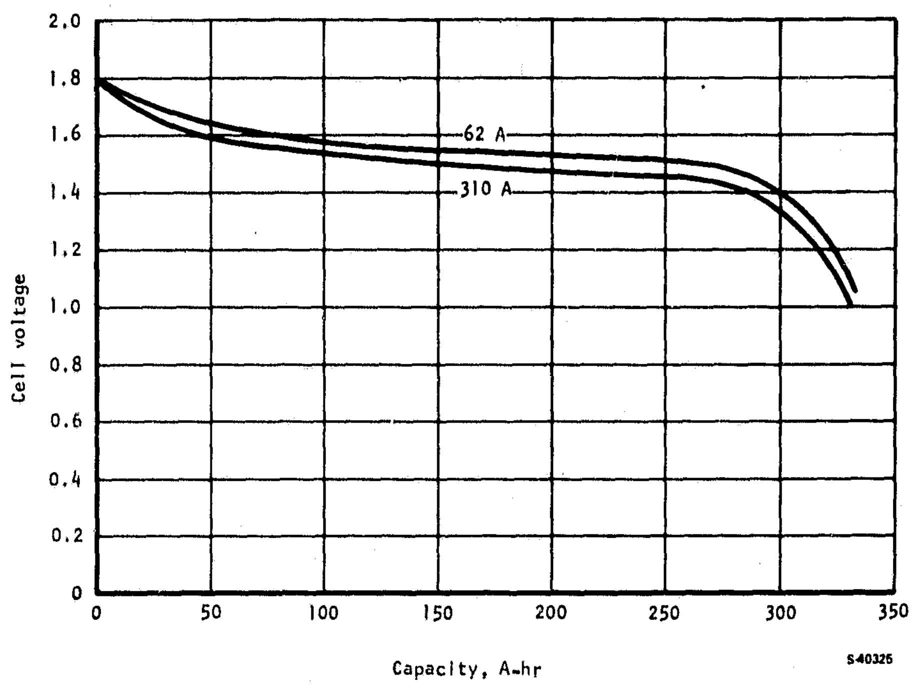

Figure 28.--Estimated performance of nickel-zinc cell.

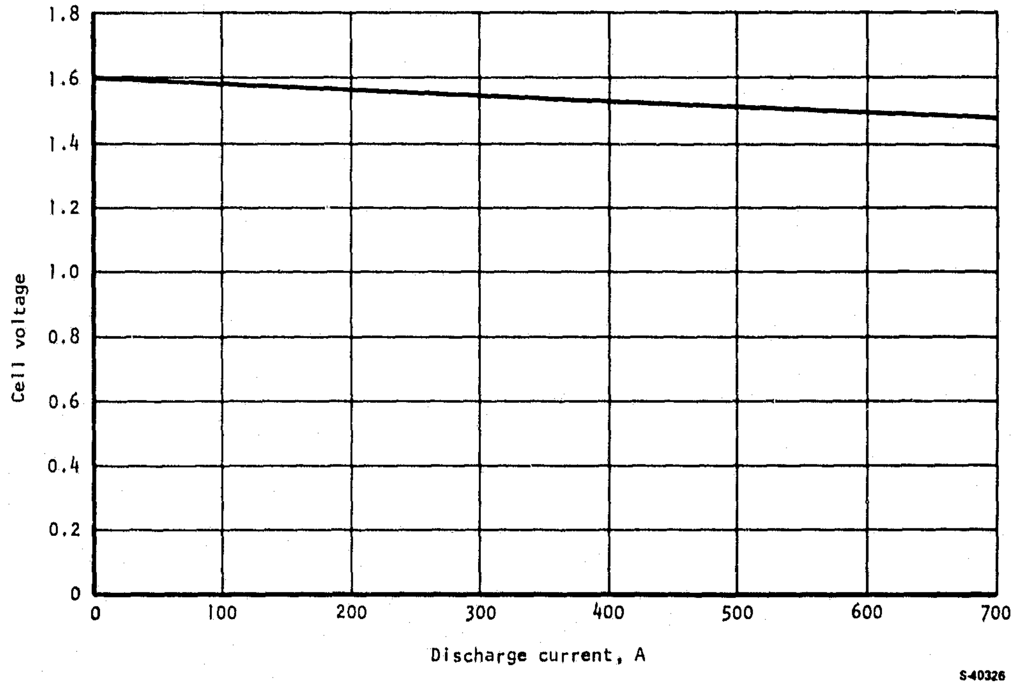

Figure 29.--Nominal volt-ampere characteristics of nickel-zinc cell.

be enhanced. Recent tests (ref. 10) have failed to discover any enhancement effect, however, and in fact pulsed discharge may result in considerable energy losses over what is experienced in constant current discharge. It appears that the losses may depend heavily on the frequency and duration of the pulses.

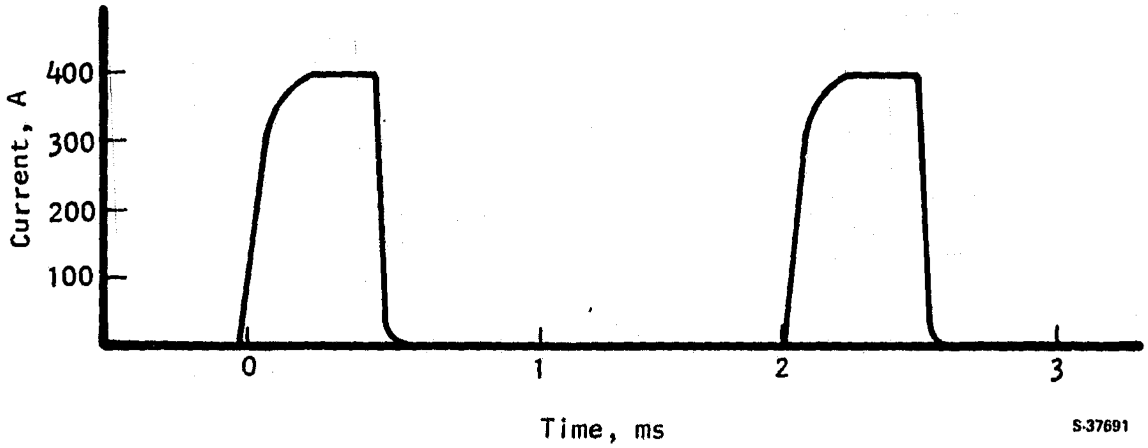

Figure 30.--Typical oscilloscope trace of chopper discharge pulses at 400-amp peak current, 100-amp average current, and 500-Hz frequency.

Subjecting a battery to high power pulses will affect the concentration gradient as well as the size and distribution of crystals on the plates (ref. 4). Although the concentration of ions in the bulk of the electrolyte is determined by the average power rate, the gradient near the plates is very dependent on instantaneous power. High power peaks will tend to deplete the electrolyte within the pores, suppress the voltage, and lead to earlier cutoff.

Regenerative braking.--During regenerative braking, energy that would otherwise be dissipated as heat is returned to the battery. This returned energy can condition the battery so that the total energy output can exceed the regenerated input; however, there are definite limits to the rate at which regeneration can take place. Battery tests have shown that the maximum charging current that a battery can tolerate without damage depends on the temperature of the electrolyte and the state of discharge.

In one reported example (ref. 3), a golf cart battery that was only slightly discharged was subjected to a changing current of 400 A for 9 s. The terminal voltage rose above 7.35 V in less than 0.5 s, and the battery exhibited violent gassing, which caused the electrolyte to foam up out of the cells. When the test was rerun with the battery initially discharged by 40 percent, the violent gassing did not occur, although a high terminal voltage was experienced. High terminal voltages during charging are known to limit battery life.

From a system standpoint, the limits of regenerative braking must be carefully considered to ensure that the benefits of energy management are not outweighed by a shortening of battery life. The simplest procedure appears to be the use of some current limit for regeneration, and if possible, a temperature compensation for the current limit.

POWER TRAIN CHARACTERISTICS

In the initial effort to compare 17 configurations, some with common components, component performance maps were prepared that could be used conveniently in the computer simulation. The power train performance maps were based on available information for components currently being developed, or proposed for near term development. This procedure was adopted to meet the required criterion for components that they be suitable for reduction to practice by 1983. In most cases, some extrapolation of existing data was required to meet the desired power and speed characteristics. The estimated weights for the propulsion systems are based on the weights of the principal components and do not include an allowance for structure, mounting, cabling, ducting, or instrumentation; this is considered part of the vehicle fixed weight allowance discussed previously.

Electric Motors and Controllers

The traction motor must be considered in conjunction with a controller to achieve a particular performance characteristic. In the previously described basic motor sizing, the nominal motor power is designated as 30 kw, with capability of 200-percent overload. The motor also must be capable of functioning as a generator to achieve regenerative braking. In general, the approach is to use motors operating at a speed as high as possible to achieve the required power with minimum motor size and weight.

Dc shunt motor.--Shunt-wound dc motors are particularly well-suited as traction motors where close speed control is desired. Using a separately excited field, with the field winding shunting the armature winding, the speed control is achieved by varying the relatively low power in the shunt circuit.

The dc motor with a separately excited field can provide constant horsepower from base speed to rated speed. This feature shapes the torque-speed relationship so that the torque at base speed is approximately 250 percent of the torque at rated speed. Base speed is defined as the lowest equilibrium speed reached by the motor when full armature voltage is applied and the field is fully excited. Below base speed, the torque can be held constant by decreasing the armature voltage in proportion to the speed reduction. The motor develops full power at base speed, with maximum efficiency. Above base speed, the power that can be developed remains nearly constant, using field weakening to control velocity, subject to the power constraints of commutation limit, saturation limit, and thermal limit. The motor performance map used for the dc shunt motor is shown in fig. 31, and it includes the losses associated with field control. This map represents the estimated performance for a motor with 100 percent rated continuous power of 30 kW; however, the map can be used for machines with rated power within a range of ± 10 percent.

Direct current machinery is limited by the requirement for a commutator and brush network to supply armature power. The brushes wear and require periodic maintenance, and the limitation on peripheral speed of the commutator in turn limits the amount of size reduction, with speed increase, which can be accomplished to improve power density. The estimated motor size to achieve the performance in fig. 31 is 82 kg. This size and performance is based on current high-performance motor designs.

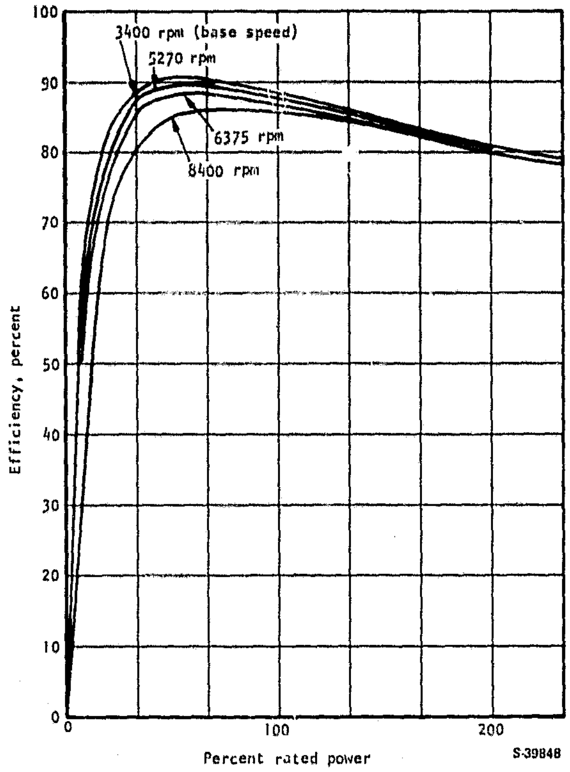

Figure 31.--Dc shunt motor performance.

It is apparent that the optimum dc shunt motor performance is achieved at base speed. When the motor is used in a system with a variable transmission, the transmission is employed to allow the motor to reach base speed as soon as possible, and to operate close to base speed over as much of the driving cycle as possible. In this case the motor starting operation can be accomplished by the simple expedient of reduced voltage applied to the armature in steps to limit current, and this regime of operation is so short, up to a vehicle speed of approximately 6 km/hr, that the efficiency of operation is not a significant concern.

For the single case, configuration 1, where the motor must be operated for a longer period below base speed, motor control is accomplished by use of a chopper. The chopper limits current by switching the circuit on and off. The effective power supplied may be controlled by varying the on-time pulse width, the repetition rate, or both. The losses, characterized as switching losses and resistance losses are modeled as

Chopper loss = (Battery current) x (1.5 V) + 0.03 (Motor power)

Ac induction machine.--Polyphase induction motors are indicated for several of the propulsion system configurations, some with constant frequency inverter controls and some with variable frequency inverters. The basic motor design is similar for either type of application, giving a 16-kg machine of approximately 30 kW continuous output rating operating at a maximum speed of close to 30 000 rpm. Estimated performance at constant frequency is shown in fig. 32, and estimated performance with variable frequency operation is shown in fig. 33.

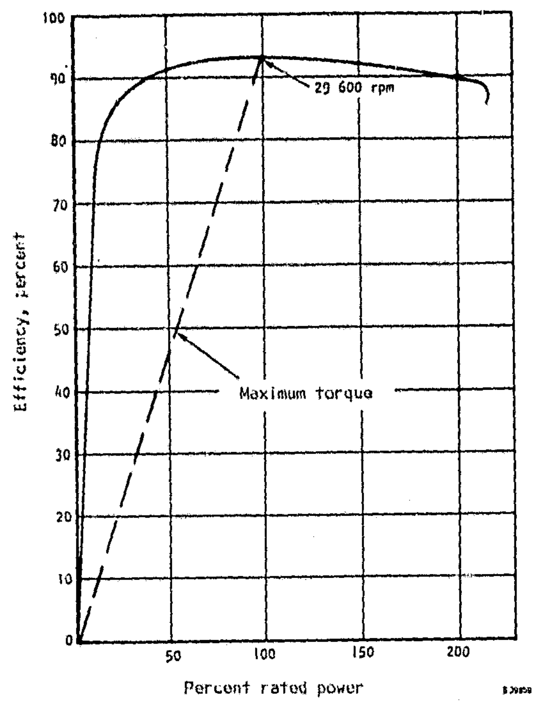

Figure 32.--Ac induction motor, constant frequency control.

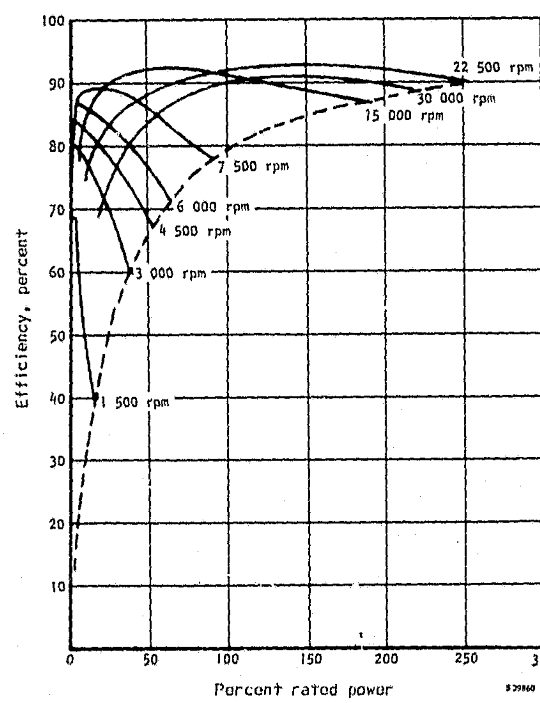

Figure 33.--Ac induction motor, variable frequency control.

The rated speed and power of an induction motor are established by the condition of maximum torque and a corresponding speed that usually represents about 14-percent slip. When loaded beyond this point, the speed will decrease and the efficiency will suffer up to about 150 percent of rated torque at the thermal limit. Stall torque is about half of the maximum torque capability at rated conditions.

The selected ac machine configurations do not have brushes, and thus are free of the commutation limit associated with dc machines. Consequently, much higher rotational speeds are possible, permitting reductions in motor size for a given power output. Constant frequency operation is characterized by a loss in efficiency at low power output, while variable frequency operation permits reduction in speed with maintenance of high efficiency at low power. This improved efficiency with variable frequency operation is secured at greater complexity and cost of the inverter.

Constant frequency inverters are established as induction motor controllers and do not require any significant advance in application technology. Cost and size, however, can be favorably reduced by advances in electronic component technology.

The variable frequency controller for the ac traction motor drive requires variable voltage, variable frequency, and controlled slip to meet the necessary output conditions. The inverter can consist of six silicon-controlled rectifiers (SCR's) plus one series transistor operated in pulse-width modulation (PWM) mode or six transistors operated in both PWM and commutation mode. The PWM is necessary to condition the input voltage down to the required volts per Hertz that constitutes adequate torque at the lowest current that is drawn.

The advantages in ac machinery and controls result from the following recent technological advances:

(1) Development of fast, high-surge current thyristors that can be made immune to high rates of di/dt and dv/dt.

(2) Development of rapid signal processing and compact logic that provides gates, time delays, counters, thresholds, memory, and combinations at rates sufficient to drive ac motors. The logic and input/output (I/O) signal capacity in one compact microprocessor or one large-scale integrated (LSI) circuit can handle the ac motor/generator plus energy management logic.

The inverter losses for the performance simulation are modeled as follows:

(1) Constant frequency inverter

Inverter loss = (Battery current) x (3.0 V) + 0.03 (Motor power)

(2) Variable frequency inverter

Inverter loss = (Battery current) x (3.0 V) + 0.035 (Motor power)

Permanent-magnet motor.--The permanent-magnet (PM) motor provides a minimum motor size and high efficiency for the required power. The following particular features of the design contribute to this performance:

(1) Field losses are eliminated.

(2) Field cooling, which can be a problem in relatively small high-speed machines, is not required.

(3) Slip rings are not required.

(4) A variable voltage field power supply is not required.

(5) The performance equivalent of field weakening can be achieved in the electronic commutator by varying the switching angle with respect to motor back emf.

The disadvantage of the PM machine is the fixed field, which tends to cause undesirable losses at high speed. The losses can be minimized by using thin laminations and low flux densities.

A permanent-magnet brushless dc motor produces a speed-torque curve that is linear as the speed is increased from stall to rated speed. The voltage applied also must vary linearly with velocity. For a traction motor application, it is necessary to have a suitable transmission so that the motor speed can be maintained within the optimum range for all driving conditions. In addition, a variable frequency inverter-type controller is used to tailor motor operation to the imposed load.

The estimated motor performance shown in fig. 34 is for a 14-kg motor of approximately 30 kW continuous rating, whose characteristics are based on a permanent magnet motor, designated an advanced dc motor, currently being developed under a NASA contract.

Differentials and Gearboxes

All the propulsion system configurations employ a differential to permit relative motion of the wheels during change in vehicle direction, and to permit a reduction in drive train shaft speed. All except five configurations also have some type of variable ratio transmission. In addition, there is a need for a fixed-ratio gearbox in several of the configurations to supplement the basic speed reduction in the differential or transmission. In practice, such a gearbox could be incorporated in the design of the differential or transmission, but to simplify the analysis procedure, it has been considered as a separate element.

Differential.--The design of differentials is well advanced due to the many years of automobile applications; however, as recent studies have emphasized, the design criteria for typical automotive components are not completely suitable for electric vehicle use (refs. 1 and 2). The use of hypoid gears in differentials is popular because it permits not only a 90-deg change in shaft direction, but an offset in the axis as well, so that the drive shaft can be lowered below

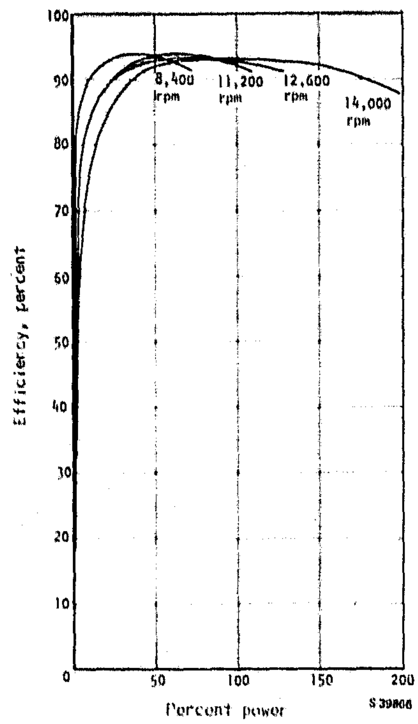

Figure 34.--Permanent-magnet motor performance.

the axle level. This arrangement is very desirable for a front engine drive to the rear wheels; however, for a close-coupled drive train mounted either in the front or the rear of a vehicle, a differential can be constructed using skew bevel gears or chain drives, which are more efficient than the typical hypoid gearing. This improved efficiency is particularly important for vehicles that use power regeneration, since hypoid gearing is very inefficient with reverse power flow (ref. 11). Also, improvements in lubrication techniques can eliminate the oil churning losses associated with the usual splash-type lubrication.

The overall differential and axle efficiency used in the Task I analysis is shown in fig. 35. This performance map is based on work done on gas turbine transmissions (ref. 12) and illustrates the effect of both power and speed on efficiency. Rated power and speed for the transmission are the maximum vehicle conditions, and it is apparent they should not be overstated if maximum operating efficiency is to be obtained. The values are considered representative of current good design practice, and can probably be improved with careful design for a specific application.

Gearbox.--Fixed-ratio gearboxes using straight spur or helical gear sets can be extremely efficient if proper care is taken to minimize bearing and lubrication losses. Maximum efficiency also depends on the reduction ratio, with 1 to 1 being the best possible. The performance map (ref. 12) presented in fig. 36 has been used as representative of all the required gearboxes, though actual operating efficiency depends on the individual power and speed ratings used in each case.

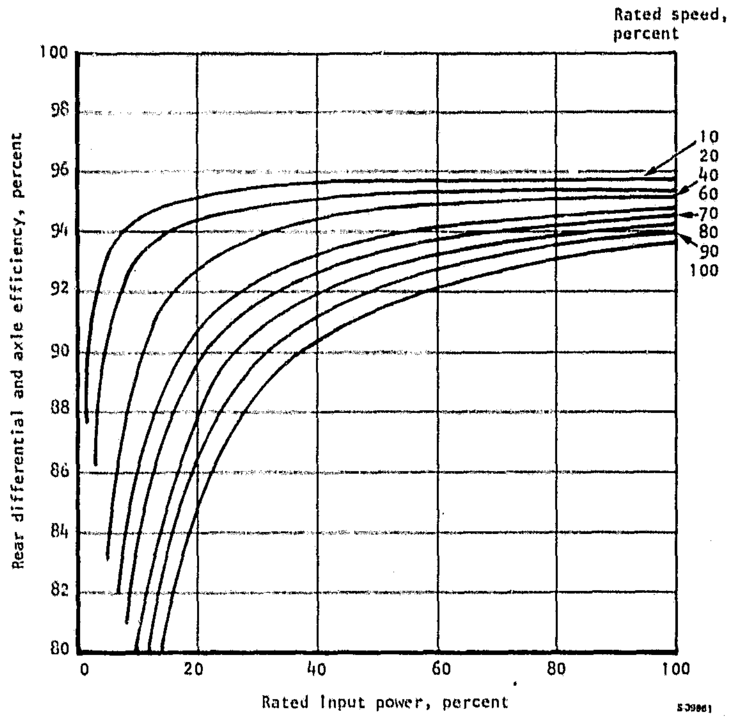

Figure 35.--Combined rear differential and axle overall efficiency.

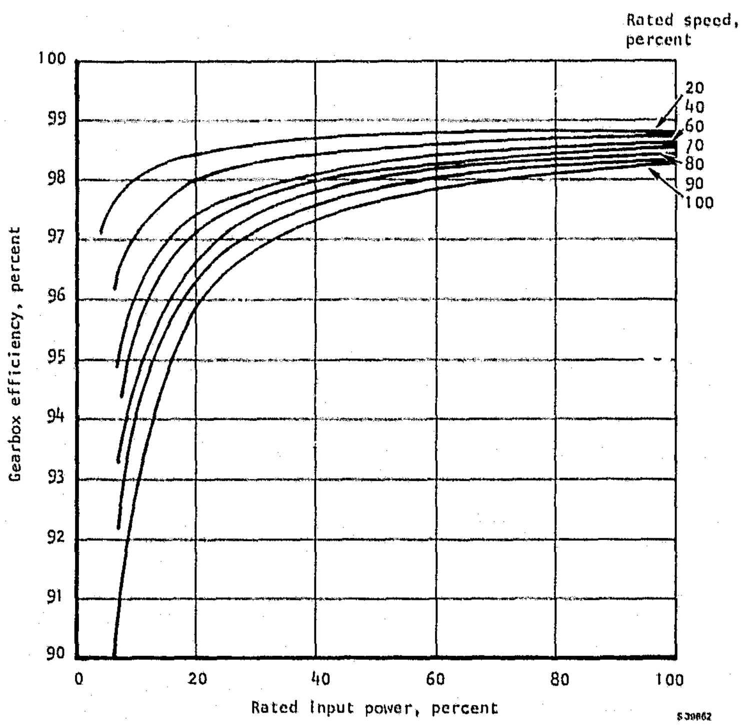

Figure 36.--Gearbox efficiency.

Transmissions

Four basic types of transmissions are considered in the various configurations:

(1) Multiple-shift mechanical gear

(2) Electric drive (generator, motor, and controls)

(3) Hydrostatic or hydromechanical power-splitting

(4) Continuously variable speed ratio (toroidal drive and belt drive)

The very low power required by the automobile at normal urban cruise speeds emphasizes the need for a highly efficient transmission. Efficiencies of a typical current automobile three-speed automatic gearbox and a typical forward and reverse gearbox are usually between 80 and 90 percent in the normal urban speed range (ref. 2). Such efficiencies can be improved by careful sizing of capacity and design of components, when tailored for electric vehicle service.

Multiratio transmissions.--Two of the configurations employ multiratio transmissions. The two transmissions are quite different as the speeds of the two traction motors are much different. The speed relations of the unit used with the dc motor are shown in fig. 37. The gear ratios are selected to allow the motor to accelerate to base speed as quickly as possible, in this case at a vehicle speed of approximately 5.4 km/hr. Subsequently, the shift points are set so the motor will not drop below base speed, and so that efficiency at 72 km/hr cruise will be good. Gearbox efficiencies are used as shown in fig. 36.

The multiratio transmission used with the ac motor has the speed relations shown in fig. 38. In this case, a rapid initial rise in speed also is desirable, and subsequent shift points are set to maintain motor speed as high as possible to achieve the best motor efficiency.

An actual transmission design would have to allow for some speed overlap in shifting up and shifting down, but these details do not significantly affect the simulation. One effect of speed change that has been considered in the simulation is the energy associated with a rapid change in motor speed. Although the motor rotor inertia is not large, the energy involved is significant.

Traction transmission.--The distinction between a continuously variable transmission (CVT) and an infinitely variable transmission (IVT) as used in this program is that the IVT can be varied down to an infinite ratio of input/output, while the CVT will have some finite limit. Thus the IVT can have full input speed with zero output. It can be made to provide smooth control from full forward speed, through zero, and into reverse, though the reverse capability sometimes adds to complexity. A CVT, such as a belt drive, may have an advantage in simplicity, with the limitation that there is some minimum transmission ratio, which in starting may require an accommodation such as motor speed control or a slipping clutch.

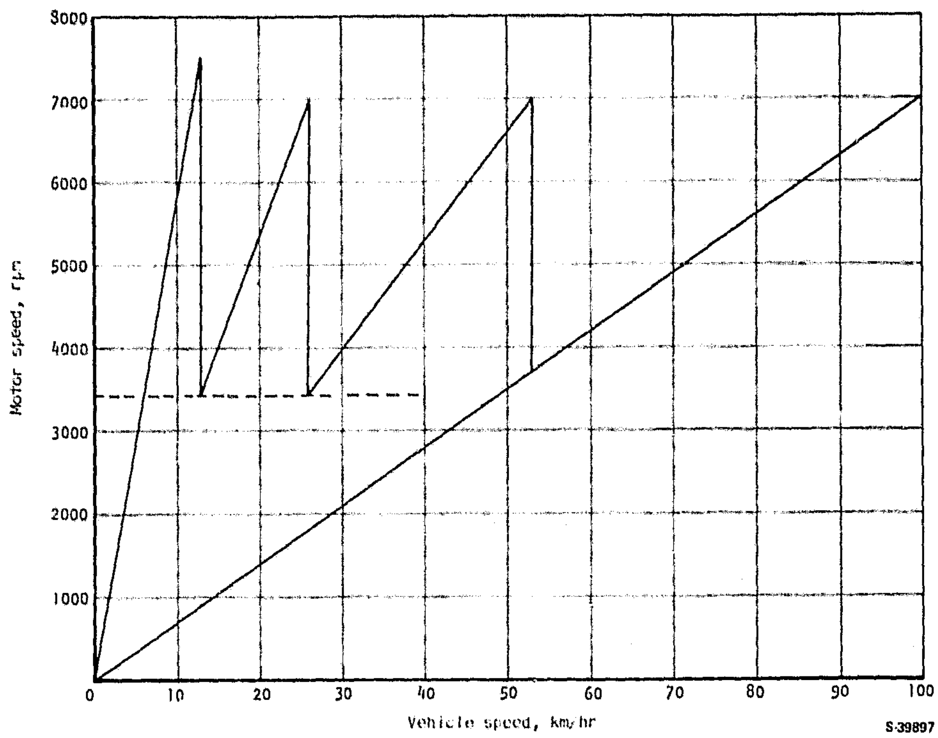

Figure 37.--Multiratio transmission, configuration 3.

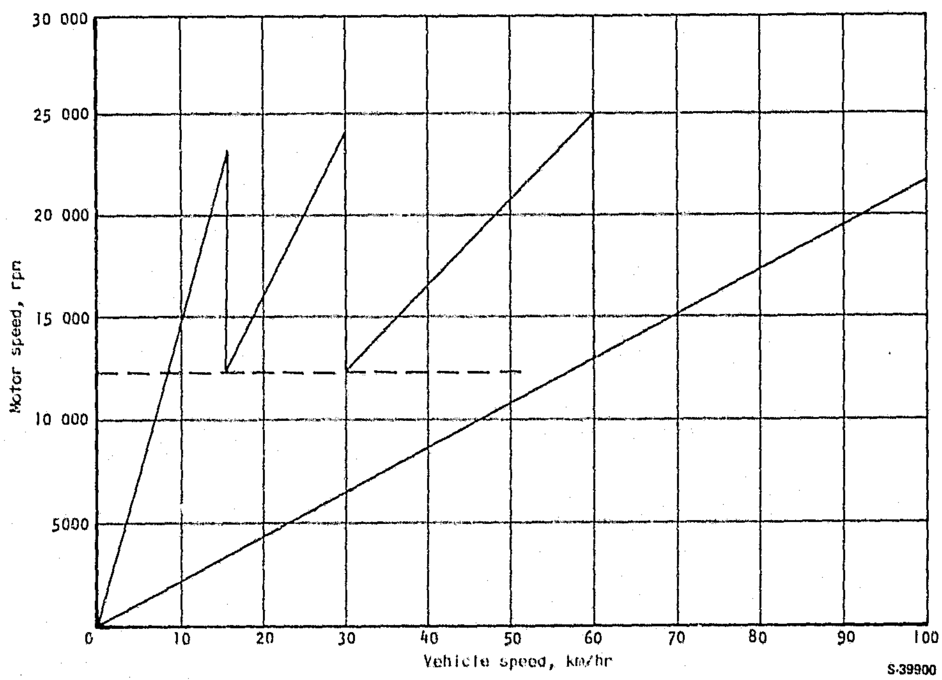

Figure 38.--Multiratio transmission, configuration 4.

A traction transmission employs some type of traction element in which power is transmitted through smooth rolling elements loaded against each other. By varying the position of the rolling elements, the speed ratio of the input and output can be smoothly and continuously varied from the minimum to the maximum value.

The transmission of power between smooth rolling surfaces requires a substantial normal force, but contact loads must be low enough to ensure an adequate fatigue life. Power transmission also is limited by the possibility of slip between the rollers, since slip leads to rapid wear failure. The method used to increase these limits involves the use of modern traction lubricants, which provide high resistance to slip and high viscosity to reduce wear. These new lubricants have considerably extended the power range of traction transmissions.

The information on proven traction transmissions is rather modest in power rating due to previous limitations in traction capacity. Now that higher powers are available, it appears entirely reasonable that automotive traction transmissions can be available by 1983. The performance map shown in fig. 39 is extrapolated from data on small-power traction units (refs. 1 and 13).

Belt transmission.--Variable speed belt drives have been used for many years in low-power applications such as industrial variable speed drives. Recent advances in belt construction have made belt drives acceptable as automobile transmissions such as for the small DAF automobile (ref. 1). The combination of

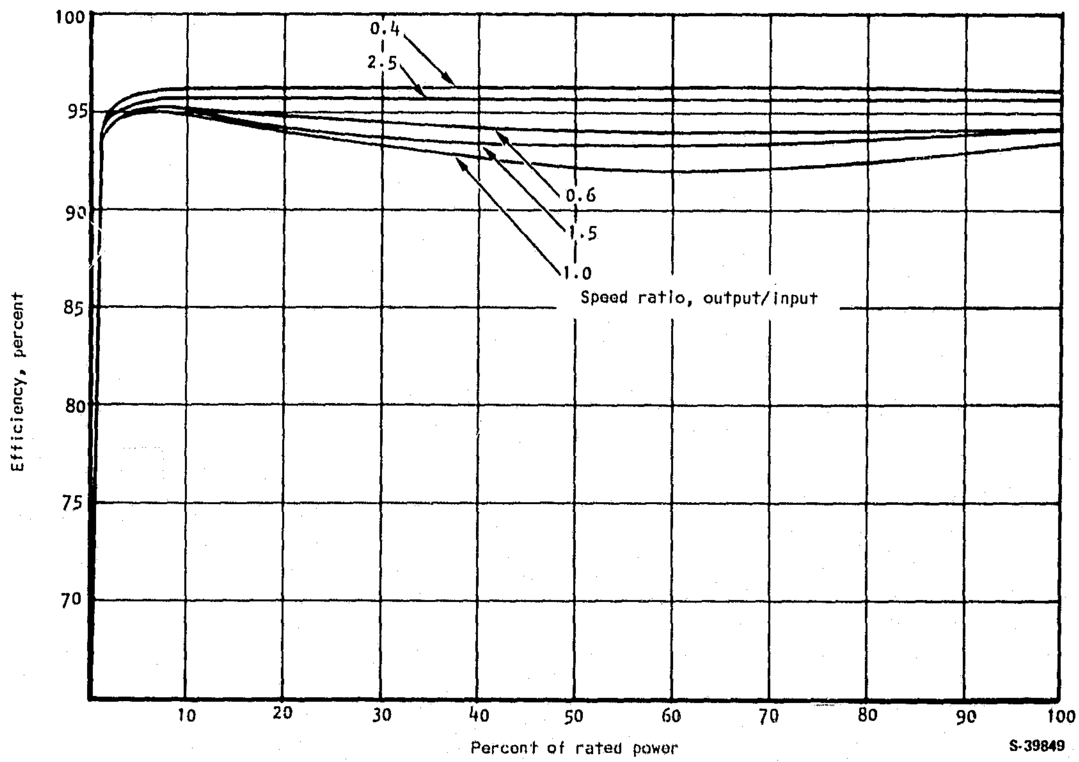

Figure 39.--Traction variable transmission.

high power level and broad change in speed ratio is still difficult to achieve, but there is sufficient evidence to suggest that a suitable unit could be developed by 1983 (ref. 14).

Variable speed belt drives are currently used on several types of small vehicles. A configuration of an electric postal vehicle being built and tested at AiResearch uses a belt drive having an overall change in ratio of 7 to 1, and the unit has been tested at overall ratio changes of 9 to 1. The estimated performance presented in fig. 40 represents an extrapolation (ref. 12) to an overall ratio change of 10 to 1. Belt efficiencies are typically very high, but low belt life at high power levels would necessitate periodic maintenance.

Hydromechanical transmission.--The hydromechanical transmission is a device that uses two power paths, a hydrostatic unit to provide variable control, and a mechanical path to achieve improved efficiency at high power levels. One such device in an advanced development stage is the Orshansky transmission, being developed by the Orshansky Transmission Corporation.

The Orshansky hydromechanical transmission (HMT) is a split-path type that transmits the majority of the power through planetary gear sets, using the hydraulic pump and motor at low vehicle speeds and to provide a smooth transition between the gear steps. Only a small fraction of the total power goes through the higher loss hydraulic components. The complexity of the HMT is partially offset by utilizing components with a long history of commercial use and service.

The performance map shown in fig. 41 is derived from published data (ref. 15) on a development model of the transmission. The preproduction prototype is rated at 75-kW capacity, 3600-rpm maximum input speed, and a weight of 78 kg.

Hydrostatic transmission.--Hydrostatic transmissions are an entire hydraulic system. A pump is connected to the prime power source to supply hydraulic flow and pressure to a hydraulic motor that is connected to the load. Speed and power control is achieved by using a variable displacement pump or a variable displacement motor, or both the pump and motor with variable displacement.

Hydrostatic drives can provide a wide variation in speed and power control smoothly and continuously. In the past, these virtues have been offset by relatively high cost, large size, and low efficiency, as compared to mechanical systems; however, improvements in pump and motor design and in the servo controls have made the hydrostatic drive a possible alternative as an automotive transmission.

The estimated performance map shown in fig. 42 is based on the use of a high efficiency pump and motor. To achieve a minimum size for the unit, maximum system pressure should be as high as 35 MPa (ref. 16). The performance shown assumes some improvement over current levels, although the levels should be achievable by 1983.

Energy Storage Device

The energy storage device used on several of the configurations is a flywheel. Recent studies (ref. 17) indicate the advantages of flywheels over

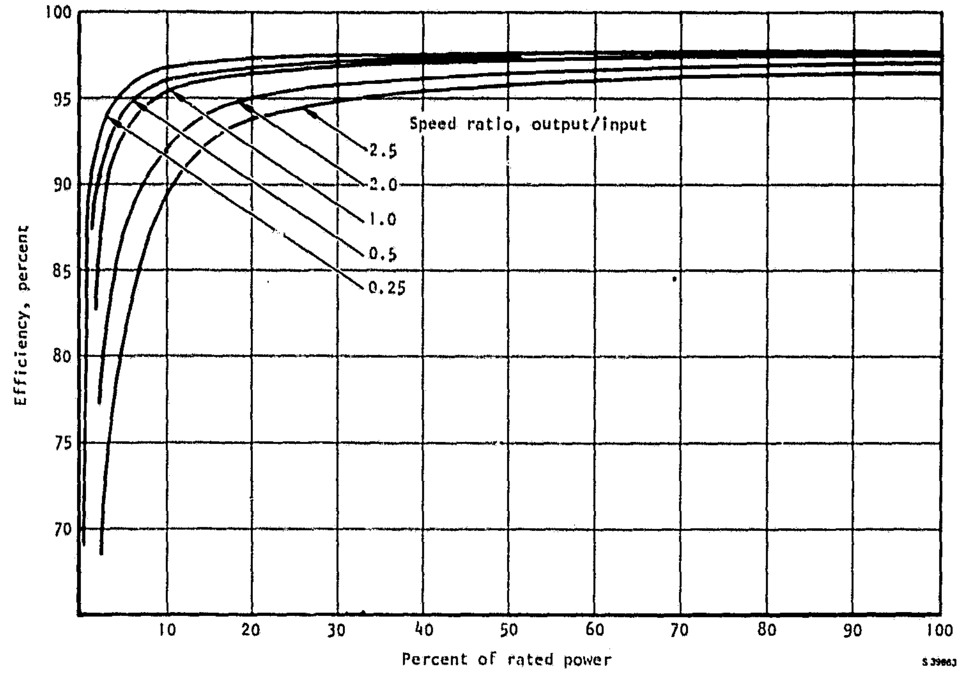

Figure 40.--Variable belt transmission.

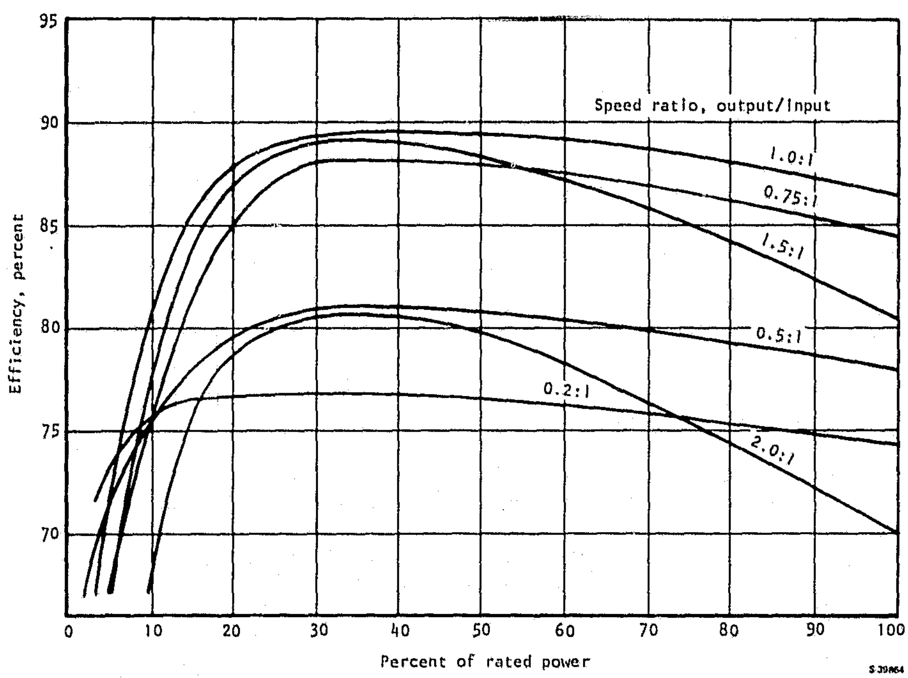

Figure 41.--Hydromechanical transmission.

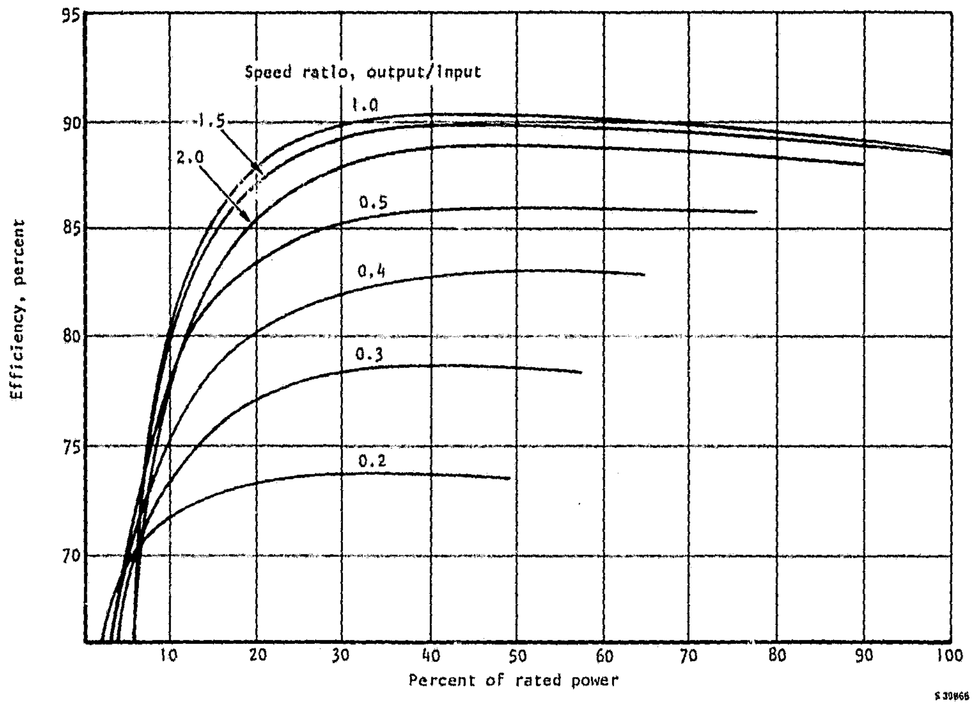

Figure 42.--Hydrostatic transmission.

alternative devices, such as hydraulic or pneumatic systems, and flywheels are currently being used in various automotive applications. Since the energy storage device is required only for maximum acceleration conditions and not for long grade situations, the required energy storage is not large. Based on units already being built, the energy storage capability was selected as 250 W-hr at full speed, as discussed in the section "Performance Parameters."

Energy storage.--The energy stored in a flywheel may be expressed by the relationship:

$$E = 1/2 \; I \omega^2$$

Where E is the kinetic energy of the flywheel, I is the moment of inertia of the flywheel about the axis of rotation, and ω is the angular rate of rotation. With a speed range from full speed to half speed, 75 percent of the flywheel energy can thus be used to accelerate the vehicle.

A useful index of the energy that can be stored in a flywheel is the specific energy, defined as:

$$\text{Specific Energy} = \frac{\text{kinetic energy}}{\text{weight}}$$

There is a relationship between these terms and the flywheel geometry and material, expressed as follows:

$$\frac{\text{Kinetic energy}}{\text{Weight}} = K_S \; (\sigma/\delta)$$

where: K_S = nondimensional shape factor

σ = allowable working stress

δ = weight density

For flywheels fabricated from isotropic materials such as steel, a variety of shapes are possible; some common forms are shown in fig. 43. Filament composite materials, which can sustain stress only in one direction, are limited to certain methods of utilization (ref. 18), and some current design configurations shown in fig. 44. The composite flywheels have a relatively low shape factor (K_S); however, the high strength-to-weight ratio of composite materials more than compensates for their shape factor and provides a much higher specific energy and low cost, as shown in fig. 45. Therefore, the selected flywheel configuration is a composite type.

The characteristics presented in fig. 45 do not represent specific designs, but are considered typical based on a number of units that have been built and operated (refs. 19 and 20). The relatively high containment weight for the steel flywheel is necessary because of the worst-case failure mode where relatively large pieces of material having appreciable energy must be contained. In contrast, the failure of a composite flywheel results in a mass of material in the form of fluff, which dissipates energy in internal friction. The cost numbers are based on material costs projected for 100,000 units. Costs include estimates of fabrication and assembly costs.

Operating losses.--To reduce frictional drag, the flywheel is operated within a housing maintained at a low vacuum. A vacuum pump is required, which introduces some continuous power drain attributable to the flywheel. Some power is also required to overcome bearing friction and to provide bearing lubrication. Flywheel losses were established as 300 W, which results in a loss of flywheel speed that must be made up by periodic charging.

Flywheel configuration		Typical relative shape factor, K_s
1. Flat disc (with hole)		0.30
2. Flat disc (no hole)	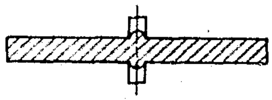	0.61
3. Modified constant stress disc (with hole)	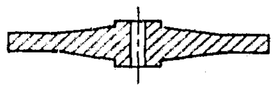	0.45
4. Modified constant stress disc (no hole)	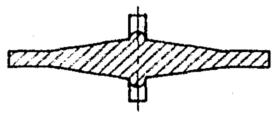	0.90
5. Rimmed disc	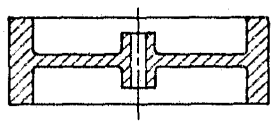	0.40
6. Constant stress disc (no hole)	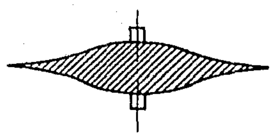	1.0 (OD $\rightarrow \infty$)

S-40158 -A

Figure 43.--Flywheel geometry comparison.

Flywheel configuration	Typical relative shape factor, K_s
1. Laminated disc with bonded hub (General Electric) 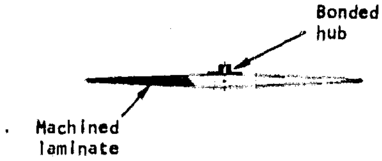	0.30
2. Circumferential core with tape overwrap (Rockwell) 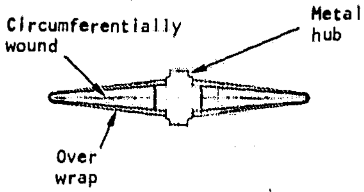	0.30
3. Filament wound rim with radial bands (Sandia) 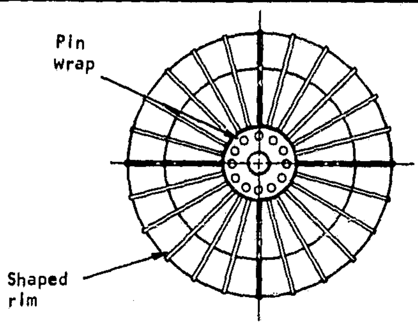	0.35
4. Concentric cylinders with composite catenary spokes (Brobeck) 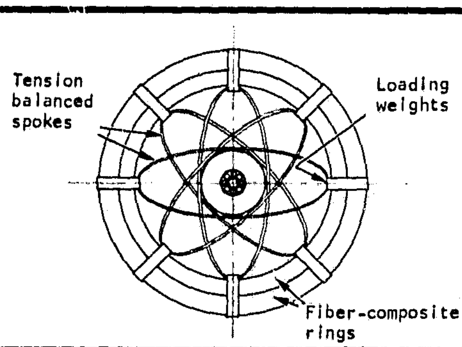	0.35
5. Concentric cylinders with solid hub (AiResearch) 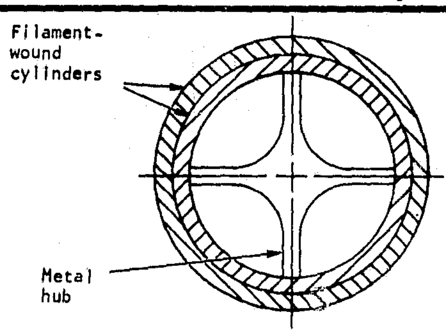	0.35

S-40188-A

Figure 44.--Composite flywheel configurations.

	Laminated rotor 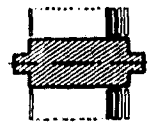	Multi-drum 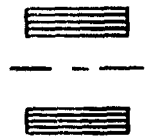	Multi-drum 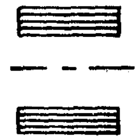
Material	Steel	E-glass epoxy	Kevlar epoxy
Rotor specific energy (W-hr/kg)	12.3	26.0	44.1
Rotor weight (relative)	1.0	0.47	0.28
Approx. housing and containment weight (relative to laminated rotor)	0.5	0.3	0.3
Flywheel assembly energy per assembly volume (W-hr/cm^3)	0.027	0.016	0.016
Flywheel assembly specific energy (W-hr/kg)	8.1	16.1	21.3
Flywheel assembly cost ($/W-hr)	0.5	0.3	0.4

S-40129-A

Figure 45.--Flywheel weight and cost comparisons.

PRELIMINARY ANALYSIS AND TRADEOFFS

An analysis was made of the 17 propulsion system configurations previously described, as well as the baseline configuration. On the basis of this initial comparison, five candidate configurations were selected for further design tradeoff evaluations in Task II, where the selection was narrowed to two configurations for the final conceptual design studies.

Preliminary Range Comparisons

Initial comparisons were based on the range that is achievable when successive SAE J227a schedule D cycles are driven. Battery weight was varied in a series of calculations to determine range as a function of battery weight, shown summarized in fig. 46. In the integration of system components, an effort was made to match the component performance to secure the best system performance; however, in a preliminary analysis, it cannot be assumed that all systems are fully optimized. Therefore, some tolerance must be applied to the final standings, and small differences in performance may not have any great significance.

The computer procedure that was used has been described previously in the section "Technical Approach." Component losses are computed and tabulated as shown in figs. 47 through 64. Battery drain is computed as described in the battery model, and is tabulated for each segment of the driving cycle. The comparisons are based on use of an ISOA lead-acid battery of 168-V nominal voltage, but with the capacity assumed to vary with battery weight. Components were sized for approximately 30-kW continuous power and 60-kW maximum power, as discussed in the preceding section.

All systems were able to achieve the specified range of 161 km using the J227a schedule D cycle, except two: configurations 9 and 10. Configuration 9 has a hydrostatic transmission, and configuration 10 has a hydromechanical transmission. Both of these systems were at a disadvantage because the best operating points of the transmissions are not optimally suited for a constant high-speed motor drive, and a large speed-reduction stage must be incorporated into the transmission input. Efficiencies at the low power associated with constant speed operation also were poor.

Individual plots and tabulations are presented for all the configurations in figs. 47 through 64. The principal system characteristics are listed for reference. The configurations of group 4, which have two electrical machines, are characterized as having an "electrical transmission." It may be noted that a number of the configurations with flywheel energy storage units achieve a greater range for a given battery weight than the basic systems, even though the energy consumption per cycle is higher. This is because the energy storage units provide load leveling, and the steady drain on the battery is less taxing than the power surges experienced by the basic systems.

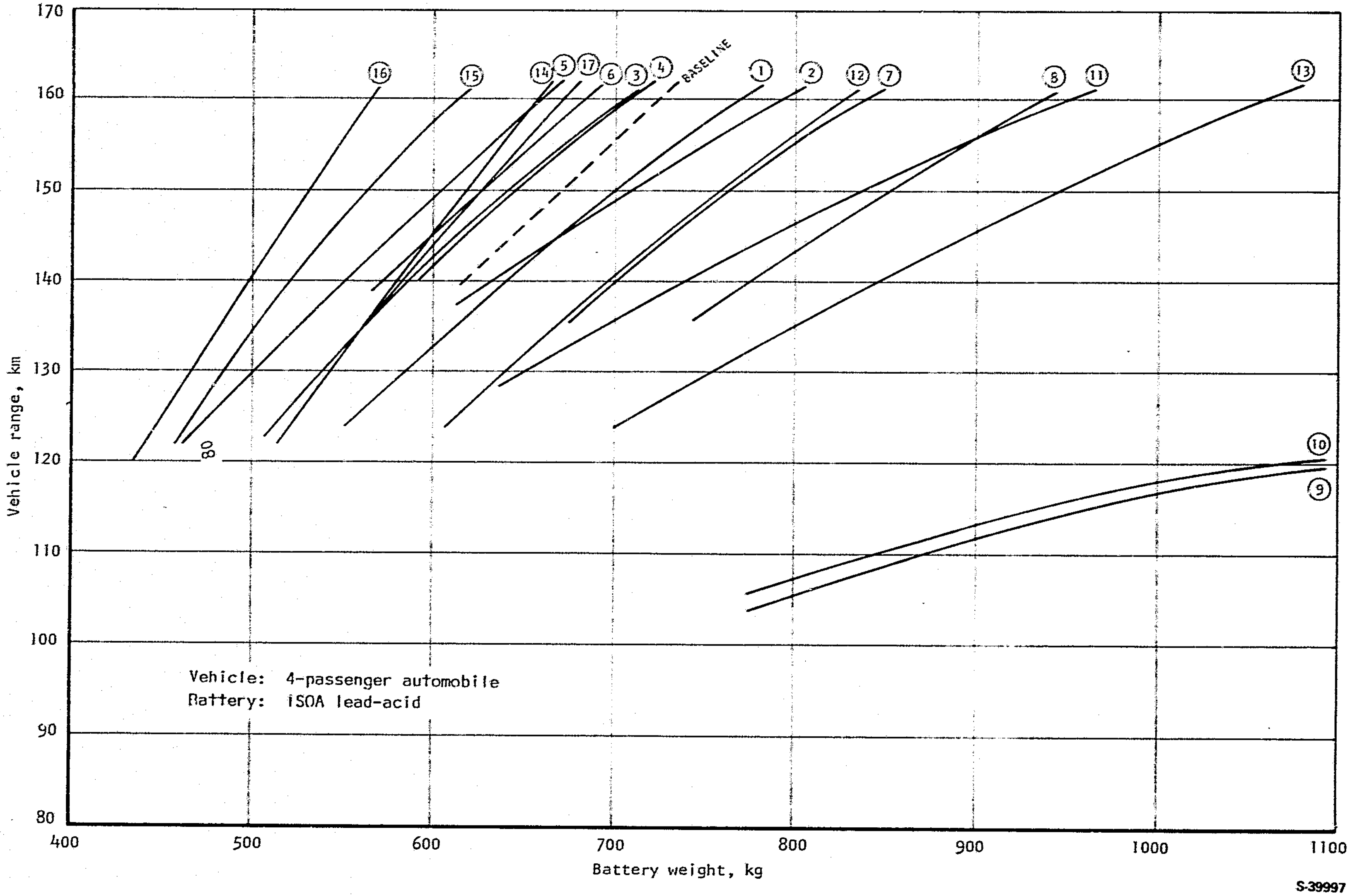

Figure 46.--Comparison of advanced propulsion systems for electric vehicles driving the SAE J227a schedule D cycle.

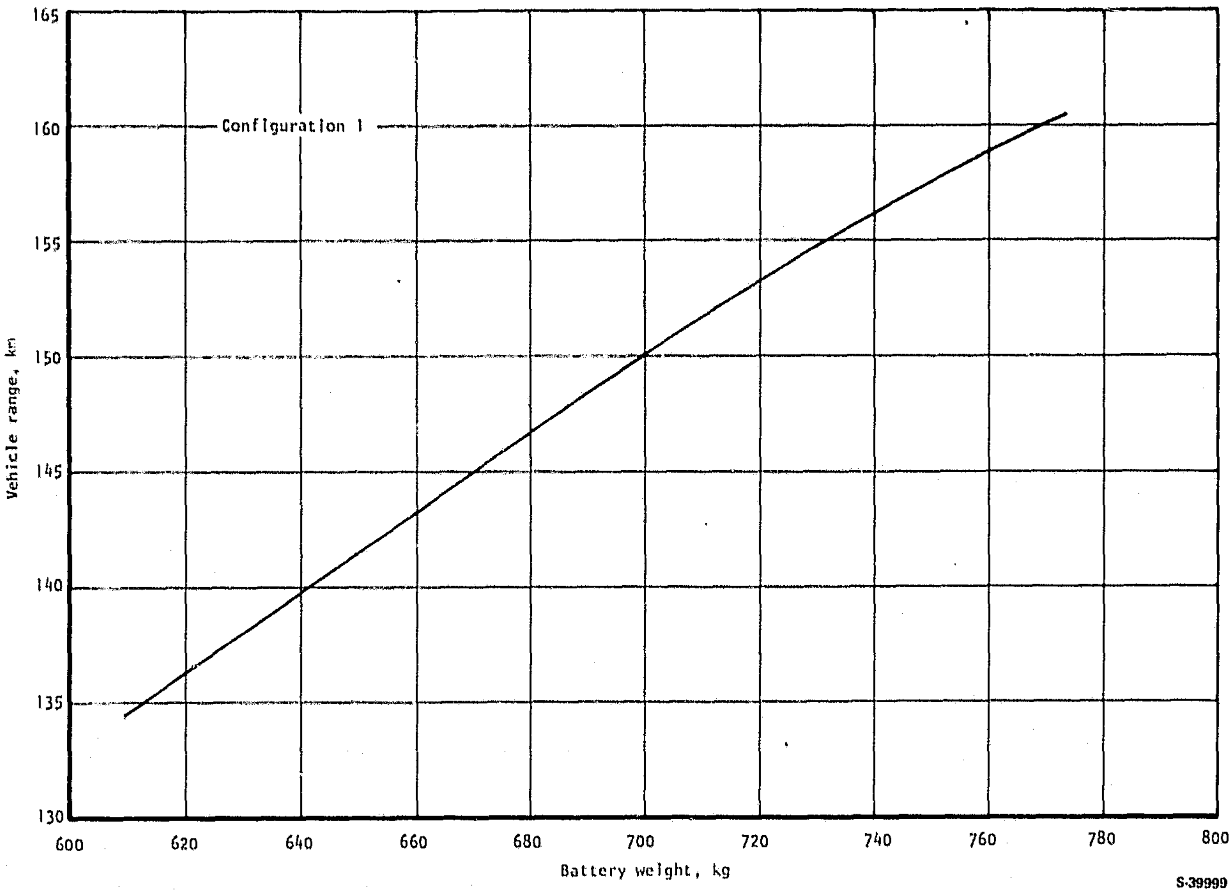

Electric vehicle simulation:

Traction motor	Dc shunt
Transmission	Gear box
Energy buffer	None
Driving cycle	J227a schedule D
Vehicle weight, kg	1805.7
Propulsion system weight, kg	124.7
Battery weight, kg	772.0
Total range, km	160.2

Summary of energy losses in driving cycle, W-hr

	Acceleration	Cruise	Coast	Brake	Dwell	Total
Road drag	24.746	83.836	14.910	4.586	.000	128.078
Differential	9.541	14.322	4.931	4.071	.000	32.865
Transmission	2.669	4.113	2.465	1.139	.000	10.386
Motor	22.603	23.967	.822	11.979	.000	59.371
Controller	1.879	.000	.000	1.240	.000	3.119
Brake	.000	.000	.000	0.391	.000	0.391
Total	61.438	126.238	23.128	23.406	.000	234.210
Battery	169.718	126.238	.000	-61.746	.000	234.210

Figure 47.--Performance of configuration 1.

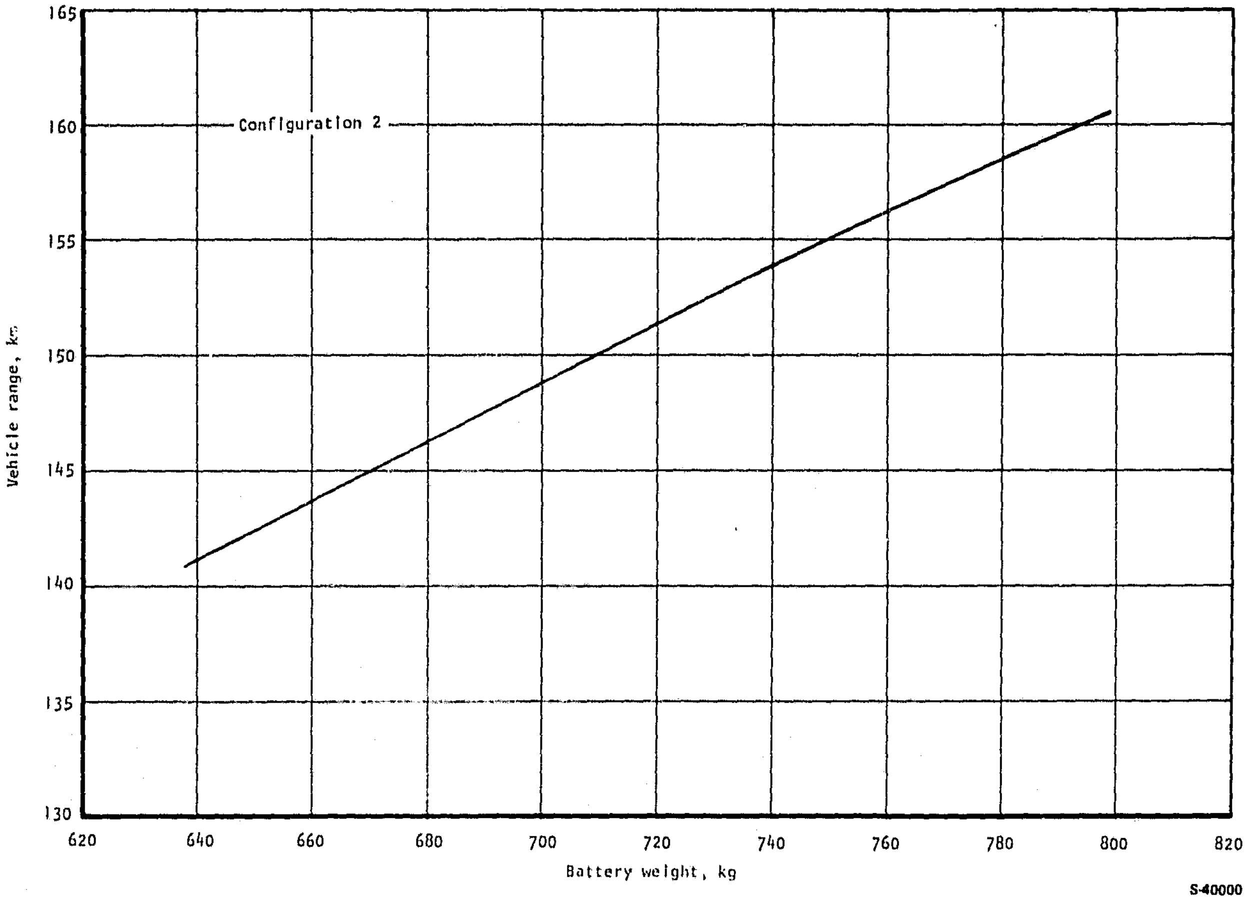

Electric vehicle simulation:

Traction motor	Ac variable frequency
Transmission	Gear box
Energy buffer	None
Driving cycle	J227a schedule D
Vehicle weight, kg	1763.6
Propulsion system weight, kg	70.8
Battery weight, kg	793.8
Total range, km	160.0

Summary of energy losses in driving cycle, W-hr

	Acceleration	Cruise	Coast	Brake	Dwell	Total
Road drag	23.259	82.788	14.789	4.552	.000	125.388
Differential	9.195	14.287	4.099	4.040	.000	31.621
Transmission	2.695	4.103	2.049	1.132	.000	9.979
Motor	19.087	18.312	0.683	12.155	.000	50.237
Controller	8.481	5.987	.000	3.216	.000	17.684
Brake	.000	.000	.000	5.809	.000	5.809
Total	62.717	125.477	21.620	30.904	.000	240.718
Battery	169.125	125.476	.000	-53.883	.000	240.718

Figure 48.--Performance of configuration 2.

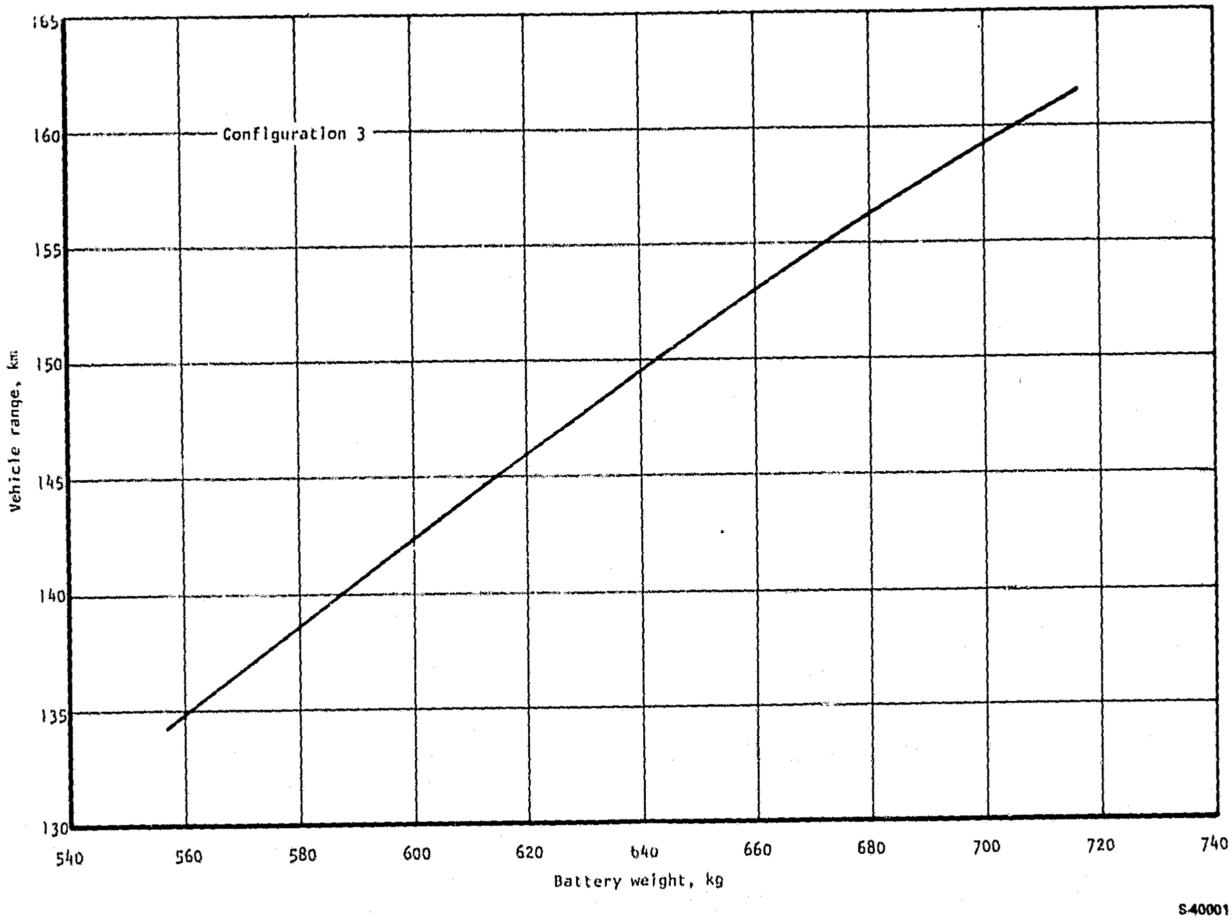

Electric vehicle simulation:

Traction motor	Dc shunt
Transmission	Multiratio 4 speed
Energy buffer	None
Driving cycle	J227a schedule D
Vehicle weight, kg	1748.6
Propulsion system weight, kg	140.6
Battery weight, kg	712.1
Total range, km	161.0

Summary of energy losses in driving cycle, W-hr

	Acceleration	Cruise	Coast	Brake	Dwell	Total
Road drag	24.235	82.404	14.513	4.409	.000	125.561
Differential	9.388	14.273	4.757	3.889	.000	32.307
Transmission	2.346	2.588	2.854	1.043	.000	8.831
Motor	17.854	21.314	1.903	11.115	.000	52.186
Controller	.000	.000	.000	.000	.000	.000
Brake	.000	.000	.000	0.498	.000	0.498
Total	53.823	120.579	24.027	20.954	.000	219.383
Battery	156.948	120.579	.000	-58.144	.000	219.383

Figure 49.--Performance of configuration 3.

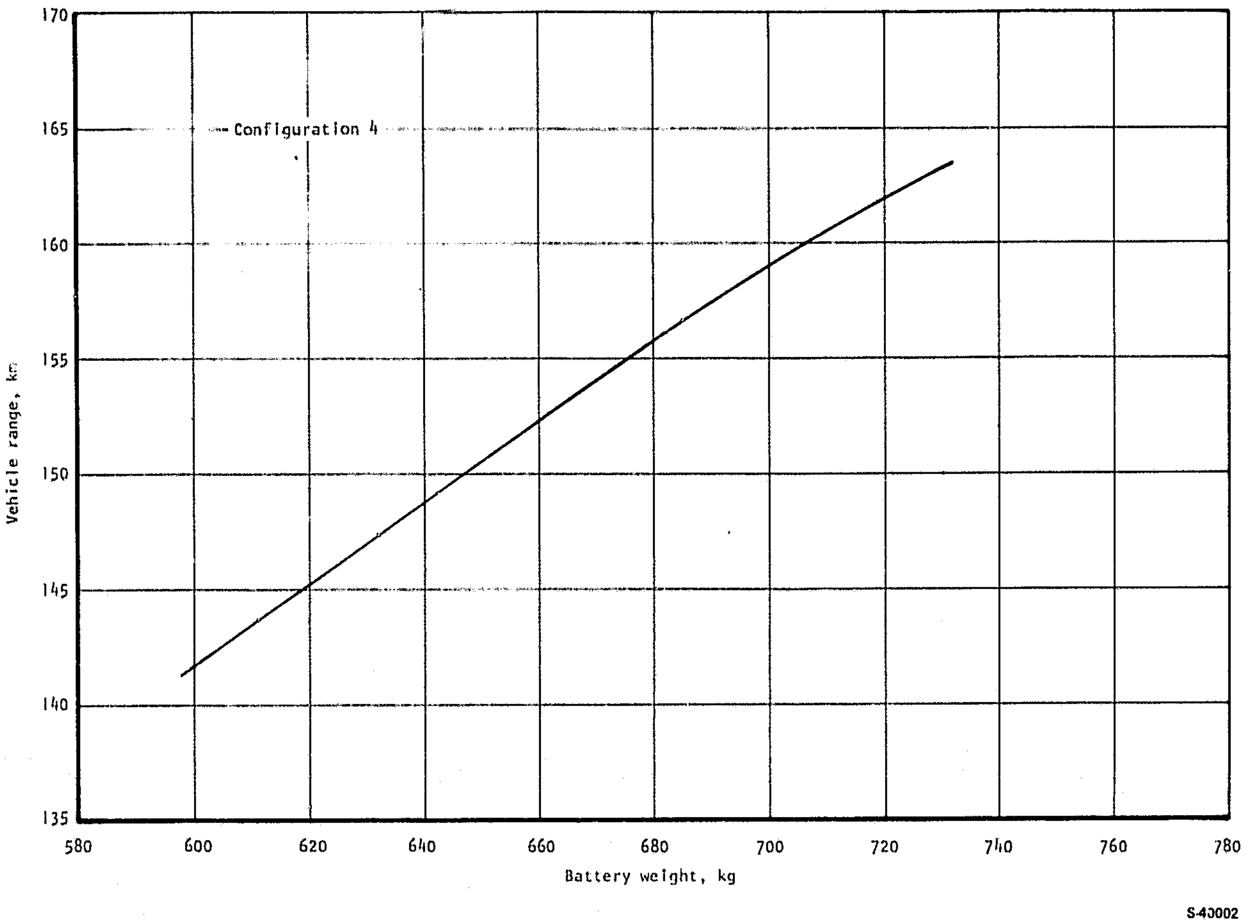

Electric vehicle simulation:

Traction motor	Ac variable frequency
Transmission	Multiratio 4 speed
Energy buffer	None
Driving cycle	J227a schedule D
Vehicle weight, kg	1722.3
Propulsion system weight, kg	107.0
Battery weight, kg	725.7
Total range, km	162.6

Summary of energy losses in driving cycle, W-hr

	Acceleration	Cruise	Coast	Brake	Dwell	Total
Road drag	22.908	81.755	14.443	4.402	.000	123.508
Differential	9.078	14.249	4.156	3.895	.000	31.378
Transmission	2.493	2.475	2.493	1.037	.000	8.498
Motor	12.502	13.285	1.662	6.253	.000	33.702
Controller	8.161	5.739	.000	3.468	.000	17.368
Brake	.000	.000	.000	0.439	.000	0.439
Total	55.142	117.503	22.754	19.494	.000	214.893
Battery	157.996	117.503	.000	-60.606	.000	214.893

Figure 50.--Performance of configuration 4.

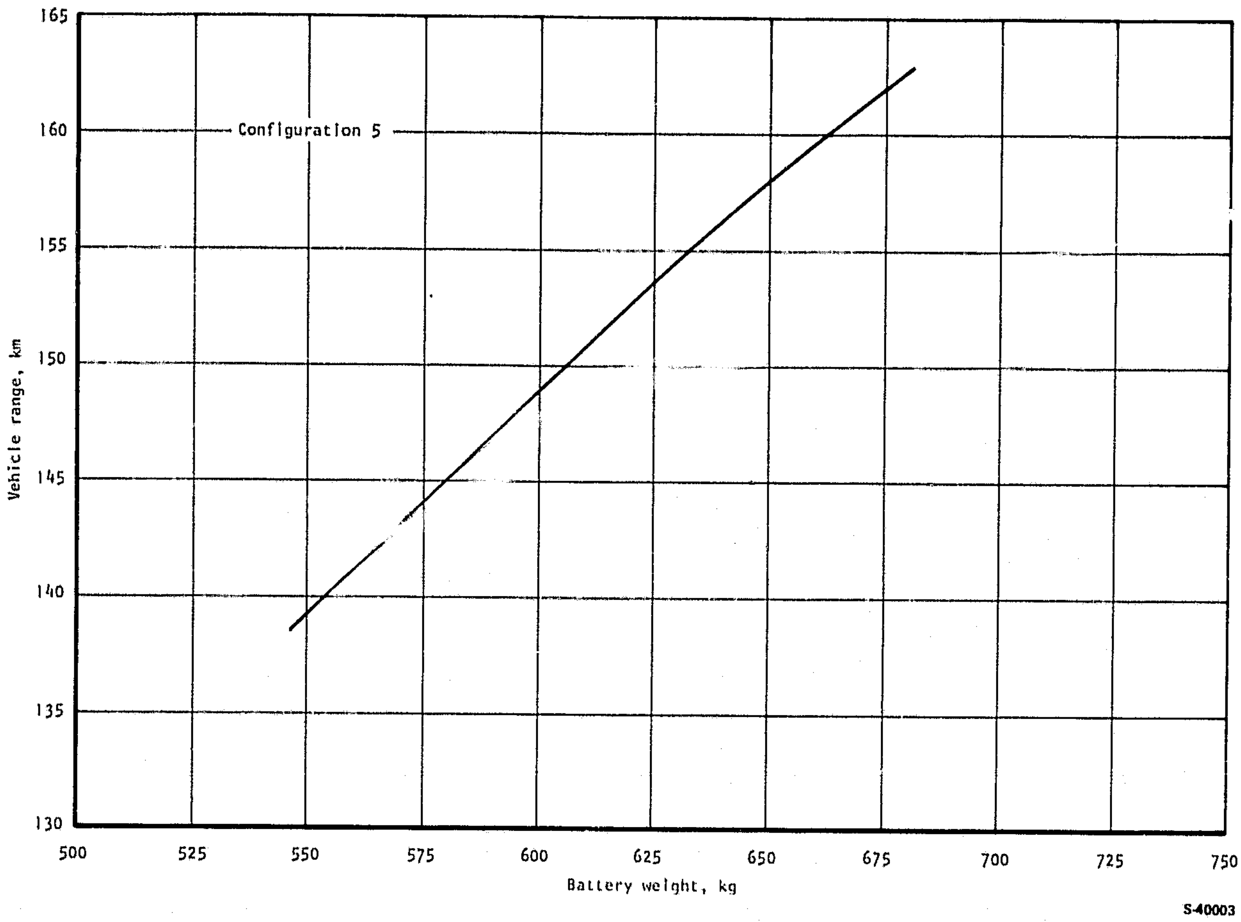

Electric vehicle simulation:

Traction motor	Dc permanent magnet
Transmission	Traction CVT
Energy buffer	None
Driving cycle	J227a schedule D
Vehicle weight, kg	1668.3
Propulsion system weight, kg	110.7
Battery weight, kg	680.4
Total range, km	163.2

Summary of energy losses in driving cycle, W-hr

	Acceleration	Cruise	Coast	Brake	Dwell	Total
Road drag	23.520	80.397	14.402	4.405	.000	122.724
Differential	8.240	11.495	4.036	3.740	.000	27.511
Transmission	9.884	6.264	0.807	4.684	.000	21.639
Motor	10.739	5.400	0.538	4.823	.000	21.500
Controller	8.251	5.551	.000	3.319	.000	17.121
Brake	.000	.000	.000	0.189	.000	0.189
Total	60.634	109.107	19.783	21.160	.000	210.684
Battery	160.007	109.107	.000	-58.430	.000	210.684

Figure 51.--Performance of configuration 5.

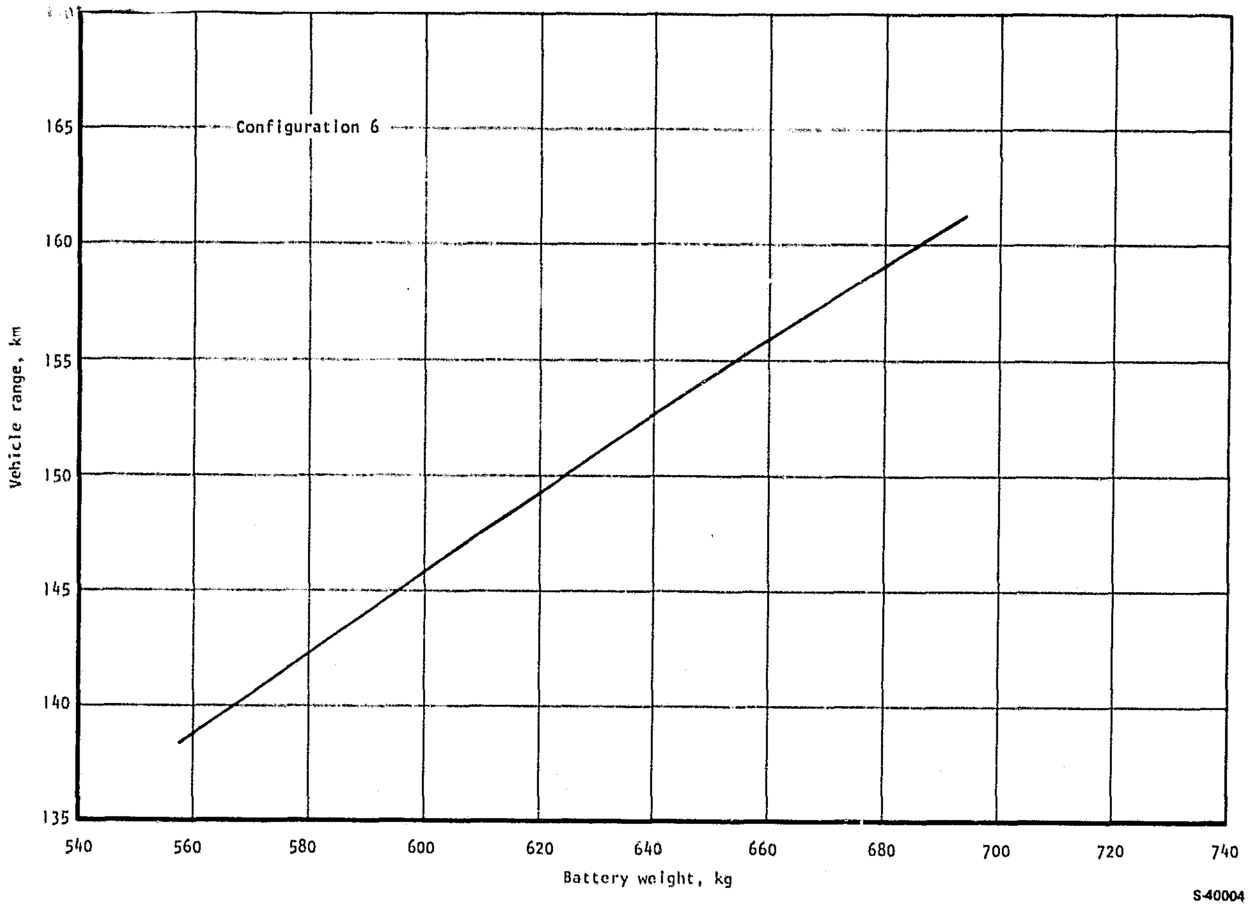

Electric vehicle simulation:

Traction motor	Dc shunt
Transmission	Traction CVT
Energy buffer	None
Driving cycle	J227a schedule D
Vehicle weight, kg	1707.3
Propulsion system weight, kg	140.6
Battery weight, kg	680.4
Total range, km	159.2

Summary of energy losses in driving cycle, W-hr

	Acceleration	Cruise	Coast	Brake	Dwell	Total
Road drag	23.867	81.371	14.579	4.475	.000	124.292
Differential	9.272	14.234	4.290	3.965	.000	31.761
Transmission	5.621	5.931	0.858	3.110	.000	15.520
Motor	15.410	17.882	0.572	9.966	.000	43.830
Controller	.000	.000	.000	.000	.000	.000
Brake	.000	.000	.000	0.133	.000	0.133
Total	54.170	119.418	20.299	21.649	.000	215.536
Battery	155.996	119.418	.000	-59.878	.000	215.536

Figure 52.--Performance of configuration 6.

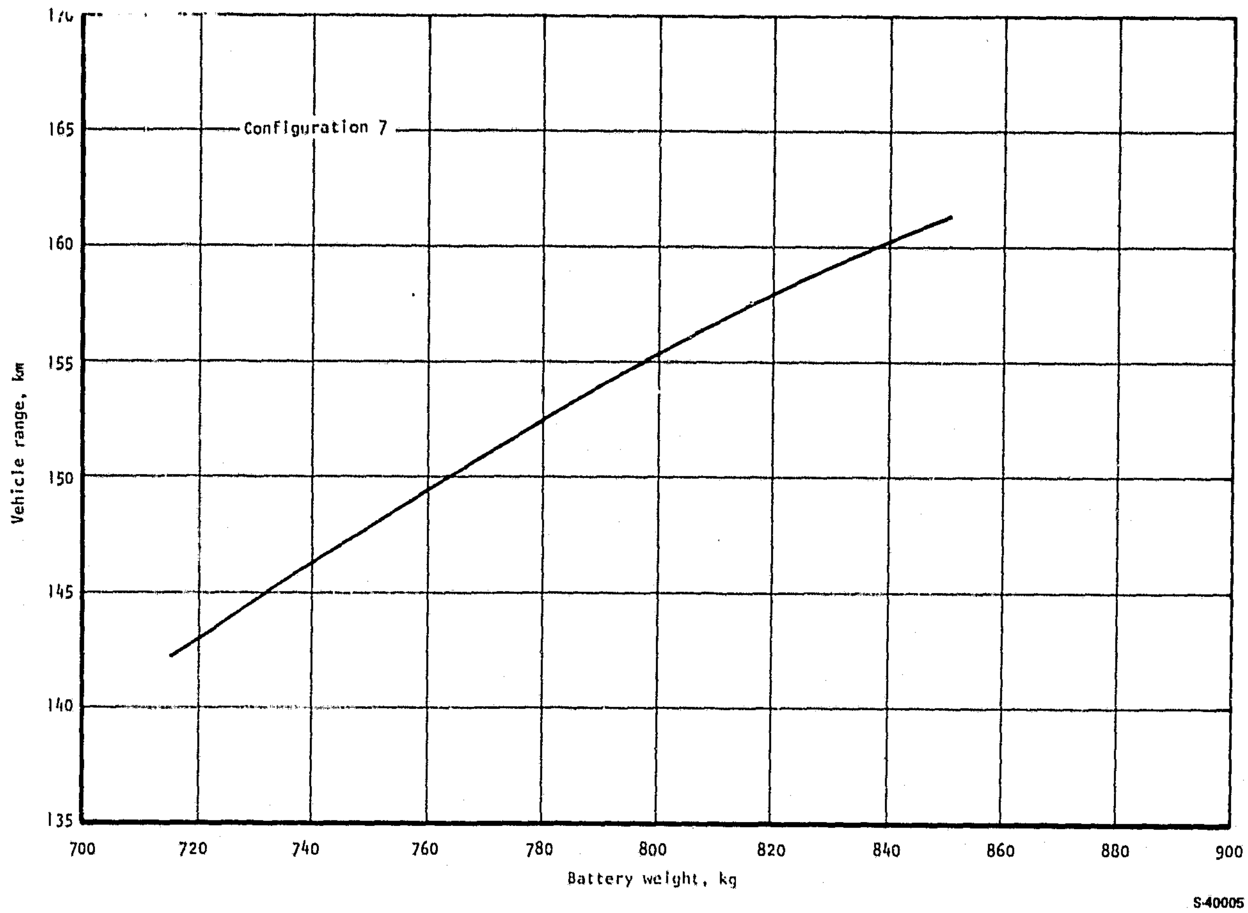

Electric vehicle simulation:

Traction motor	Ac constant frequency
Transmission	Traction CVT
Energy buffer	None
Driving cycle	J227a schedule D
Vehicle weight, kg	1867.0
Propulsion system weight, kg	104.8
Battery weight, kg	839.1
Total range, km	160.2

Summary of energy losses in driving cycle, W-hr

	Acceleration	Cruise	Coast	Brake	Dwell	Total
Road drag	25.293	85.370	15.282	4.752	.000	130.697
Differential	9.714	14.369	5.554	4.227	.000	33.864
Transmission	7.997	10.808	1.111	3.662	.000	23.578
Motor	14.914	13.159	0.741	7.495	.000	36.309
Controller	8.522	5.839	.000	3.527	.000	17.888
Brake	.000	.000	.000	0.255	.000	0.255
Total	66.440	129.545	22.688	23.918	.000	242.591
Battery	181.307	129.545	.000	-68.261	.000	242.591

Figure 53.--Performance of configuration 7.

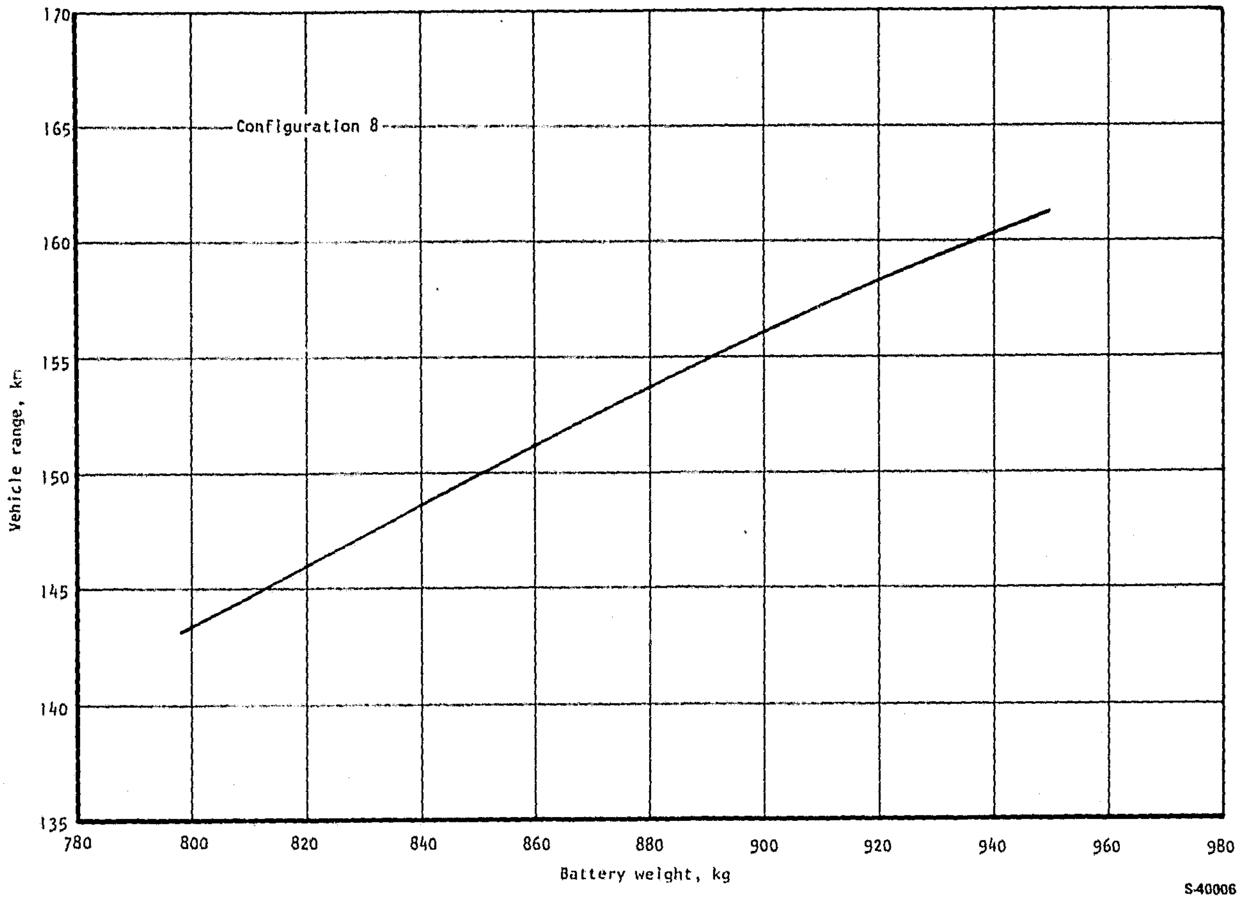

Electric vehicle simulation:

Traction motor	Ac constant frequency
Transmission	Belt CVT
Energy buffer	None
Driving cycle	J227a schedule D
Vehicle weight, kg	1996.2
Propulsion system weight, kg	113.9
Battery weight, kg	930.0
Total range, km	159.4

Summary of energy losses in driving cycle, W-hr

	Acceleration	Cruise	Coast	Brake	Dwell	Total
Road drag	26.450	88.617	15.898	5.017	.000	135.982
Differential	10.057	14.449	4.087	4.484	.000	33.077
Transmission	10.753	10.997	3.270	4.923	.000	29.943
Motor	17.393	13.474	0.817	8.828	.000	40.512
Controller	9.142	6.015	.000	3.668	.000	18.825
Brake	.000	.000	.000	0.257	.000	0.257
Total	73.795	133.552	24.072	27.177	.000	258.596
Battery	195.636	133.552	.000	-70.592	.000	258.596

Figure 54.--Performance of configuration 8.

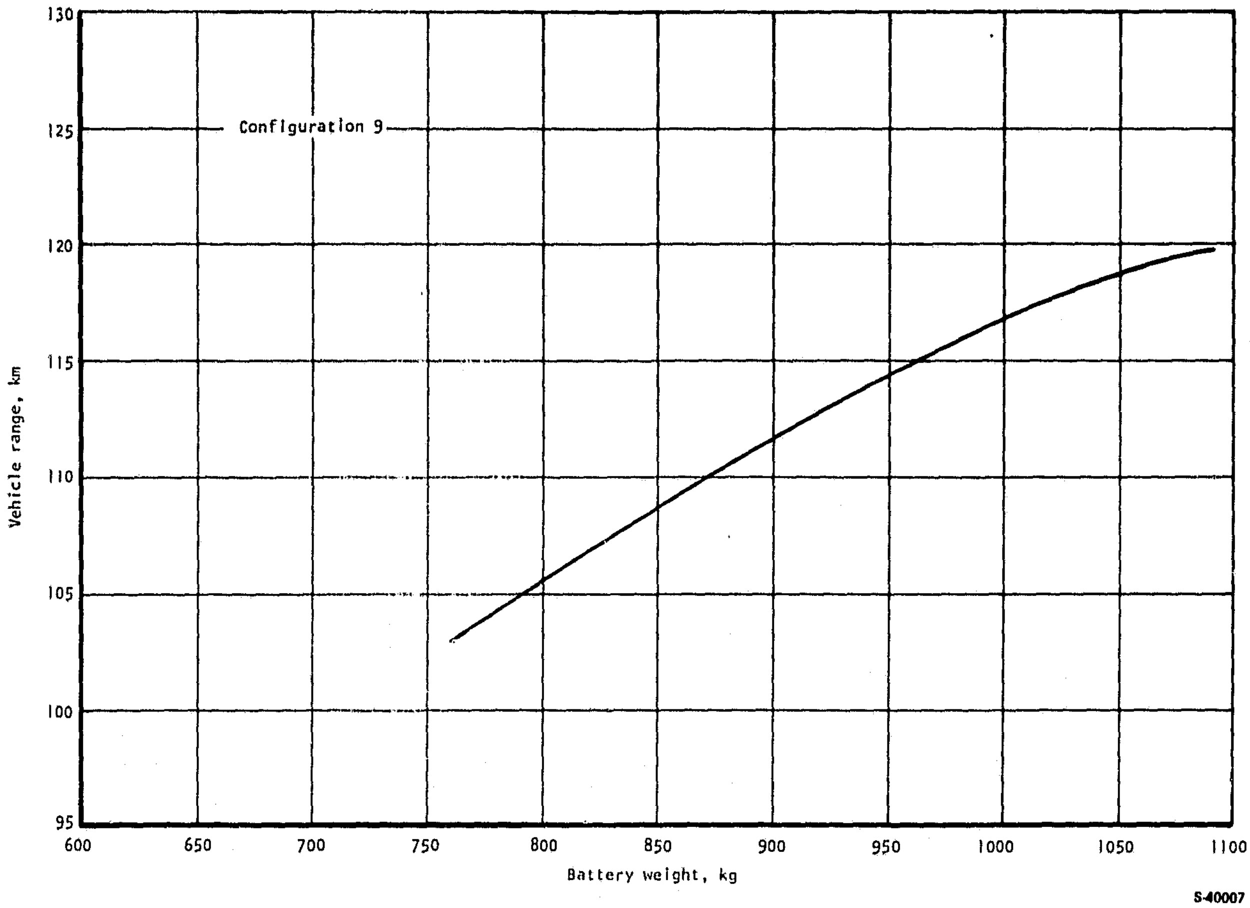

Electric vehicle simulation:

Traction motor	Ac constant frequency
Transmission	Hydrostatic
Energy buffer	None
Driving cycle	J227a schedule D
Vehicle weight, kg	2238.9
Propulsion system weight, kg	142.0
Battery weight, kg	1088.6
Total range, km	119.7

Summary of energy losses in driving cycle, W-hr

	Acceleration	Cruise	Coast	Brake	Dwell	Total
Road drag	28.617	94.698	17.146	5.699	.000	146.150
Differential	10.703	14.717	4.128	5.005	.000	34.553
Transmission	33.683	21.999	3.303	16.583	.000	75.568
Motor	17.223	14.939	0.826	7.987	.000	40.975
Controller	11.225	6.916	.000	3.707	.000	21.848
Brake	.000	.000	.000	0.202	.000	0.202
Total	101.452	153.268	25.403	39.183	.000	319.306
Battery	237.251	153.269	.000	-71.214	.000	319.306

Figure 55.--Performance of configuration 9.

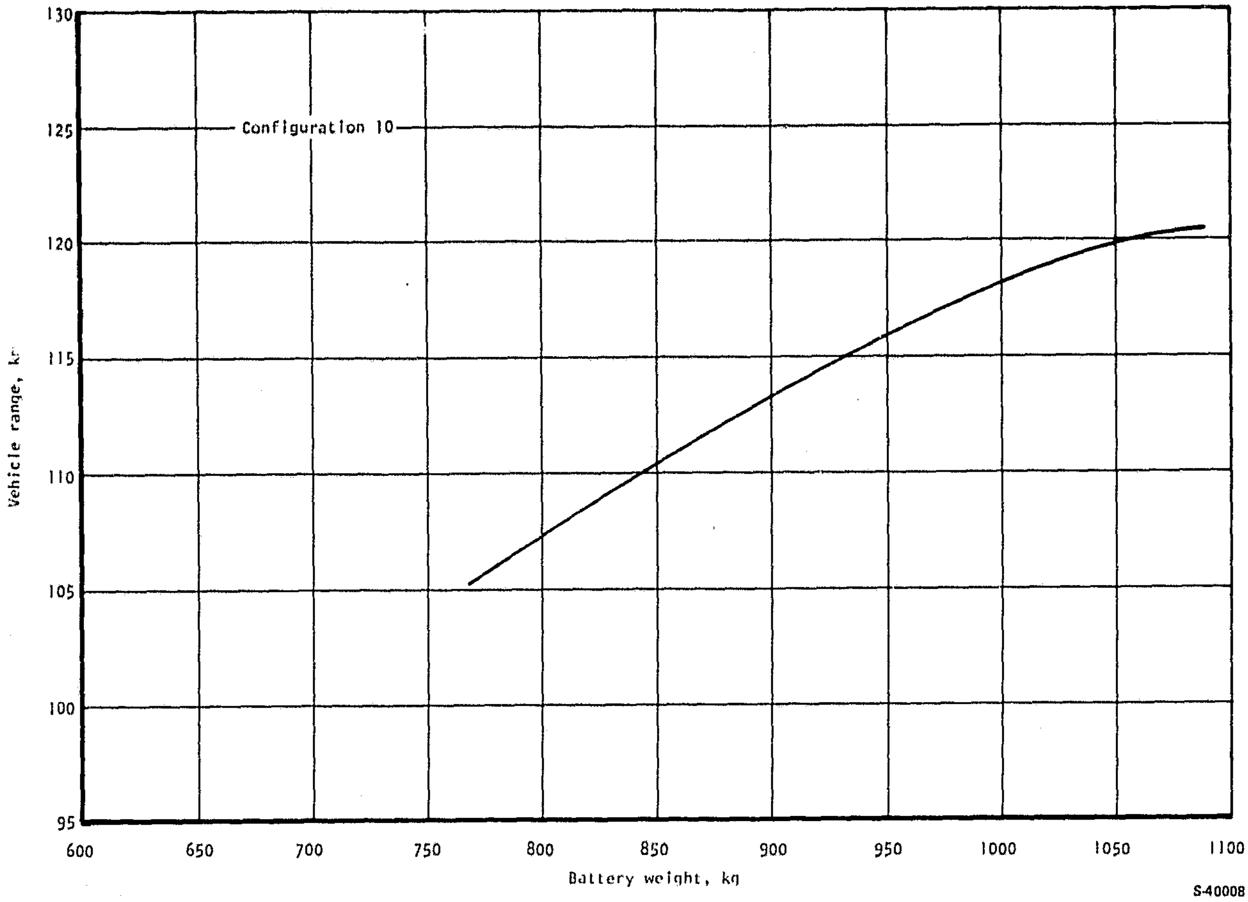

Electric vehicle simulation:

Traction motor	Ac constant frequency
Transmission	Hydromechanical
Energy buffer	None
Driving cycle	J227a schedule D
Vehicle weight, kg	2202.6
Propulsion system weight, kg	113.9
Battery weight, kg	1088.6
Total range, km	120.5

Summary of energy losses in driving cycle, W-hr

	Acceleration	Cruise	Coast	Brake	Dwell	Total
Road drag	28.291	93.783	16.959	5.598	.000	144.631
Differential	10.607	14.653	4.124	4.931	.000	34.315
Transmission	35.521	22.291	3.300	18.417	.000	79.529
Motor	17.266	14.883	0.825	7.496	.000	40.470
Controller	11.185	6.880	.000	3.557	.000	21.622
Brake	.000	.000	.000	0.209	.000	0.209
Total	102.870	152.490	25.208	40.208	.000	320.776
Battery	236.617	152.489	.000	-68.330	.000	320.776

Figure 56.--Performance of configuration 10.

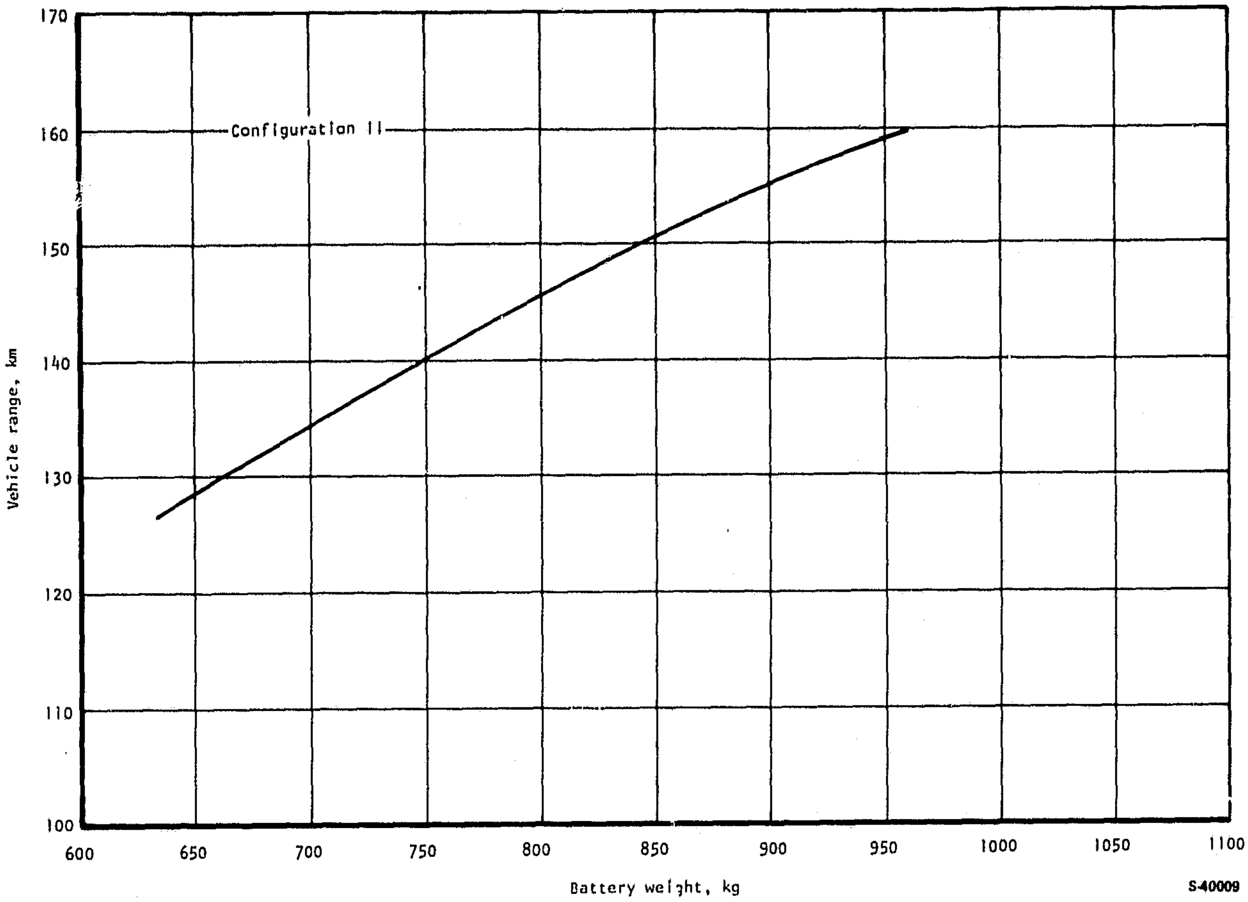

Electric vehicle simulation:

Traction motor	Dc shunt
Transmission	Electrical
Energy buffer	Flywheel/motor/generator
Driving cycle	J227a schedule D
Vehicle weight, kg	2120.1
Propulsion system weight, kg	195.5
Battery weight, kg	943.5
Total range, km	159.2

Summary of energy losses in driving cycle, W-hr

	Acceleration	Cruise	Coast	Brake	Dwell	Total
Road drag	27.554	91.716	16.541	5.335	.000	141.146
Differential	10.392	14.507	4.546	4.731	.000	34.176
Transmission	2.885	4.236	2.066	1.199	.000	10.386
Motor	24.773	23.803	1.653	14.786	.000	65.015
Controller	7.443	0.703	3.937	5.508	0.825	18.416
Brake	.000	.000	.000	0.680	.000	0.680
Flywheel	1.658	1.927	0.389	0.640	2.049	6.663
Flywheel motor	15.853	1.961	5.107	7.717	2.999	33.637
Total	90.558	138.853	34.239	40.596	5.873	310.118
Battery	77.053	145.070	64.505	9.981	13.509	310.118

Figure 57.--Performance of configuration 11.

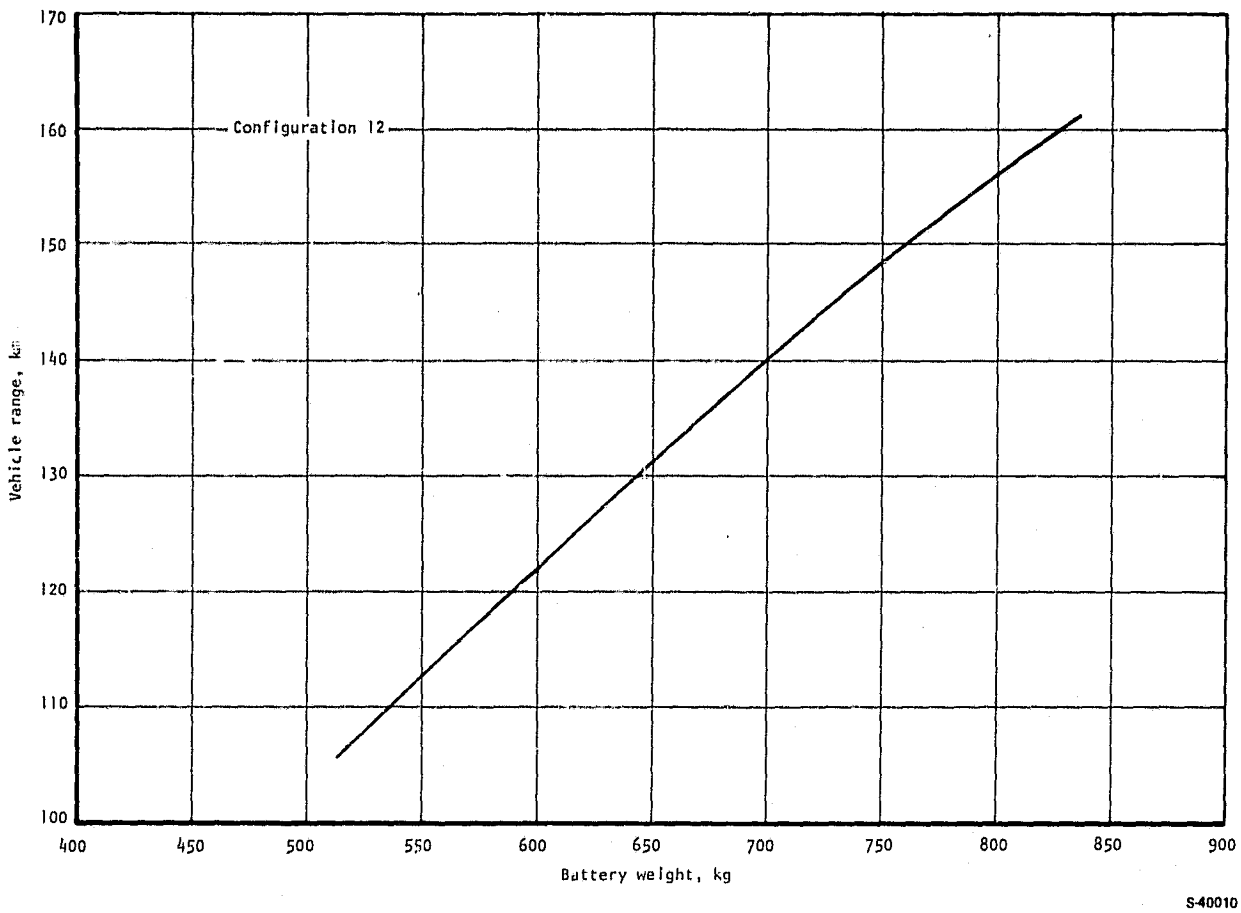

Electric vehicle simulation:

Traction motor	Ac variable frequency
Transmission	Electrical
Energy buffer	Flywheel/motor/generator
Driving cycle	J227a schedule D
Vehicle weight, kg	1848.4
Propulsion system weight, kg	113.4
Battery weight, kg	816.5
Total range, km	158.7

Summary of energy losses in driving cycle, W-hr

	Acceleration	Cruise	Coast	Brake	Dwell	Total
Road drag	25.130	84.913	15.230	4.735	.000	130.008
Differential	9.664	14.356	3.767	4.213	.000	32.000
Transmission	2.676	4.132	1.712	1.100	.000	9.620
Motor	25.141	18.522	1.370	13.223	.000	58.256
Controller	11.296	10.392	2.565	6.261	0.936	31.450
Brake	.000	.000	.000	0.825	.000	0.825
Flywheel	1.742	2.246	0.466	0.642	2.043	7.139
Flywheel motor	15.676	3.757	4.926	7.578	3.393	35.330
Total	91.325	138.318	30.036	38.577	6.372	304.628
Battery	80.742	150.060	42.019	16.477	15.330	304.628

Figure 58.--Performance of configuration 12.

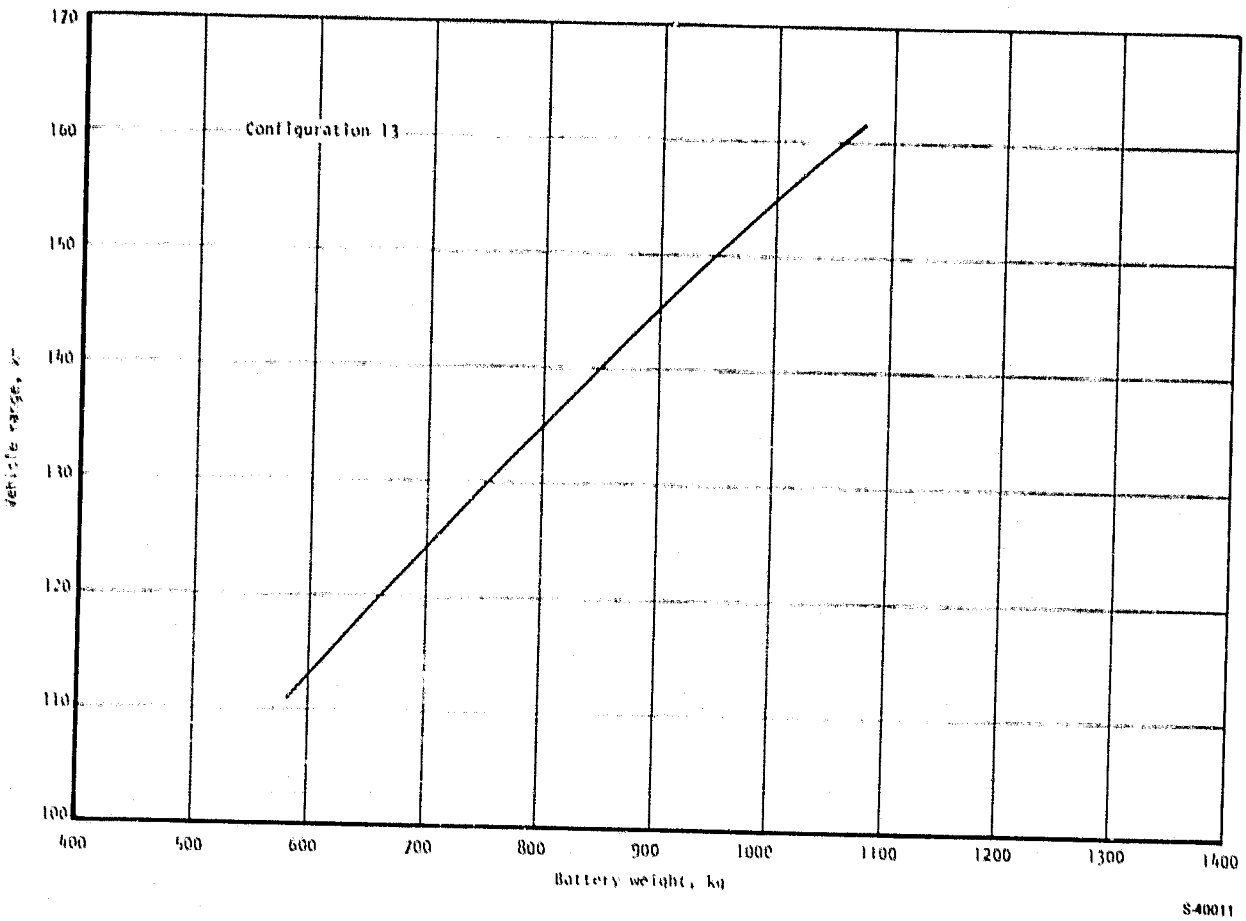

Electric vehicle simulation:

Traction motor	Dc shunt
Transmission	Electrical
Energy buffer	Flywheel/motor/generator
Driving cycle	J227a schedule D
Vehicle weight, kg	2352.3
Propulsion system weight, kg	251.7
Battery weight, kg	1065.9
Total range, km	160.8

Summary of energy losses in driving cycle, W-hr

	Acceleration	Cruise	Coast	Brake	Dwell	Total
Road drag	29.622	97.531	17.730	6.156	.000	151.043
Differential	11.006	14.904	4.562	5.291	.000	35.762
Transmission	3.048	4.318	2.073	1.334	.000	10.774
Motor	26.595	23.512	1.659	15.006	.000	66.772
Controller	8.080	0.931	.000	6.704	.000	15.715
Brake	.000	.000	.000	2.543	.000	2.543
Flywheel	2.119	2.257	0.455	0.816	6.803	12.451
Flywheel motor	19.611	4.696	7.693	14.910	5.941	52.851
Total	100.086	146.149	34.172	52.760	12.744	347.911
Battery	84.982	154.590	65.967	18.267	24.105	347.911

Figure 59.--Performance of configuration 13.

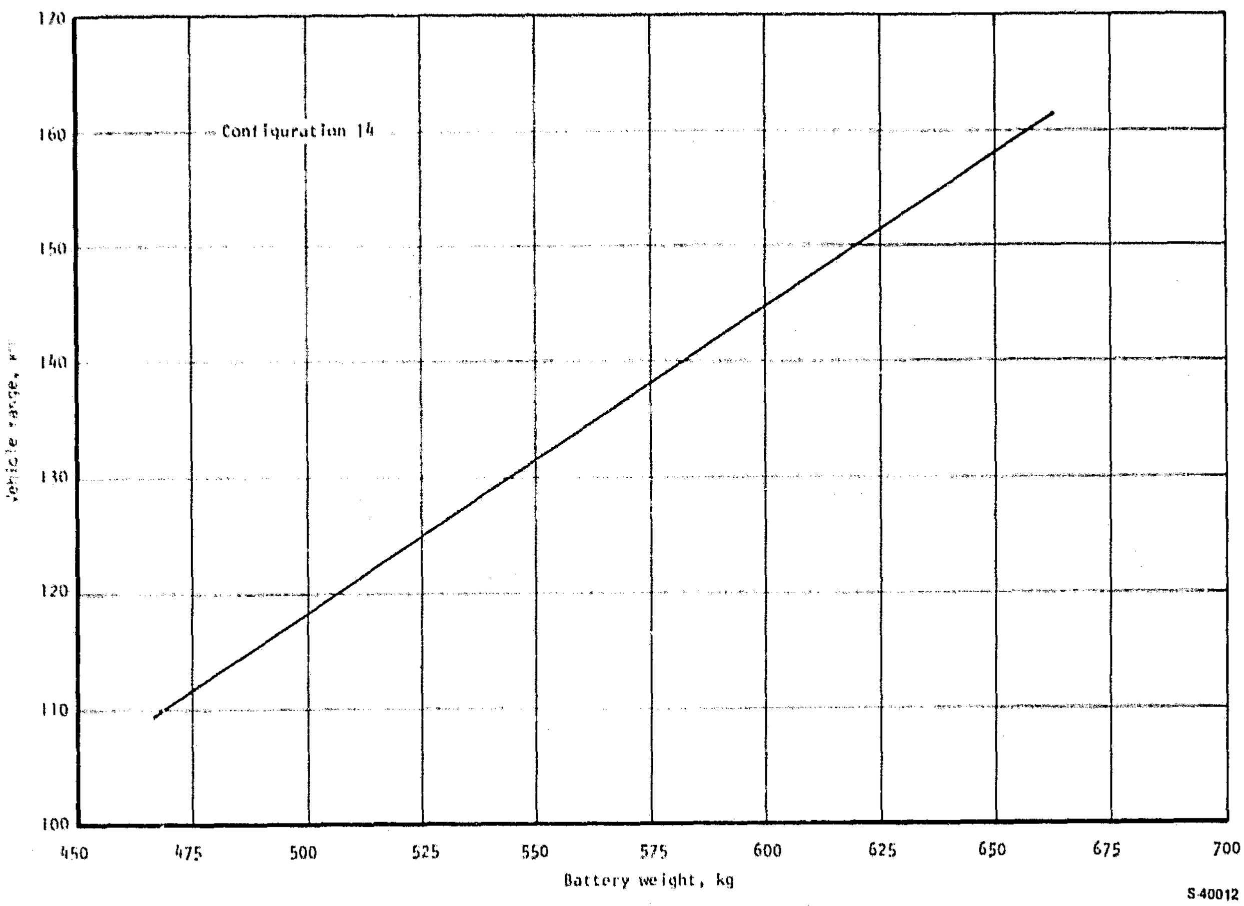

Electric vehicle simulation:

Traction motor	Dc shunt
Transmission	Traction CVT
Energy buffer	Flywheel
Driving cycle	J227a schedule D
Vehicle weight, kg	1698.2
Propulsion system weight, kg	156.5
Battery weight, kg	657.7
Total range, km	160.6

Summary of energy losses in driving cycle, W-hr

	Acceleration	Cruise	Coast	Brake	Dwell	Total
Road drag	23.788	81.150	14.384	4.377	.000	123.699
Differential	9.246	14.226	4.035	3.872	.000	31.379
Transmission	7.608	4.720	3.587	4.038	.000	19.953
Motor	11.854	26.778	6.942	5.866	4.109	55.549
Controller	.000	.000	.000	.000	.000	.000
Brake	.000	.000	.000	2.899	.000	2.899
Flywheel	4.356	4.279	0.893	1.114	10.414	21.056
Flywheel motor	.000	.000	.000	.000	.000	.000
Total	56.852	131.153	29.841	22.166	14.523	254.535
Battery	60.196	131.153	24.931	21.736	16.519	254.535

Figure 60.--Performance of configuration 14.

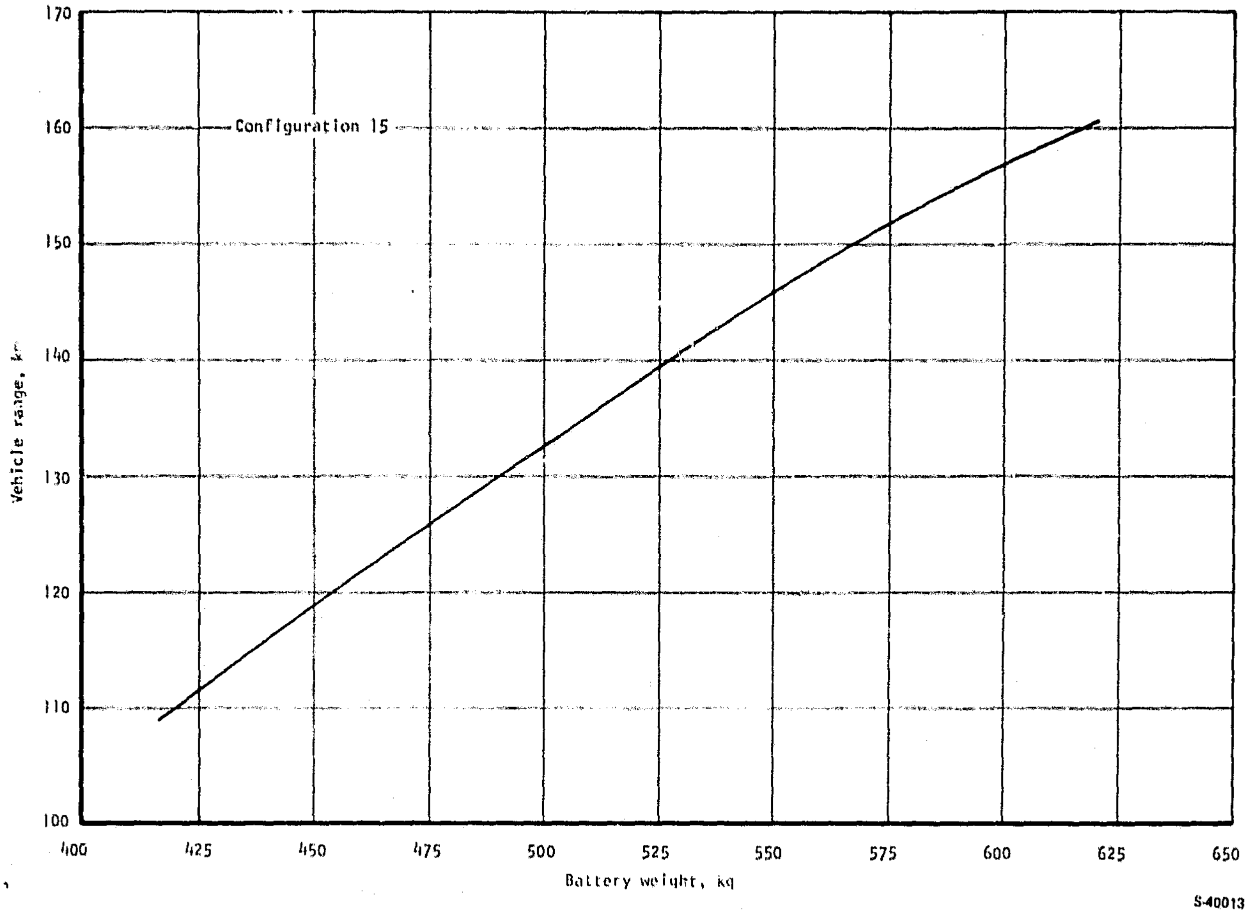

Electric vehicle simulation:

Traction motor	Dc shunt
Transmission	Traction CVT
Energy buffer	Flywheel
Driving cycle	J227a schedule D
Vehicle weight, kg	1642.4
Propulsion system weight, kg	158.8
Battery weight, kg	612.3
Total range, km	159.7

Summary of energy losses in driving cycle, W-hr

	Acceleration	Cruise	Coast	Brake	Dwell	Total
Road drag	23.288	79.747	14.370	4.402	.000	121.807
Differential	9.086	14.168	4.101	3.904	.000	31.259
Transmission	10.539	6.643	3.523	5.693	.000	26.398
Motor	7.564	23.831	4.805	7.369	5.348	48.917
Controller	.000	.000	.000	.000	.000	.000
Brake	.000	.000	.000	2.002	.000	2.002
Flywheel	3.062	4.215	0.895	1.114	6.238	15.524
Flywheel motor	.000	.000	.000	.000	.000	.000
Total	53.539	128.604	27.694	24.484	11.586	245.907
Battery	51.479	132.417	26.961	21.654	13.396	245.907

Figure 61.--Performance of configuration 15.

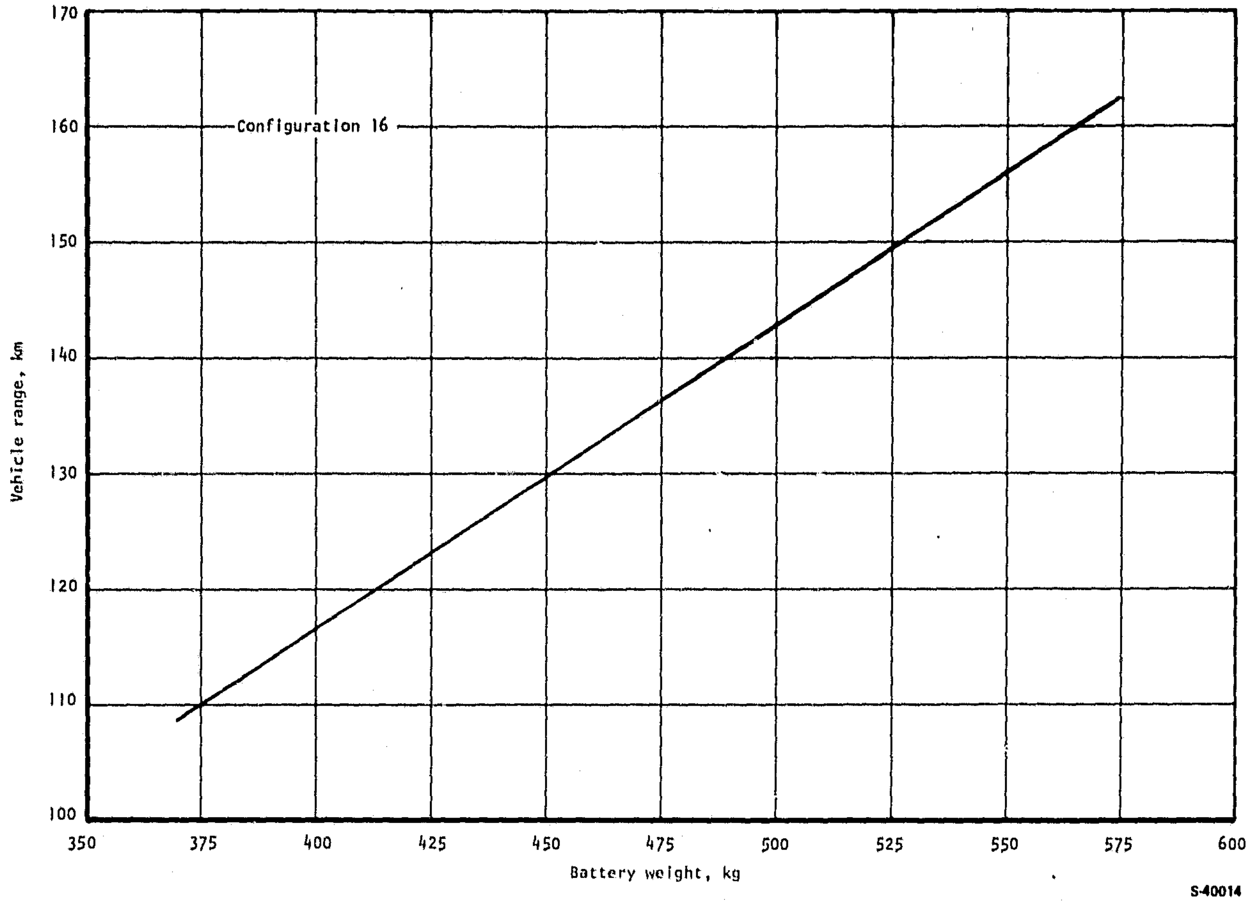

Electric vehicle simulation:

Traction motor	Dc shunt
Transmission	Traction CVT
Energy buffer	Flywheel
Driving cycle	J227a schedule D
Vehicle weight, kg	1583.5
Propulsion system weight, kg	158.8
Battery weight, kg	567.0
Total range, km	160.8

Summary of energy losses in driving cycle, W-hr

	Acceleration	Cruise	Coast	Brake	Dwell	Total
Road drag	22.762	78.272	13.777	4.126	.000	118.938
Differential	8.914	14.101	4.016	3.625	.000	30.656
Transmission	7.367	4.648	3.570	3.777	.000	19.361
Motor	10.258	27.168	5.580	5.807	0.855	49.668
Controller	.000	.000	.000	.000	.000	.000
Brake	.000	.000	.000	0.589	.000	0.589
Flywheel	1.855	2.598	0.555	0.674	2.084	7.766
Flywheel motor	.000	.000	.000	.000	.000	.000
Total	51.156	126.787	27.498	18.598	2.939	226.978
Battery	48.654	128.016	27.778	19.109	3.421	226.978

Figure 62.--Performance of configuration 16.

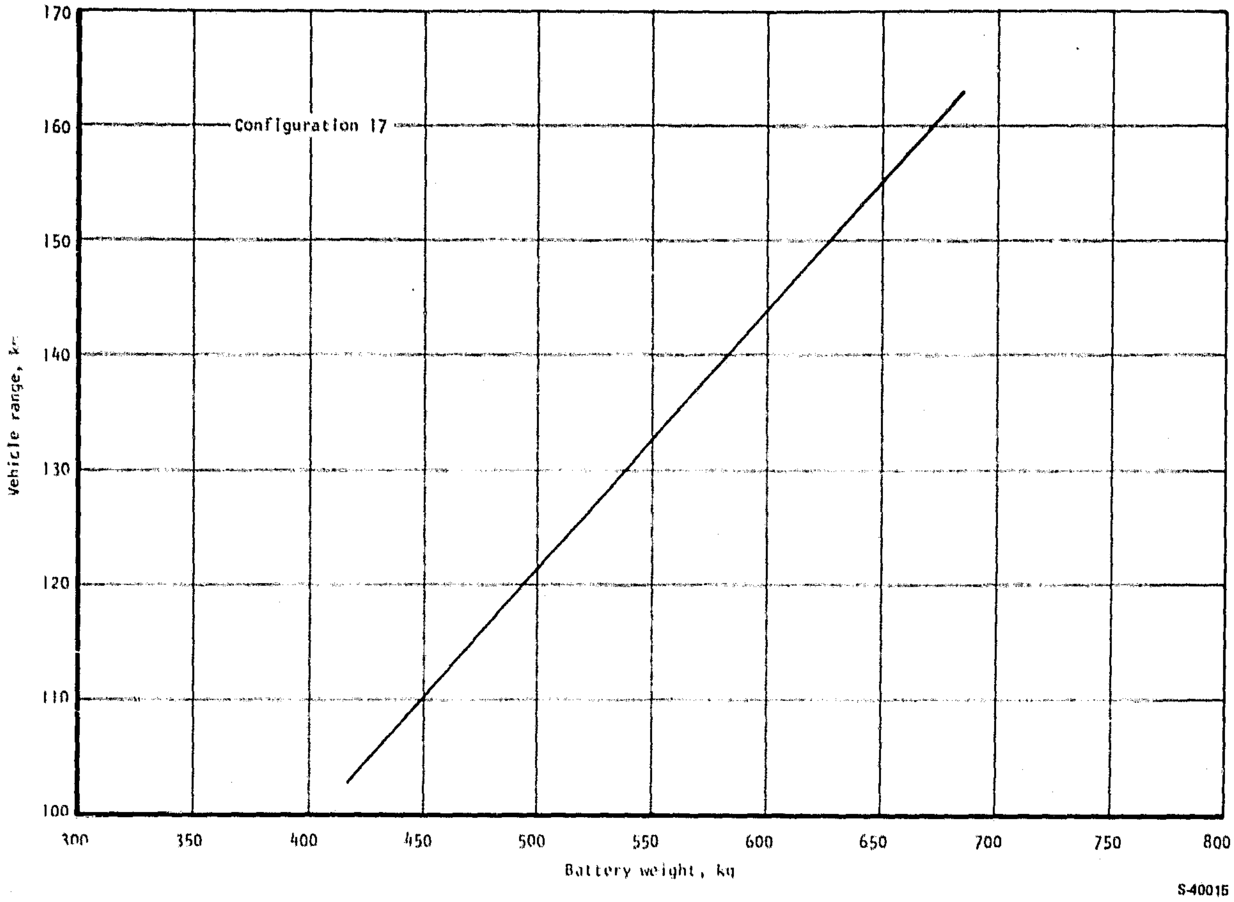

Electric vehicle simulation:

Traction motor	Ac variable frequency
Transmission	Traction CVT
Energy buffer	Flywheel
Driving cycle	J227a schedule D
Vehicle weight, kg	1686.9
Propulsion system weight, kg	125.2
Battery weight, kg	680.4
Total range, km	161.9

Summary of energy losses in driving cycle, W-hr

	Acceleration	Cruise	Coast	Brake	Dwell	Total
Road drag	23.688	80.869	14.325	4.353	.000	123.235
Differential	9.214	14.215	4.033	3.849	.000	31.311
Transmission	10.578	15.384	3.585	4.473	.000	34.020
Motor	9.126	22.672	4.778	5.469	2.192	44.237
Controller	2.393	6.953	1.382	1.202	0.437	12.367
Brake	.000	.000	.000	1.431	.000	1.431
Flywheel	3.033	4.049	0.875	1.100	6.243	15.300
Flywheel motor	.000	.000	.000	.000	.000	.000
Total	58.032	144.142	28.978	21.877	8.872	261.901
Battery	51.040	145.842	29.160	26.203	9.656	261.901

Figure 63.--Performance of configuration 17.

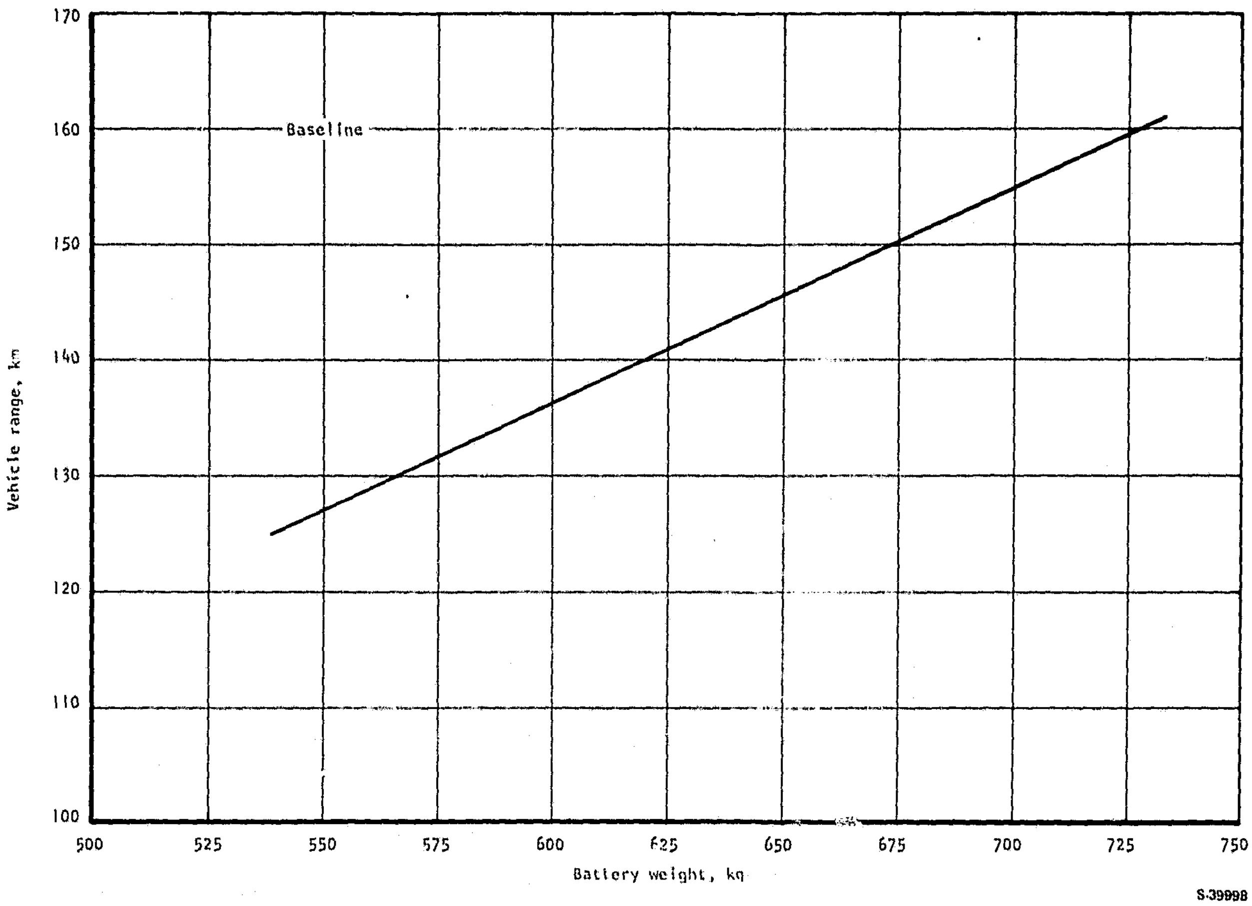

Electric vehicle simulation:

Traction motor	Dc shunt
Transmission	Electrical
Energy buffer	Flywheel
Driving cycle	J227a schedule D
Vehicle weight, kg	1940.9
Propulsion system weight, kg	267.6
Battery weight, kg	733.5
Total range, km	161.8

Summary of energy losses in driving cycle, W-hr

	Acceleration	Cruise	Coast	Brake	Dwell	Total
Road drag	25.955	87.230	14.340	4.234	.000	131.759
Differential	15.129	16.554	3.663	4.736	.000	40.082
Transmission	.000	.000	.000	.000	.000	.000
Motor	17.799	30.388	7.823	8.542	.000	64.552
Controller	3.454	8.301	1.581	1.128	.000	14.464
Brake	.000	.000	.000	0.840	.000	0.840
Flywheel	1.713	1.875	0.415	0.536	1.879	6.418
Flywheel motor	10.215	3.368	4.496	12.787	9.357	40.223
Total	74.265	147.716	32.318	32.803	11.236	298.338
Battery	56.626	136.076	25.915	18.484	61.237	298.338

Figure 64.--Performance of baseline configuration

Range Limits

The driving cycle range calculations were used for the initial comparisons, and some of the data generated were then used to calculate the range achievable at a constant 72 km/hr. The required range at constant speed is 209 km, and several of the flywheel systems could not meet this range with the minimum battery pack needed to meet the driving cycle range. Therefore, the basic battery pack for these flywheel systems was established by the 209-km range requirement.

The battery pack weight and range of each system is presented in table 6. The battery weight is the major factor in establishing the vehicle weight and total system cost. The stated battery weight is the minimum needed for both range requirements, established by the most difficult requirement. There is an implied assumption that the lead-acid batteries could be configured to provide the calculated energy at the exact weight allowance needed.

First Cost Comparisons

The initial cost comparison was based on the acquisition cost of the propulsion system components and the battery pack. Table 6 shows the relative costs, using configuration 1 as the reference, and table 7 ranks the systems by battery weight and relative cost. The differences between adjoining configurations in the ranking are not large, and design variations can be reflected in the rankings of the top systems to cause a shift in placement by as much as two ranks.

The acquisition cost of the propulsion system is the initial factor in determining life-cycle costs, but only the final system selections received full cost evaluations. The initial cost estimates were, in part, based on comparisons with items that are currently produced in large quantity, such as automotive parts (refs. 21 and 22). Projections were also made for large-scale production of high-technology parts currently in limited production (ref. 23). It is assumed that all components would be fully developed by 1983. There are wide variations in the various data sources with regard to the assumptions used to develop costs; therefore, this initial cost presentation was made comparative, rather than absolute, as a means of relative evaluations of the various systems.

Initial System Selection

The Task I effort was concluded by selection of five propulsion systems for further study in Task II. These five systems were selected partly on the basis of their rating in performance and cost, as may be seen in table 6, but also on the basis of technological risk and the advantages of one configuration over a closely similar configuration.

All the configurations are listed in table 7 with their ranking based on cost and performance, and an assessment of technological risk and growth. It is apparent that several of the systems require such a large battery weight

TABLE 6.--PERFORMANCE OF ADVANCED ELECTRIC VEHICLE PROPULSION SYSTEMS

Configuration number	Battery weight, kg	Range on J227a (D) cycle, km	Range at constant 72 km/hr, km	Relative cost
1	776	161.0	250.9	1.00
2	799	161.0	261.1	1.19
3	712	161.0	244.7	0.95
4	719	161.0	256.2	1.17
5	671	161.0	240.0	1.16
6	688	161.0	238.9	0.93
7	843	161.0	264.2	1.30
8	939	161.0	283.2	1.39
9	1089	119.7	270.5	1.54
10	1089	120.5	272.6	1.54
11	954	161.0	256.3	1.48
12	828	161.0	210.7	1.35
13	1067	161.0	261.9	1.46
14	670	164.1	209.0	1.03
15	678	174.6	209.0	1.05
16	667	187.3	209.0	1.01
17	765	178.6	209.0	1.26
Baseline	730	161.0	209.8	1.23

TABLE 7.--COMPARISON OF PROPULSION SYSTEMS

Config. No.	Power control	Traction motor	Transmission type	Energy storage	Weight ranking	Cost ranking	Technical risk	Improvement potential
1	Field control	Dc shunt	-	-	10	3	Low	Low
2	Inverter	Ac induction	-	-	11	9	Low	Low
3	Field control	Dc shunt	Multiratio	-	6	2	Medium	Medium
4	Inverter	Ac induction	Multiratio	-	7	8	Medium	Medium
5	Inverter	Dc PM	CVT	-	3	7	Medium	High
6	Field control	Dc shunt	CVT	-	5	1	Medium	High
7	Inverter	Ac induction	CVT	-	13	12	Medium	Medium
8	Inverter	Ac induction	Belt	-	14	14	Medium	Medium
9	Inverter	Ac induction	Hydrostatic	-	18	18	High	High
10	Inverter	Ac induction	Hydro-mechanical	-	17	17	High	High
11	Inverter	Ac-dc	Electrical	Flywheel	15	16	High	High
12	Inverter	Ac-ac	Electrical	Flywheel	12	13	High	High
13	Inverter	Dc-dc	Electrical	Flywheel	16	15	High	High
14	Field control	Dc shunt	CVT	Flywheel	2	5	Medium	Medium
15	Field control	Dc shunt	CVT	Flywheel	4	6	Medium	Medium
16	Field control	Dc shunt	CVT	Flywheel	1	4	Medium	Medium
17	Inverter	Ac induction	CVT	Flywheel	9	11	Medium	Medium
Baseline	Field control	Dc-dc	Electrical	Flywheel	8	10	Low	Medium

that they are impractical from the standpoint of the weight and the associated cost. Some of these systems look attractive for short range, as may be seen on fig. 46, but they are at a point of diminishing returns at the 161-km range.

On the basis of weight and cost, configurations 7, 8, 9, 10, 11, 12, and 13 were eliminated. All had battery pack weights in excess of 825 kg, and the cost was more than 30 percent over the reference value.

The simplest systems, configurations 1 and 2, were relatively heavy--over 775 kg--due to their low-speed inefficiency without a transmission. Both systems were eliminated because of their weight and lack of potential for improvement.

The remaining nine systems included four basic systems with various types of traction motors and transmissions, and five flywheel systems. One of the flywheel systems was the baseline configuration. The other four flywheel systems were similar in performance, cost, and weight, but configuration 16 exhibited a clear superiority over the others. Consequently it was decided to eliminate configurations 14, 15, and 17, and retain 16 as the best representative of the group 5 systems.

The baseline configuration was a system currently being developed and thus was available to compare with the other four propulsion configurations to establish actual component performance. For this reason the baseline system was retained for use in Task II.

Of the four basic systems remaining for consideration, configurations 3, 4, 5, and 6, the traction motor for configuration 5 gives promise of the best improvement with continued development and has the lowest cost.

Configurations 3 and 6 are identical except for the transmission. Either transmission will require development for electric vehicle service, so it was decided to select configuration 6 on the basis of lower weight, and to continue the consideration of the multiratio transmission, as well as an ac motor, by retaining configuration 4. In selecting configuration 6 over 3 on the basis of weight rather than initial cost, the logic was that a lower battery pack weight means lower battery replacement costs over the life of the system, and that the lower replacement costs are more significant than first-cost advantage.

Design Tradeoffs

The five systems selected for further study and design tradeoffs in Task II, as discussed in the preceding paragraphs, were as follows:

Configuration 4: Ac induction motor, variable frequency inverter, multiratio transmission

Configuration 5: Brushless dc permanent-magnet motor, variable frequency inverter, traction continuously variable transmission

Configuration 6: Dc shunt motor, step voltage start and field control above base speed, traction continuously variable transmission

Configuration 16: Dc shunt motor, step voltage start and field control above base speed, traction continuously variable transmission, flywheel energy storage system clutched to motor

Baseline System: A resized version of the Near Term Electric Vehicle propulsion system with a dc motor, dc generator, and a flywheel energy storage system connected to a differential transmission

Cycle Operation

The five candidate systems were examined in some detail in Task II to identify areas where energy savings could be achieved and performance improved. Energy consumption during the driving cycle is shown in figs. 65 through 69. These figures represent the performance after some adjustments in gear ratios, shift points, and power management to eliminate excessive power drains.

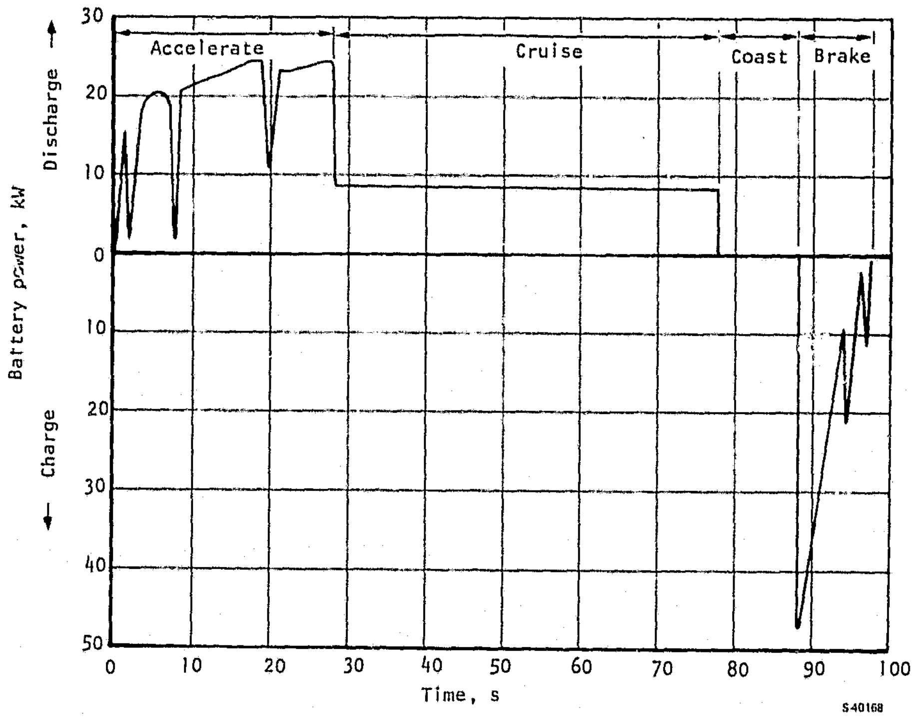

Figure 65.--Configuration 4 energy consumption during driving cycle.

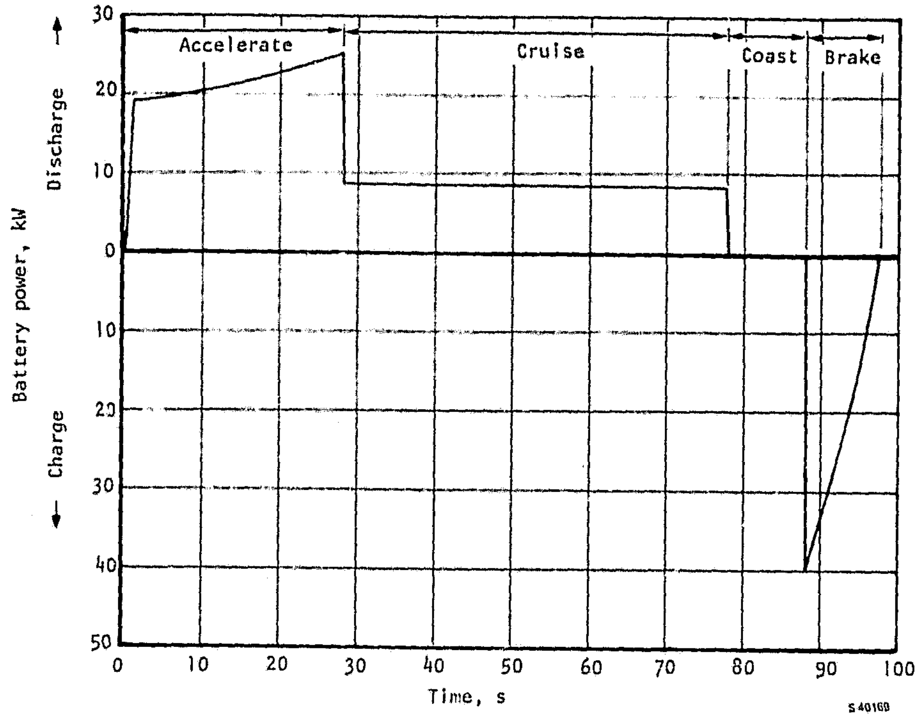

Figure 66.--Configuration 5 energy consumption during driving cycle.

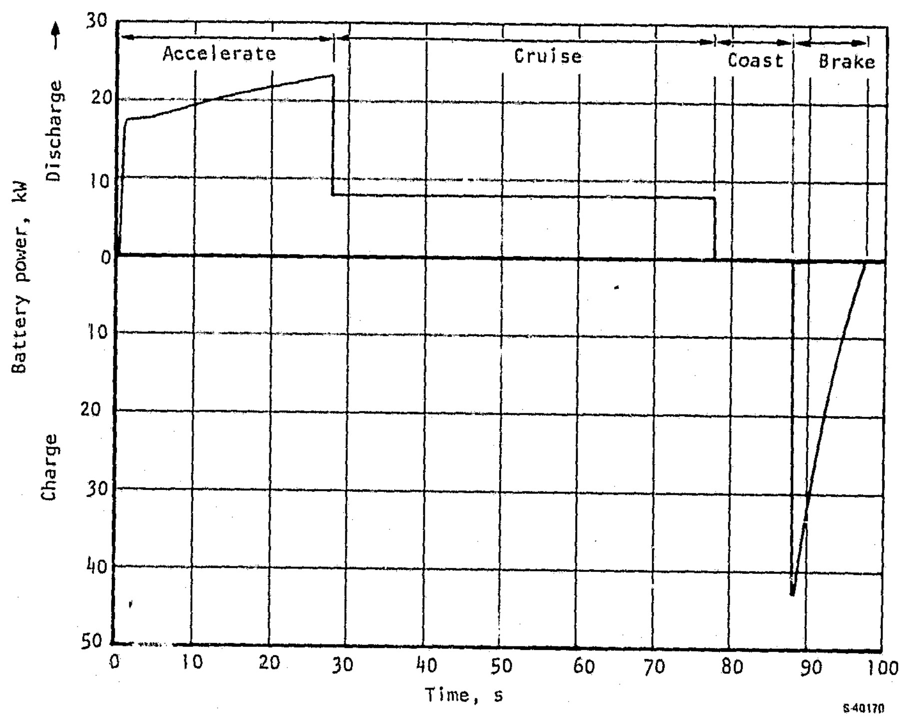

Figure 67.--Configuration 6 energy consumption during driving cycle.

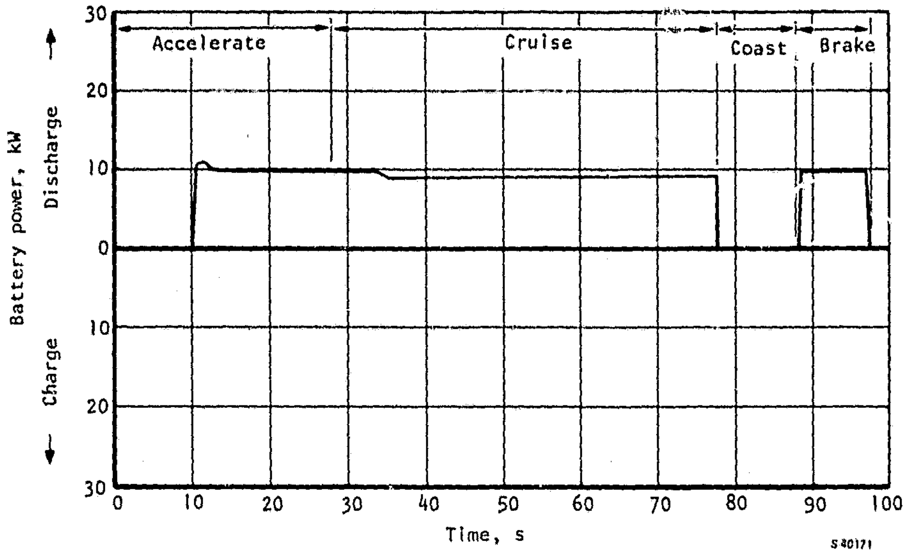

Figure 68.--Configuration 16 energy consumption during driving cycle.

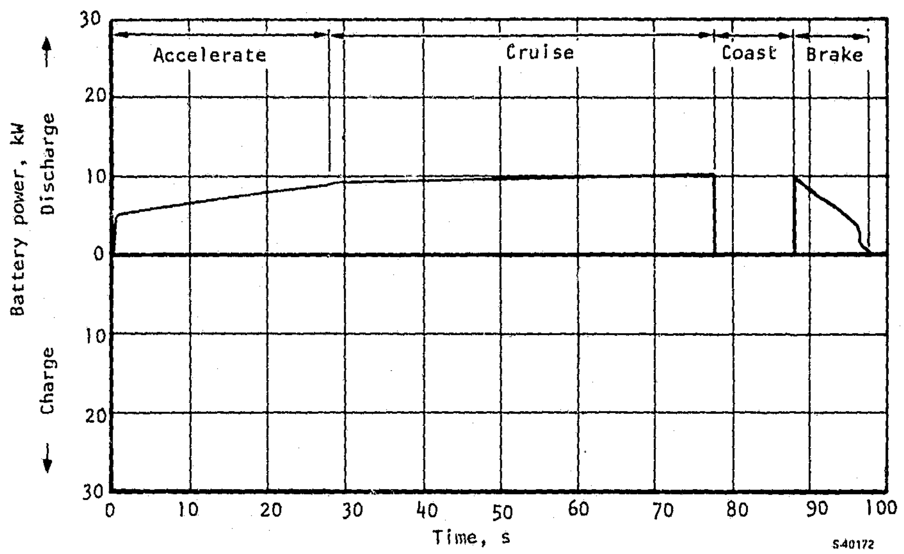

Figure 69.--Baseline configuration energy consumption during driving cycle.

Acceleration.--The acceleration schedule results in fairly uniform power drain, rising gradually during the acceleration period. Configuration 4 has change points where the transmission is shifted, while configurations 5 and 6 have smooth, stepless change with the CVT. The flywheel systems--configurations 16 and the baseline system--require low battery drain during acceleration because much of the needed power is drawn from the flywheel.

Cruise.--The power required to cruise at 72 km/hr is approximately 8 kw for all systems. The flywheel systems draw one or two kilowatts more during a portion of the cruise period to recharge the flywheel. The relatively low power at cruise, approximately 25 percent of rated power, imposes a problem in system design for all systems to maintain good efficiency at low power ratios.

Coast.--The coast condition was assumed to be a free-wheeling coast, without power regeneration. This is not a universal practice, since some degree of power regeneration could be used, giving an effect similar to coasting with the engine engaged in a standard internal combustion engine automobile.

Brake.--The brake segment uses regeneration. In configurations 4, 5, and 6, energy is returned to the battery, and the transmission is shifted to maintain the best speed of the motor, operating as a generator, down to the lowest vehicle speed possible. The rate of regeneration is limited by the maximum power capability of the electrical motor/generator.

The flywheel systems return energy to the flywheel during braking; however, the transfer of kinetic energy from the vehicle to the flywheel has losses associated with the transfer, and the flywheel speed does not increase to the full level that the energy management schedule requires. Therefore, some electrical energy from the battery is also used to power the electric motor to add additional energy to the flywheel, which makes up for the energy lost in regenerative power transfer.

Regeneration.--As mentioned in the preceding paragraphs, regeneration is not applied during coasting, but is only employed during braking. The vehicle braking system is not a part of the propulsion system, but braking and regeneration must be coordinated. A common procedure is to initiate regeneration by application of the brake, and have the separate friction brakes provide additional braking in proportion to operator pressure on the brake pedal. In the flywheel system, regeneration to the flywheel is limited by flywheel capacity, and at the maximum flywheel schedule, such as may be reached on a long grade, regeneration would then be accomplished by electrical charging of the battery.

Drive Train Efficiency.--The drive train efficiency may be defined as the ratio of the power applied at the axle to that of the power taken from the battery. By use of this simplified definition, the drive train efficiency is shown for the basic configurations in figs. 70, 71, and 72. One short-coming of the definition is that it does not account for the rotational momentum of rotating parts. Therefore, at the transmission shift points, as shown on fig. 70, the momentum transfer causes the apparent efficiency to rise or fall very abruptly. For a similar reason, the efficiency of the systems with energy storage cannot be represented in this way. These plots were used to examine the operating efficiency of the machinery in the critical portions

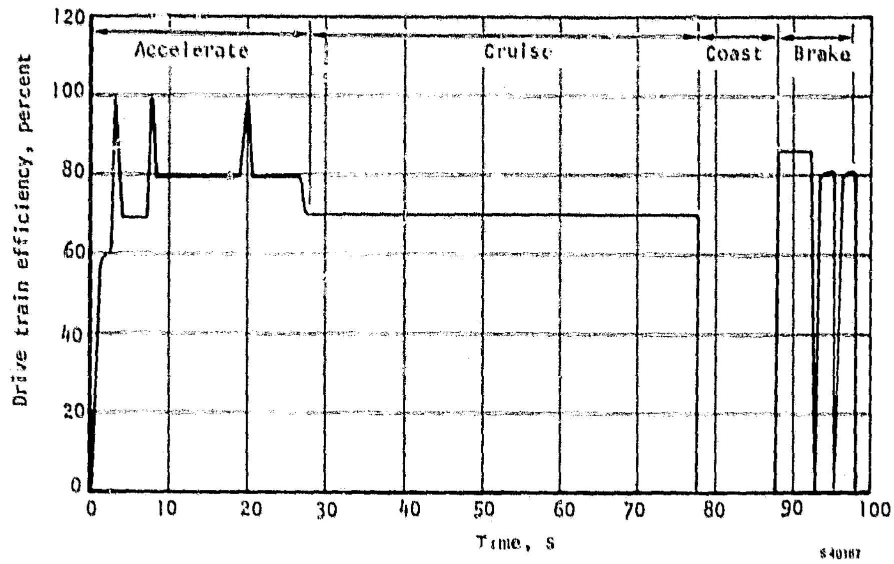

Figure 70.--Configuration 4 drive train efficiency during driving cycle.

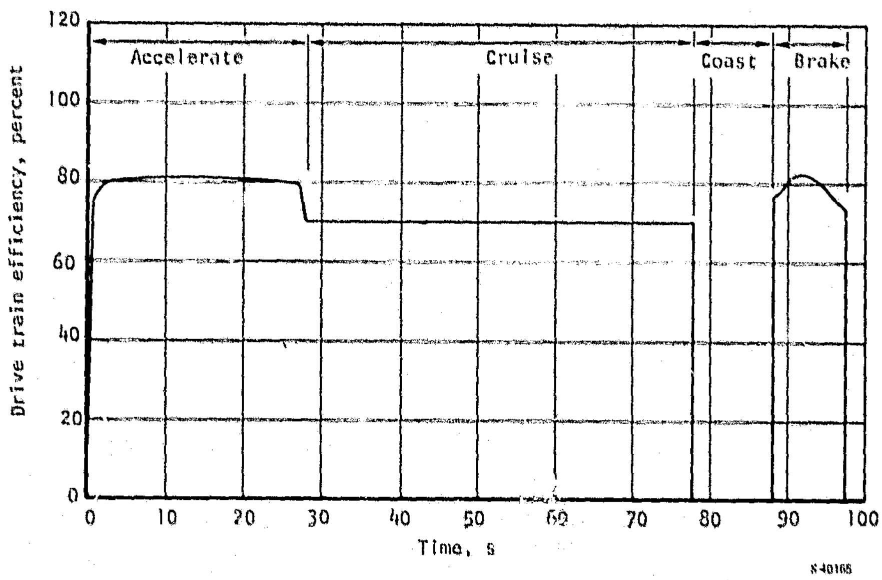

Figure 71.--Configuration 5 drive train efficiency during driving cycle.

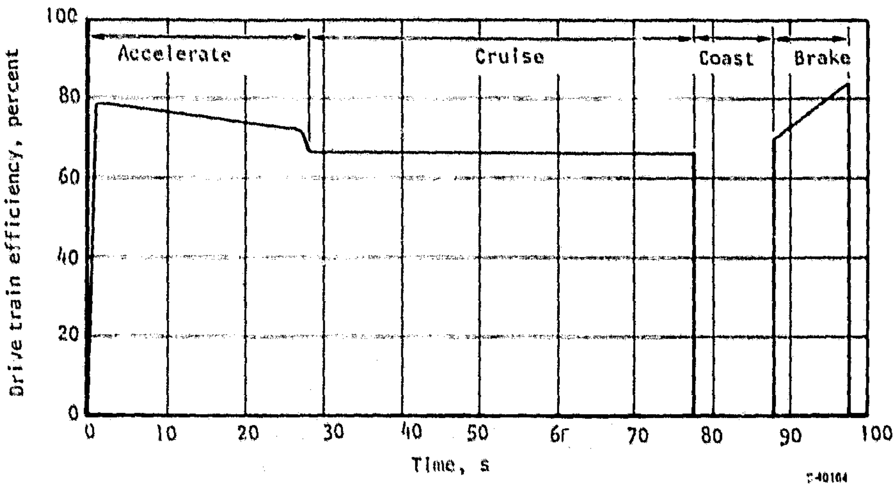

Figure 72.--Configuration 6 drive train efficiency during driving cycle.

of the cycle rather than to examine the overall energy transfer from battery to axle. This latter function was more fundamentally assessed by the vehicle range achievements.

Acceleration Performance

Acceleration performance is a critical matter with the basic propulsion systems because of the high power drain imposed on the battery. There are two major concerns: (1) the battery must have the basic power capacity to accelerate the vehicle, and (2) if the energy required for acceleration is a major percent of the battery capacity, then the vehicle will not have maximum acceleration capability after even moderate battery depletion.

The amount of power required for acceleration is directly dependent on the acceleration schedule, and battery depletion is closely dependent on the rate of power drain. Calculations were made of the battery depletion for acceleration from zero to 89 km/hr in 15 s at constant power. These results are shown in fig. 73 for the five selected systems. Configuration 6 required additional batteries to achieve the necessary power, and the battery depletion, partly because of the added weight, was quite large. The difficulty was primarily due to the drop in motor efficiency at maximum power (fig. 31). The motor map could be re-rated to a higher power to improve maximum performance, but then efficiency would be seriously depressed at the low power levels needed for the driving cycle. In either case, the size of the battery pack would increase.

The flywheel systems used flywheel energy for the acceleration, and the small amount of battery drain was used to meet losses. This battery drain during acceleration is actually determined by the energy management schedule, which was shown in fig. 12. It is possible to accelerate without using any battery power, trough charging to replace losses must be done at some point in the cycle. The principal consideration is that the charging should be done

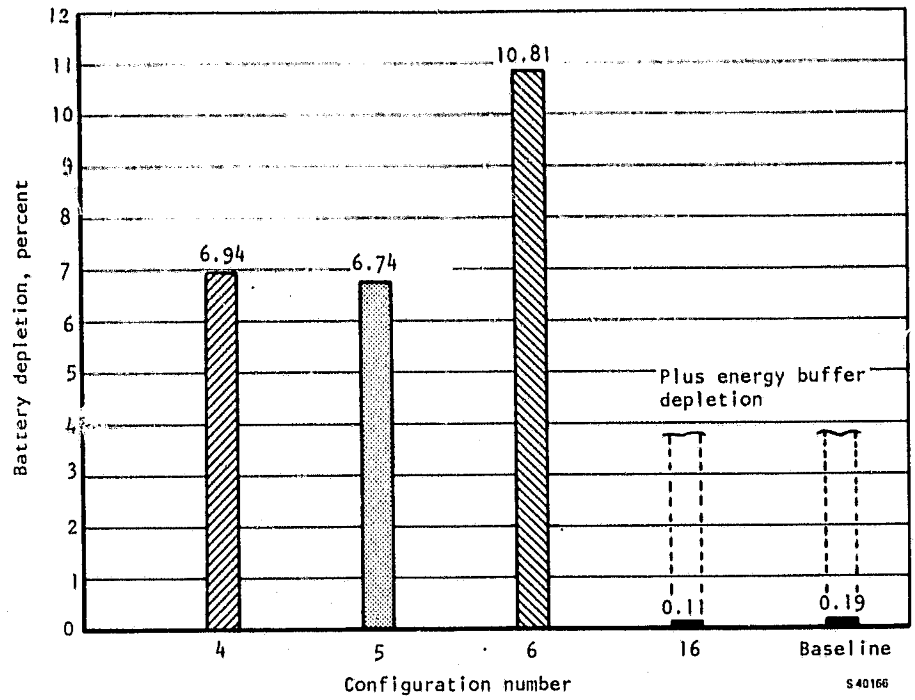

Figure 73.--Battery depletion following 0 to 89 km/hr acceleration in 15 s.

at a low enough battery drain to spare the battery and at a high enough rate that the electrical machinery is operated efficiently. The result is that the system can be operated so that it is not acceleration or power limited.

Lead-Acid Battery Weights

The necessary weight of lead-acid batteries for the five candidate systems is shown in table 8. With the weights indicated all systems will meet the indicated performance requirements of range, speed, and acceleration. The basic systems can meet the maximum acceleration requirement with a fully charged battery, but as the battery is depleted, acceleration capability is eroded, as discussed in the section "Battery Characteristics." Acceleration capability can be extended somewhat by use of a battery with high power density, such as the Globe-Union EV2-13, but there is a penalty on life, as shown in fig. 25. For a battery that meets the ISOA goals, the power and life would both be maximized, but the problem of rapid depletion during acceleration still remains a major consideration. Even with the high power density, maximum acceleration capability cannot be extended much beyond 20 to 30 percent depth of discharge for the basic systems.

The flywheel systems maintain acceleration capability even with a depleted battery, since the battery is used primarily as an energy source with the flywheel supplying power surges. A high energy density battery, such as the Eagle-Picher EP200AH, thus is well suited to the flywheel systems. Since the EP200AH battery meets the energy and life requirements of the ISOA goals, it is actually an ISOA battery as far as the flywheel systems are concerned.

TABLE 8.--BATTERY WEIGHT IN KILOGRAMS FOR VARIOUS REQUIREMENTS

Performance requirement	Configuration				
	4	5	6	16	Baseline
Range of 161 km with SAE J227a schedule D cycle	719	671	688	567	730
Range of 209 km at constant 72 km/hr	587	584	602	667	730
Acceleration of 0 to 89 km/hr in 15 s	719	671	782	567	730
Required battery pack to meet all requirements	719	671	782	667	730
Vehicle test weight with maximum battery pack	1715	1660	1840	1713	1940

System Cost Comparison

The five candidate systems were compared on the basis of manufacturing cost, as shown in table 9, with all values in 1976 dollars. Manufacturing cost was defined as the cost of direct labor, materials, and tooling, and includes the cost of acquiring small parts to fabricate and assemble the major components. Manufacturing cost does not include any corporate level costs, overhead, cost of sales, etc. The cost estimates for the indicated components are based on anticipated production of 100 000 vehicles a year, with production commencing after completion of development. Costs of standard items available for automotive service are derived from ref. 21. Costs of other mass-produced

TABLE 9.--ESTIMATED SYSTEM COSTS (1976 Dollars)

Configuration	Battery	Motor/generator	Electronics	Trans. diff.	Flywheel	Miscellaneous	Total mfg. cost
4	1438	160	570	210	---	30	2408
5	1342	290	493	233	---	30	2388
6	1564	221	75	202	---	30	2092
16	1334	162	75	233	225	60	2089
BSLN	1460	324	210	255	225	55	2529

parts are found in ref. 22, and electronic parts are covered in ref. 23, though the data base is not the same in each case. Some information was also available for the Near-Term Electric Vehicle Program (ref. 3).

Battery costs are based on the goals for ISOA lead-acid batteries as given in the statement of work, giving an acquisition cost of \$2.00 per kg. Total battery cost is for the maximum battery pack weight as given in table 8. Motor/generator costs are for the machines as defined in the section "Power Train Characteristics," and the baseline is the only configuration with two electrical machines. Electronics includes all power control and system control devices, but does not include a battery charger. The transmission and differential are combined, since the final design concept has a combined unit. Miscellaneous items include clutches,control devices, and instrumentation.

Performance With Nickel-Zinc Batteries

The five candidate systems were sized and configured for use of lead-acid batteries; however, it was required that performance of these systems should also be evaluated when nickel-zinc batteries are used. This calculation was made by use of the full mission range dynamic program previously described. The most rigorous method of using this program was to make all calculations for a common battery weight, using a total weight of batteries corresponding to 28 standard 6-V batteries.

The comparisons are shown in fig. 74. For all but the baseline system, the weight of 734 kg of batteries is a significant increase over what was originally calculated as necessary for 161-km range, accounting for the long range shown. The range achievable with the two lead-acid battery types does not differ much for the three basic systems, when the J227a schedule D cycle is driven. The nickel-zinc batteries, which have about twice the energy density of the lead-acid batteries, do not have fully twice the range. The large capacity of the nickel-zinc batteries, however, would permit a great reduction in vehicle weight to achieve the specified range.

Final Propulsion System Selections

The final selection of two systems for conceptual design in Task III was made by a process of elimination, based on the tradeoff studies.

Configuration 6 was eliminated because of the difficulty in meeting maximum acceleration performance, and because it did not appear that dc motor design (fig. 31) could be improved enough to overcome this difficulty. Design of dc motors is a relatively mature technology, and major improvements are not anticipated.

The baseline configuration was eliminated because it gave the heaviest vehicle weight, and was the most complex and expensive of the five systems. None of the drawbacks was major, but they were sufficient to give preference to the other flywheel system, configuration 16. A flywheel system was clearly desirable because of the acceleration performance capabilities.

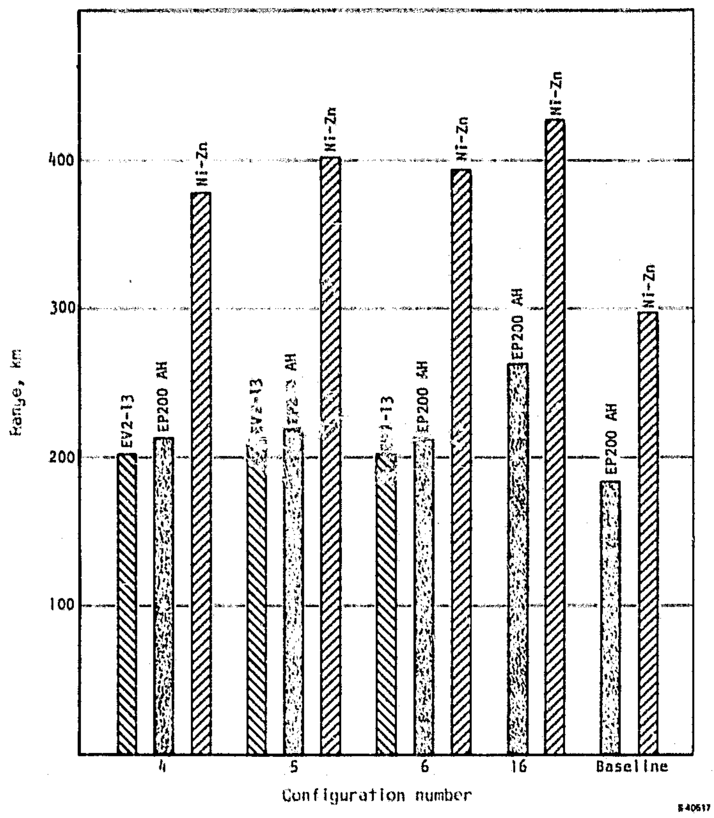

Figure 74.--Comparison of range vs battery type driving SAE J227a schedule D cycle (battery weight 734 kg).

In comparisons between the remaining basic systems (configurations 4 and 5), configuration 4 gave a vehicle weight 55 kg heavier and $20 more expensive, though neither of these differences is large. The permanent magnet motor used in configuration 5 (fig. 34) is more efficient then the induction motor of configuration 4 (fig. 33), which is reflected in a lower battery weight for configuration 5. The CVT transmission used in configuration 5 requires development effort with some technological risk, but the multiratio transmission of configuration 4 is also not available as a standard item (ref. 24). Altogether, configuration 5 appears to have a small but real advantage over configuration 4.

CONCEPTUAL DESIGNS

The preceding section discussed the selection of two propulsion system configurations for conceptual design studies. One system, configuration 5, is a basic system; the other choice, configuration 16, is a flywheel system. In the conceptual design process, some changes were made to the individual components to aid the package integration. Although maximum acceleration performance was improved, no other significant changes were made in system weight, cost, or performance. The principal features of these systems are as follows:

> Basic System--Brushless dc permanent-magnet motor, variable frequency inverter, traction continuously variable transmission (CVT)
>
> Flywheel System--Dc shunt motor, step voltage start and field control above base speed, continuously variable transmission (CVT), flywheel clutched to motor

A physical and functional description of these two systems is presented in the following paragraphs. Life-cycle cost information is presented in a subsequent section.

Description of Basic System

The basic propulsion system is configured as a front-wheel drive unit, as shown in fig. 75. The equipment is compact enough to fit easily below the hood line of a typical automobile. The drivetrain components, which transmit the power from the traction motor to the axle, are in a single, compact unit that connects to the front axles through universal joints. The electronic control unit, packaged as a separate item, is shown directly behind the drive train package.

The drivetrain unit is shown in greater detail in fig. 76. The unit is 67.3 cm long and 57.8 cm high, and has an estimated weight of 72.2 kg. The unit has self-contained cooling and lubrication, and requires only electrical power for operation and control.

A cross-sectional view of the drivetrain package is shown in fig. 77, and the major components are identified. The motor, on the left, connects through a fixed ratio speed reduction to the input of the continuously variable traction unit. The output of the CVT is through a single gear set and then a chain drive to the differential.

Traction motor--The traction motor is a brushless dc permanent-magnet (PM) motor, rated at 32 kW. This motor is identical in design to a motor currently being built under a NASA contract*, though rated power is 23 percent greater.

*NASA Contract DEN 3-77 for an Advanced Electric Motor was awarded to AiResearch Manufacturing Company of California on October 18, 1978.

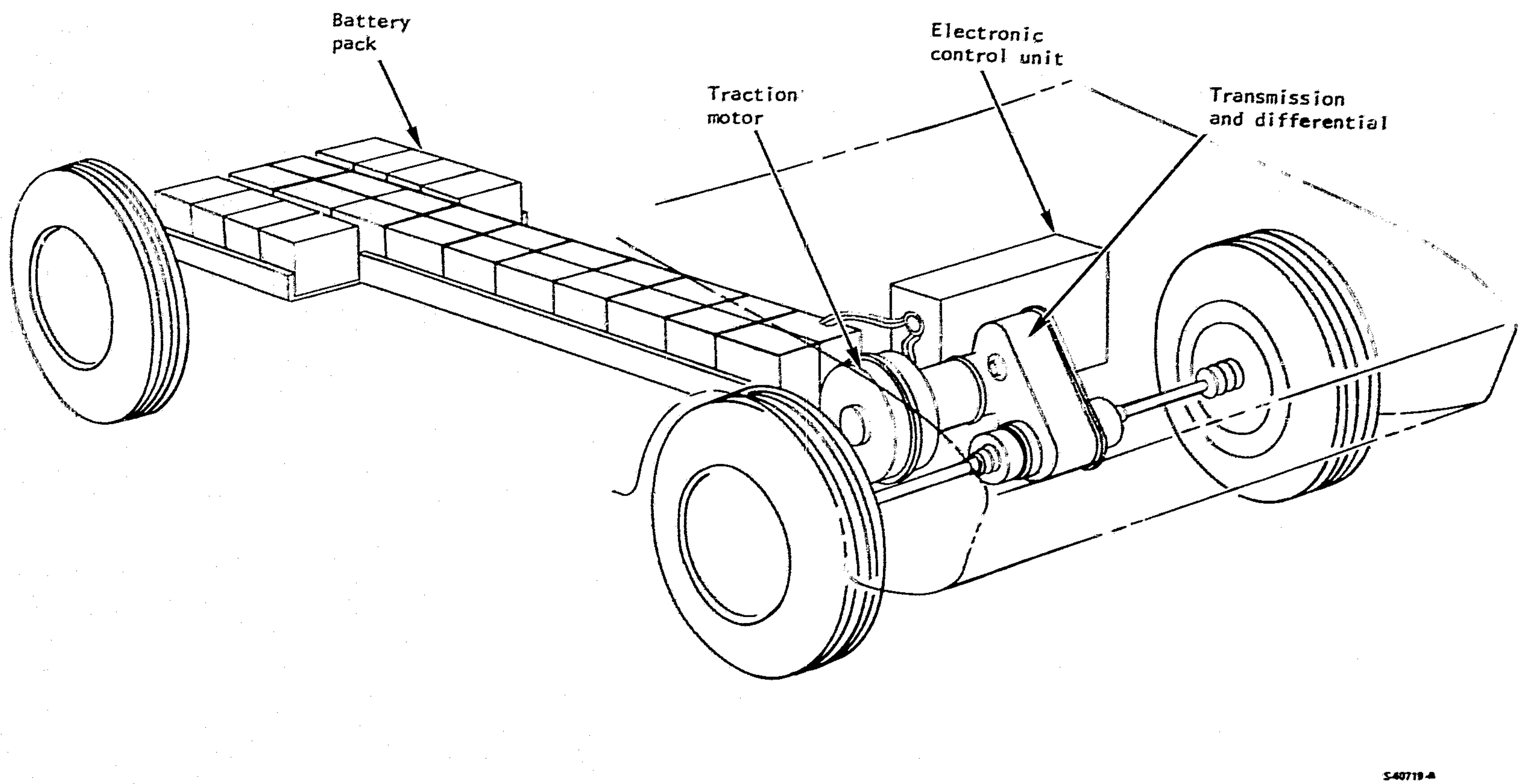

Figure 75.--Conceptual arrangement of basic propulsion system.

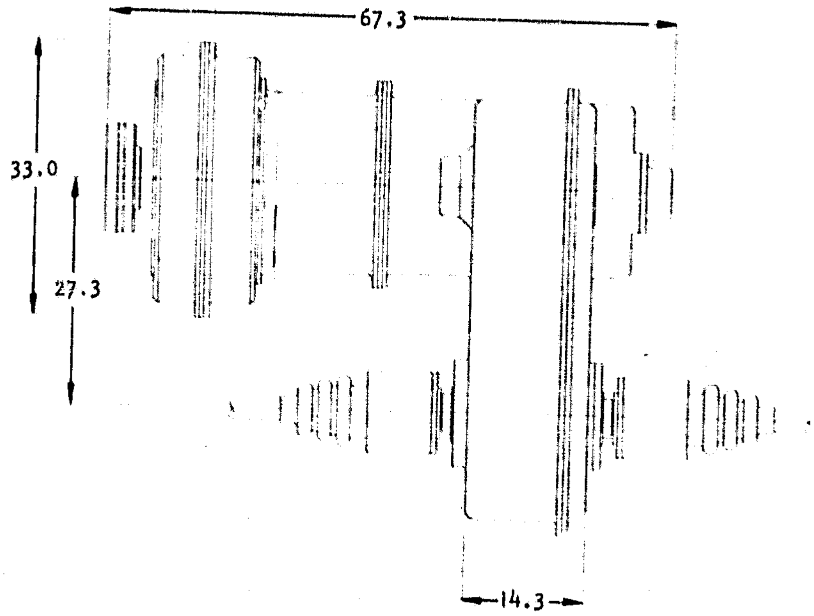

Front view

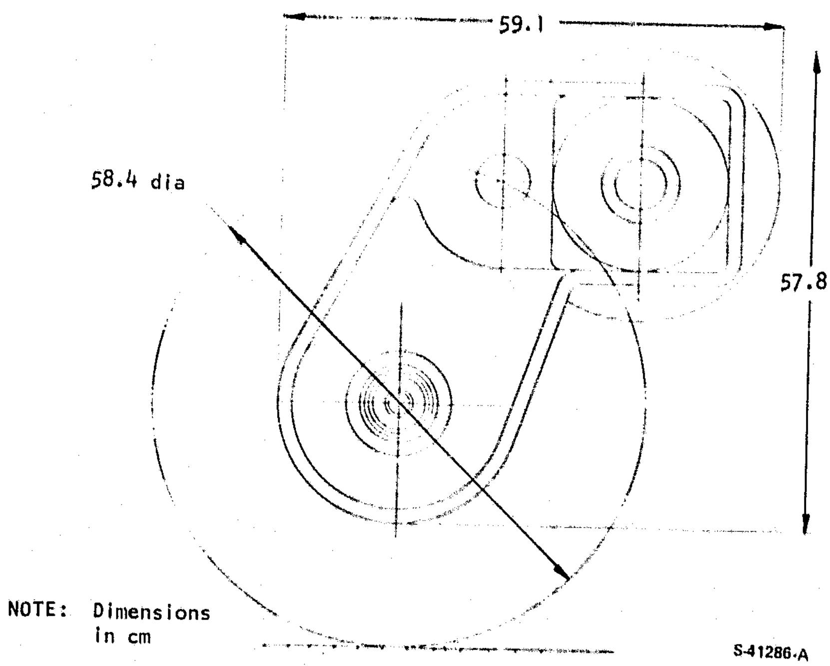

Side view

Figure 76.--Basic system drivetrain package.

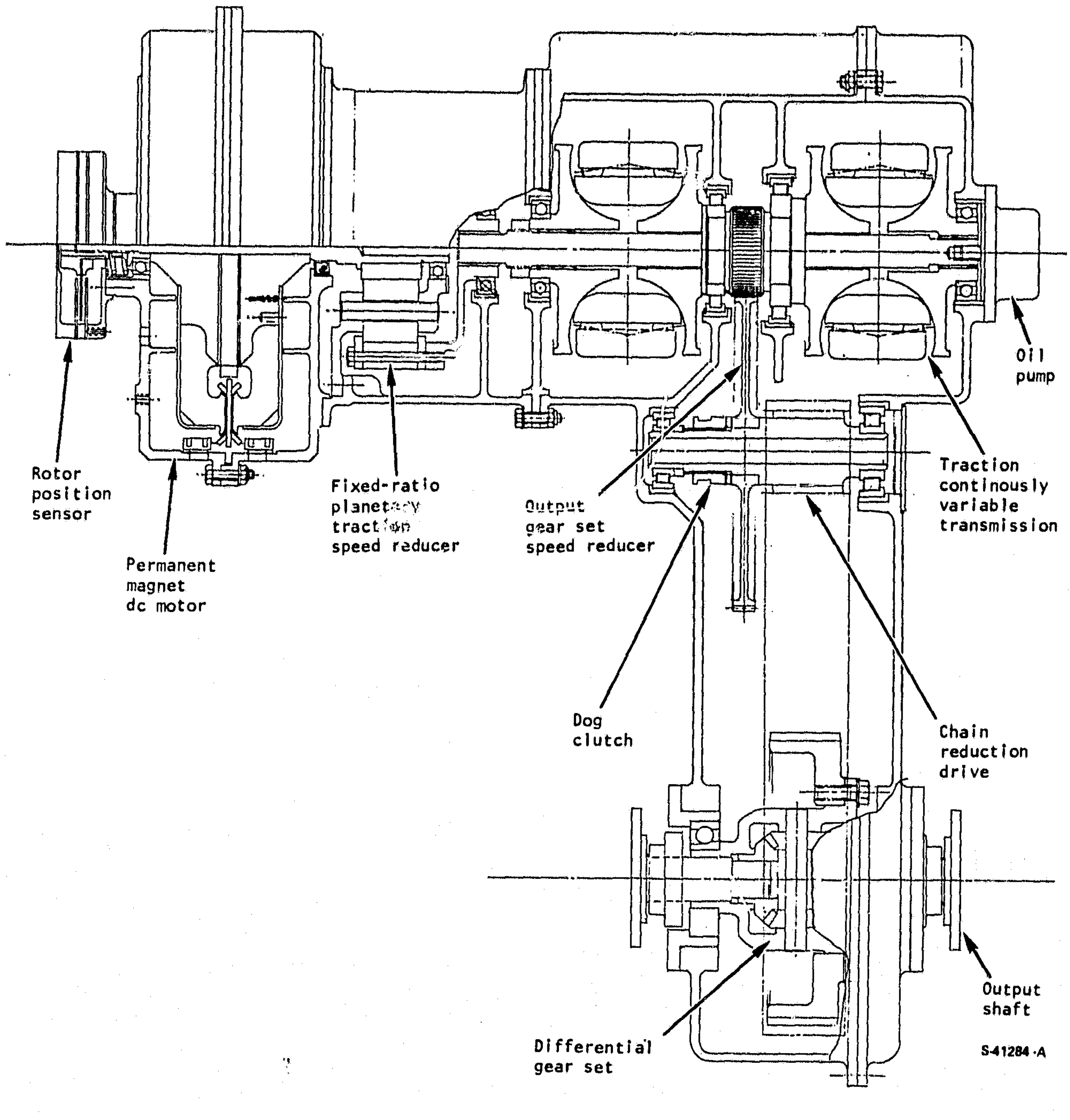

Figure 77.--Section view of basic system drivetrain.

The motor has the configuration of an axipolar machine, basically an axial-gap inductor machine with an ironless stator. Excitation is provided by a 15 MG-Oe misch metal magnet. To permit self-synchronous starting and running, the rotor position of the motor will be sensed by a six-element, solid-state, infrared source and sensor reading slots in a cylinder attached to the motor shaft. This is a proven device used in various self-synchronous PM motors to control inverter firing angle, and is contained within the housing on the left end.

During starting and running the rotor poles and the stator magnetomotive force are maintained in a synchronous relationship by inverter logic circuits so that no slip occurs. The logic circuits respond to rotor position signals up to approximately five percent of rated motor speed. Above this speed the logic circuits respond to the voltage induced in the stator winding by the rotor field. This method of operation takes into account the field distortion caused by armature current and improves the power factor of the motor as compared to what is possible by only sensing rotor position. At all times the motor is functioning as a synchronous machine. This type of operation is called self synchronous because the system is continually self adjusting, always maintaining synchronous operation, and pull-out cannot occur regardless of applied load.

A primary factor favoring the axipolar concept is its simplicity and suitability for low-cost production. The rotor is comprised of two identical, five-fingered sections separated by a magnet. The two rotor sections could be either forged or cast. An aluminum shroud covers each rotor section to direct the rotor-induced airflow over the stationary stator coils. The shroud also reduces rotor windage loss.

The stator is comprised of simple, machine-wound coils, and ribbon conductors are used to minimize eddy loss in the conductors. The ribbon conductors provide desired rigidity to the coils, which are bonded together and supported at the stator OD. Ribbon conductors provide superior heat transfer as compared to round wire, mush-wound coils or substrate-mounted, printed-circuit conductors. Ribbon conductors also provide the most efficient utilization of the space between the poles. The stator does not contain iron so the typical iron losses are eliminated.

The rotor inherently provides centrifugal fan action. Pumping loss is regulated automatically to stator heating requirements by using a butterfly valve actuated by a bimetal coil actuator in the stator exit air duct. This is similar to the choke actuator on automobile engines. Thus, at higher-speed cruise conditions with low power demand, the motor efficiency is improved by reducing airflow pumped by the motor rotor.

In the initial tradeoff studies rated motor output was established as 26 kW, and maximum power was 60 kW. It was found, however, that efficiency at 60 kW, during maximum acceleration, dropped off so much that battery drain was excessive. Therefore, it was decided to increase rated power, which required a seven percent increase in motor dimensions. The calculated motor performance characteristics are shown in fig. 78.

Rated motor power has been increased from 26 kW to 32 kW to avoid the sharp drop in efficiency at the power output of 60 kW. Top speed has been reduced from 14 000 rpm to 13 000 rpm to maintain the same peripheral velocity. The ten-pole machine has a frequency at maximum speed of 1083 Hz.

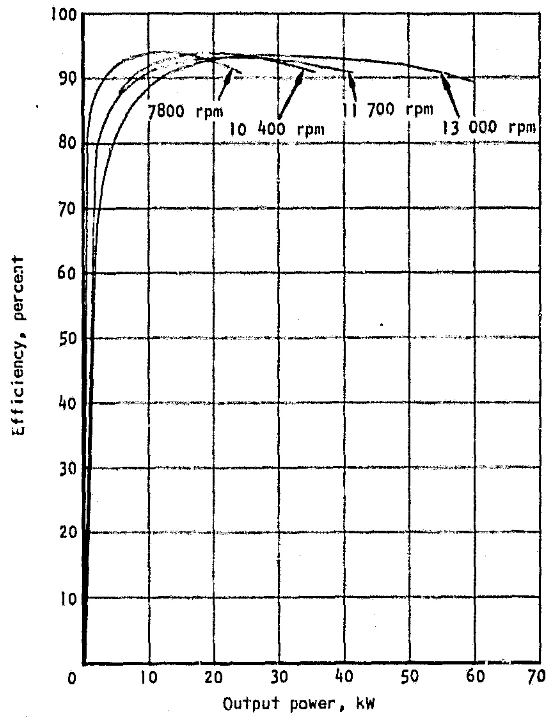

Figure 78.--Permanent magnet motor performance.

Transmission. -- The initial transmission stage is a fixed ratio 3:1 speed reducer. This device is a traction unit configured in a planetary design with the planet rollers fixed to the housing. All elements operate in pure rolling contact. This design was chosen because it provides smooth, quiet power transmission at efficiencies in excess of 97 percent. The design is similar to other units that have been built and tested (refs. 13 and 25).

The variable action of the CVT is achieved in the double-cavity toroidal drive. The main shaft of the transmission has a drive disc attached to each end; the discs have a section of toroidal shape. Two similar discs are located inboard of the outer discs, and form the two cavities. The inboard discs are mounted on separate bearings and are capable of a limited amount of axial motion. Rollers, mounted on swivel shafts, contact each set of inboard and outboard discs. The drive ratio is changed by swiveling the contact rollers from contacts close to center on the drive discs and far from center on the driven discs to the other extreme of far from center on the drive discs to close to center on the driven discs. The rollers are not forced into ratio position but are steered as the wheels of a car by low-pressure hydraulic pistons that balance internal tangential forces that are generated at the roller contacts.

The transmission of power between smooth rolling surfaces requires a substantial normal force, but the contact loads must be low enough to ensure an adequate fatigue life. Power transmission also is limited by the possibility of slip between the rollers, since slip leads to rapid wear failure. These limits have been increased by the use of modern traction lubricants that provide high resistance to slip and high viscosity to reduce wear. These new lubricants have considerably extended the power range of traction transmissions, permitted the use of higher forces, and extended transmission life. The contact forces required are heaviest when the traction contact is close to the centerline of the drive disc, and lower as the contact running radius becomes greater on the drive disc. This contact force is adjusted by a loading cam located between the two central discs that provides a separating force and thereby generates equal forces for the two cavities. The contact forces are balanced within the end disc, and no heavy thrust bearings are required for the rotating assembly.

An oil pump is located on the end of the CVT to provide pressure for the hydraulic control pistons and circulation of lubrication. Control of the pistons, which position the traction rollers, is accomplished by an electrohydraulic valve, which establishes the CVT ratio in response to an electrical control signal. The power output of the CVT is through the central gear, with a reduction ratio of 4.2:1. The CVT ratio ranges from a reduction of 2.8:1 to an overdrive of 0.35:1. The fixed-ratio planetary traction speed reducer at the CVT input reduces the motor shaft speed at 13 000 rpm to a CVT input of 4300 rpm. This input speed remains constant over most of the range of vehicle operation, except for the range of zero to 12.8 km/hr. The CVT then controls vehicle speed by changing the ratio as required, with continuous variation from reduction to overdrive. The calculated CVT performance is shown in fig. 79.

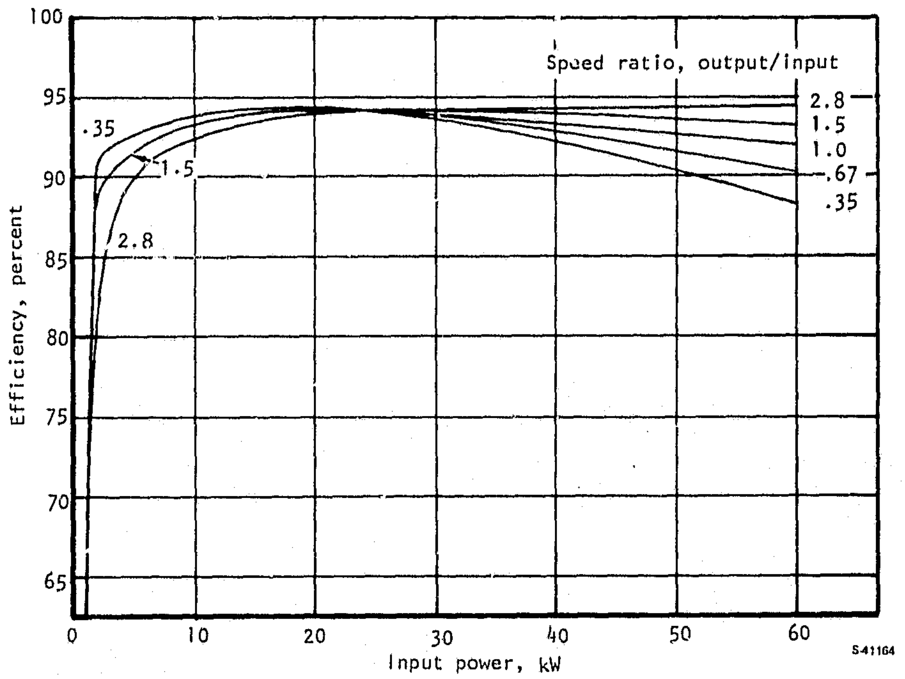

Figure 79.--Traction continuously variable transmission.

Output drive and diffential.--The output of the CVT is first through a gear reduction, and then through a chain reduction of 3:1 to the differential. This output speed reduction can be accomplished at high efficiency by careful attention to gear design, bearing selection, and lubrication control.

The losses in a speed reducer are attributed to several principal effects:

(1) Meshing Losses--Sliding losses of the tooth surfaces, proportional to load, speed, tooth accuracy, and surface finish

(2) Bearing Losses--Proportional to torque, bearing size, and the square of the speed

(3) Lubricant Churning and Pumping Losses--Proportional to the square of the speed

The design presented minimizes meshing losses by use of spur gears where the predominant motion is rolling rather than sliding. Bearing losses are minimized by the use of ball bearings carefully sized for the load. Lubricant churning and pumping losses are minimized by use of mist lubrication and avoidance of moving elements in the oil sump. Lubrication is common with the CVT, using the same lubricant and with circulation by the CVT oil pump. By proper attention to all these points, it is possible to achieve a gear mesh efficiency as high as 99 percent.

Chain drives have been shown to achieve very high efficiencies over a broad range of operation. Comparative data on gear and chain drives are shown in table 10 (ref. 11).

TABLE 10.--GEAR AND CHAIN DRIVE EFFICIENCY

Torque, N m	Hypoid gear efficiency, percent	*Hy Vo Chain	Spiral bevel gear efficiency, percent
250	96.5	98.5	98
150	93	98.5	97.5
25	89	98	94.5

*Chain manufactured by Morse Chain Company

Electronic control unit.--The electronic control unit is located in a separate package with an estimated weight of 38.5 kg. This weight includes electronic components, heat sinks, and cooling fan. The electronic control unit consists of two main systems: the power control unit for control of motor power and the system controller (a microprocessor) that controls system operation in response to drive commands.

The basic control scheme for the motor includes the following: a chopper that controls the motor current; a silicon-controlled rectifier (SCR) inverter with an auxiliary commutator for commutating the inverter switches during the motor start sequence; and a regenerative switching scheme that returns energy to the battery during braking. A block diagram of the electronic control unit is shown in fig. 80.

The electronic control unit is completely solid state. There are no relays or mechanical switches, and the basic control scheme has been structured so that state-of-the-art components (e.g., pulse width modulation integrated circuit, CMOS switches, microprocessor) can be utilized to improve flexibility and minimize cost, size, and weight. The risk involved in mechanization of the proposed controller is minimal since all of the major concepts involved have been used in previously built state-of-the-art hardware.

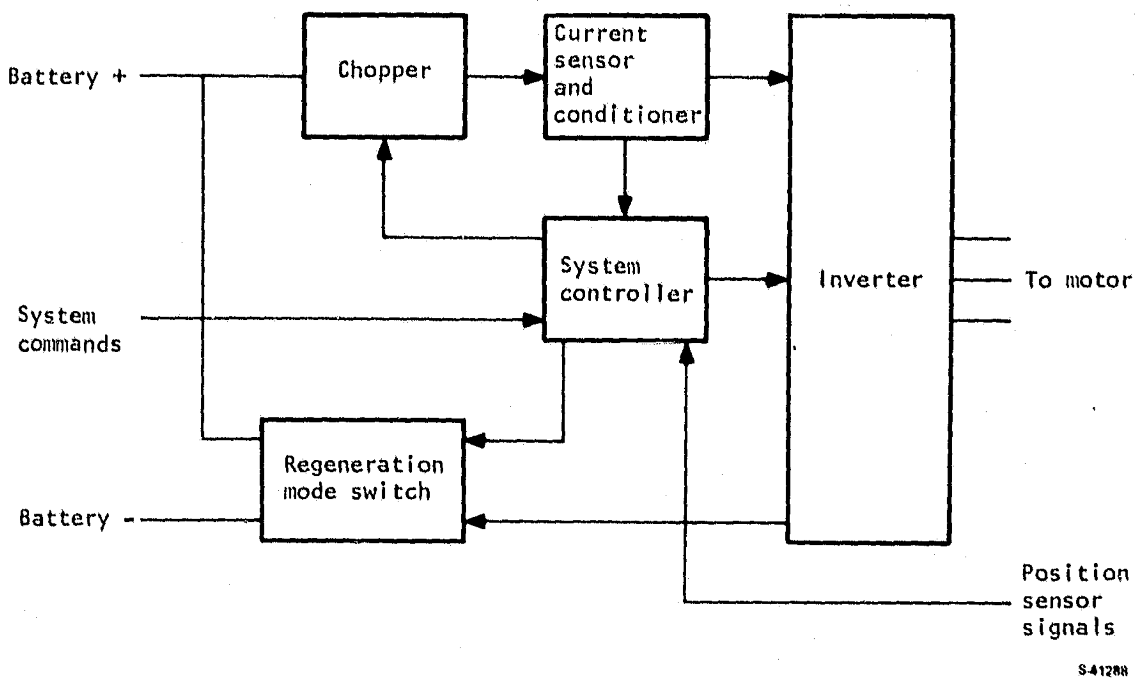

Figure 80.--Electronic control unit block diagram.

The inverter power section is functionally identical to those used for a pump motor controller. These inverter bridges are of conventional design and require minimal development effort. A schematic of the unit is shown in fig. 81.

The auxiliary commutator is also identical to that recently developed for a pump motor controller. As shown on the diagram, this commutator utilizes three significant components: a diode (CR5), an SCR (CR2), and a capacitor (C2). The inverter devices are inhibited from functioning until capacitor (C2) is charged by the chopper. When the voltage across C2 has reached a predetermined value, the inverter devices are allowed to operate under control of the inverter logic circuit. When commutation is required, SCR CR2 is turned on

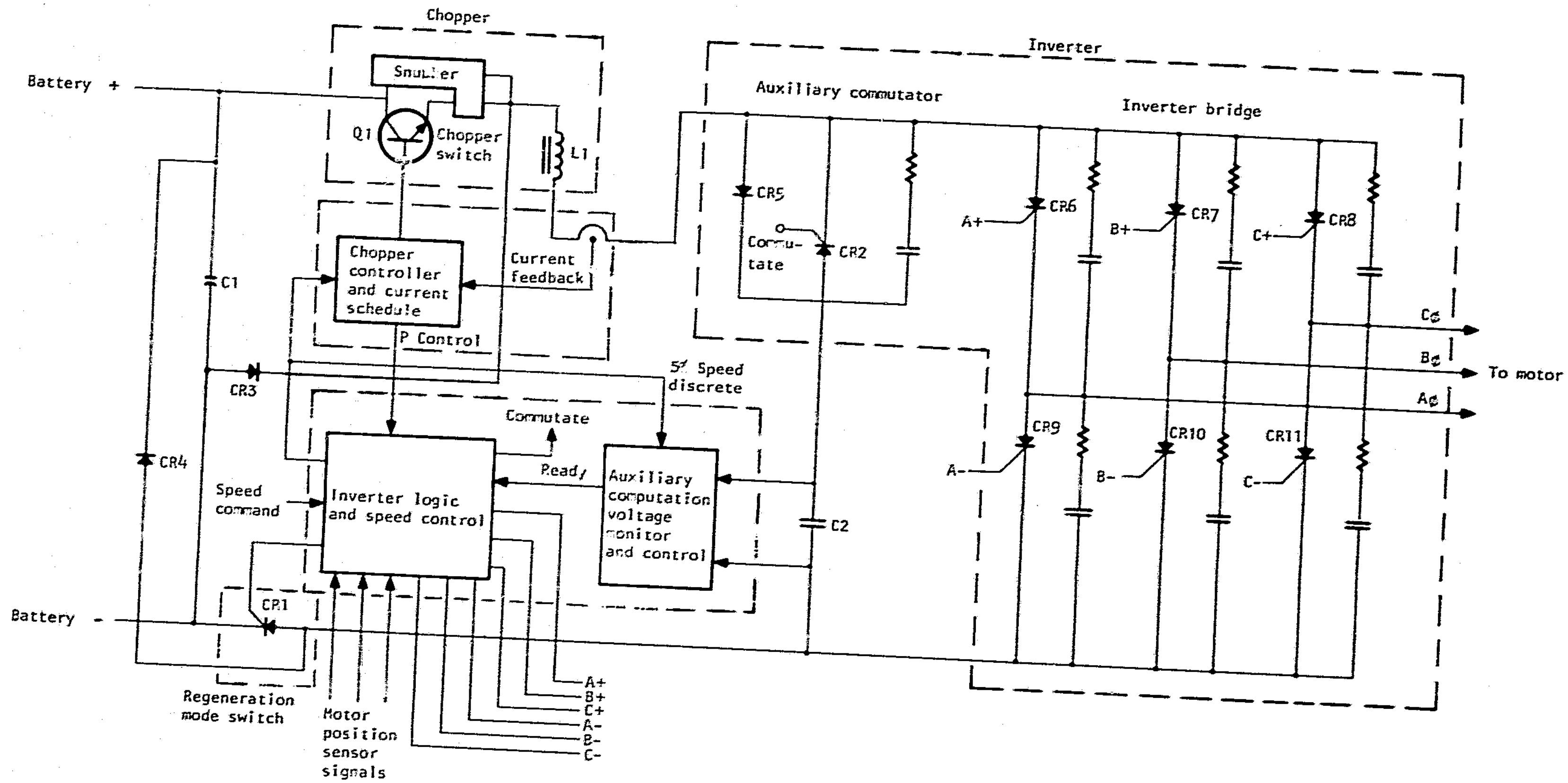

Figure 81.--Power control unit schematic.

allowing the motor inductance to resonate with capacitor C2. During the first negative half-cycle of resonance, the inverter devices that had previously been on are commutated together with SCR CR2, and the logic drive to the inverter is inhibited, which prevents any further activity in the inverter until the capacitor C2 is recharged. This sequence is repeated six times per cycle until the inverter commutation mode is changed from forced commutation to line commutation.

The motor controller has three basic modes of operation:

(1) Start mode

(2) Run mode

(3) Regeneration mode

In the start mode, the chopper is actuated by the system controller, which uses signals from the rotor position sensors to activate the inverter switches in the correct sequence for rotation. In this mode of operation, the motor current is controlled by the chopper. Inverter commutation, which is required six times per back emf cycle, is effected by the auxiliary commutation circuit. When the motor has attained a speed at which the back emf is adequate for natural commutation, the control mode is automatically changed to the run mode.

In the run mode the chopper is set to maximum duty cycle, and the motor current is controlled by varying the β angle of the inverter. Thus the system power dissipation is minimized by allowing the motor back emf to be at maximum voltage at approximately 50 percent speed. At all speeds between 50 percent and 100 percent, the β angle is adjusted to alter the effective back emf of the motor. The result is similar to field weakening in a conventional dc machine. This mechanization minimizes the size and weight and maximizes the efficiency of the system. When braking is required, the system controller selects the regeneration mode.

When braking is required, the chopper output current is commanded to zero. This allows all inverter devices, CR6-CR11, and the regeneration mode switch, CR1, to commutate. The inverter controller then selects first quadrant operation for the inverter and the motor, which is now functioning as a generator, and returns current to the battery through diode CR4. This current level is also controlled by varying the inverter angle. The current path in this mode of operation is comprised of flyback diode CR3, inductor L1, the inverter bridge, and diode CR4.

A significant portion of the power dissipated by the motor controller is in the chopper. The size and weight of the chopper/choke are also affected by the chopper frequency. The optimum chopper switch has a low saturation voltage and minimal rise and fall times. This permits high-frequency operation of the chopper (10 to 15 kc) and minimizes the size and weight of the choke. Several transistor manufacturers are involved in developing such a transistor. Power Transistor Company of Carson, California, is currently producing transistors capable of switching up to 600 A at 8 kc. Based on current market trends, other manufacturers will produce similar devices that will greatly reduce the existing cost of these devices, and improve their performance. Power Transistor Company is already producing low current (≈30-A collector current) versions of these devices.

Description of Flywheel System

The flywheel propulsion system is configured as a front-wheel drive unit, shown in fig. 82. The equipment is designed to fit below the hoodline of an automobile as may be seen by comparison to the wheel shown in the side view of fig. 83.

The drivetrain package is 57.8 cm high vertically, is 104.8 cm overall from the motor on the left to the flywheel on the right, and has an estimated weight of 152.3 kg. The unit is self-contained with regard to provisions for cooling and lubrication, and requires only electrical power for operation and control.

A cross-sectional view of the drivetrain package, which transmits the power from the traction motor to the axle, is shown in fig. 84, and the major components are identified. The motor, on the left, is connected to the main shaft of the CVT, and the flywheel, on the right, is connected to the same shaft through a gear set and clutch. The CVT has a regenerative geartrain terminating in a planetary gear set from which the CVT output is taken to a chain drive and differential.

Traction motor.--The traction motor is a dc motor, mechanically commutated, with a separately excited field. The motor is rated at 25 kW continuous duty in the speed range of 4000 to 8000 rpm. The motor design has been optimized for high efficiency at low power outputs. The motor has been slightly reduced in rated power below the value used in previous tradeoff studies, to 25 kW, because the system does not have the high overload requirements associated with maximum acceleration, and efficiency is nearly constant in the 25- to 30-kW range. Therefore, the motor can still provide adequate power for the sustained grade requirements without the need for an installed capacity of 60 kW. The motor speed range has been adjusted for use with a flywheel system operating between full speed and half speed. Motor base speed has been established as 4000 rpm and maximum speed as 8000 rpm. The calculated motor performance characteristics are shown in fig. 85

The motor laminations are made of AISI M-19 grade electrical steel, 0.046 cm thick, separated by a C-5 high-temperature insulation coating. The selection of the lamination material and coating was made to minimize both eddy current losses and hysteresis losses. The laminations and coil supports are pressed on the shaft, which is fluted in the center area. The commutator is heat shrunk on the shaft to eliminate the need for a keyway and save space. The armature coils are form wound from rectangular copper wire, which is insulated with polyimide tape. The coils are held in the slots by fiberglass slot wedges.

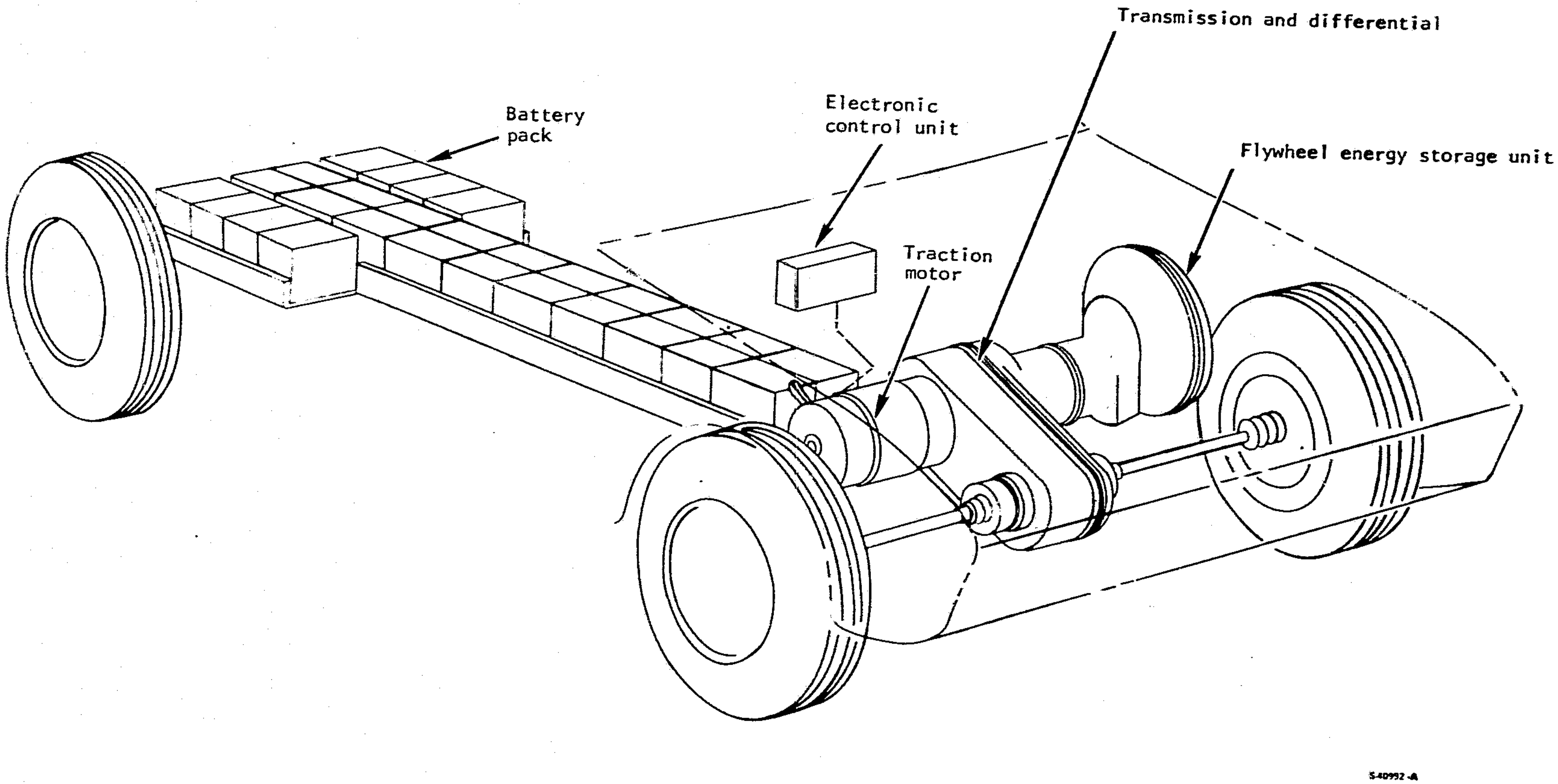

Figure 82.--Conceptual arrangement of flywheel propulsion system.

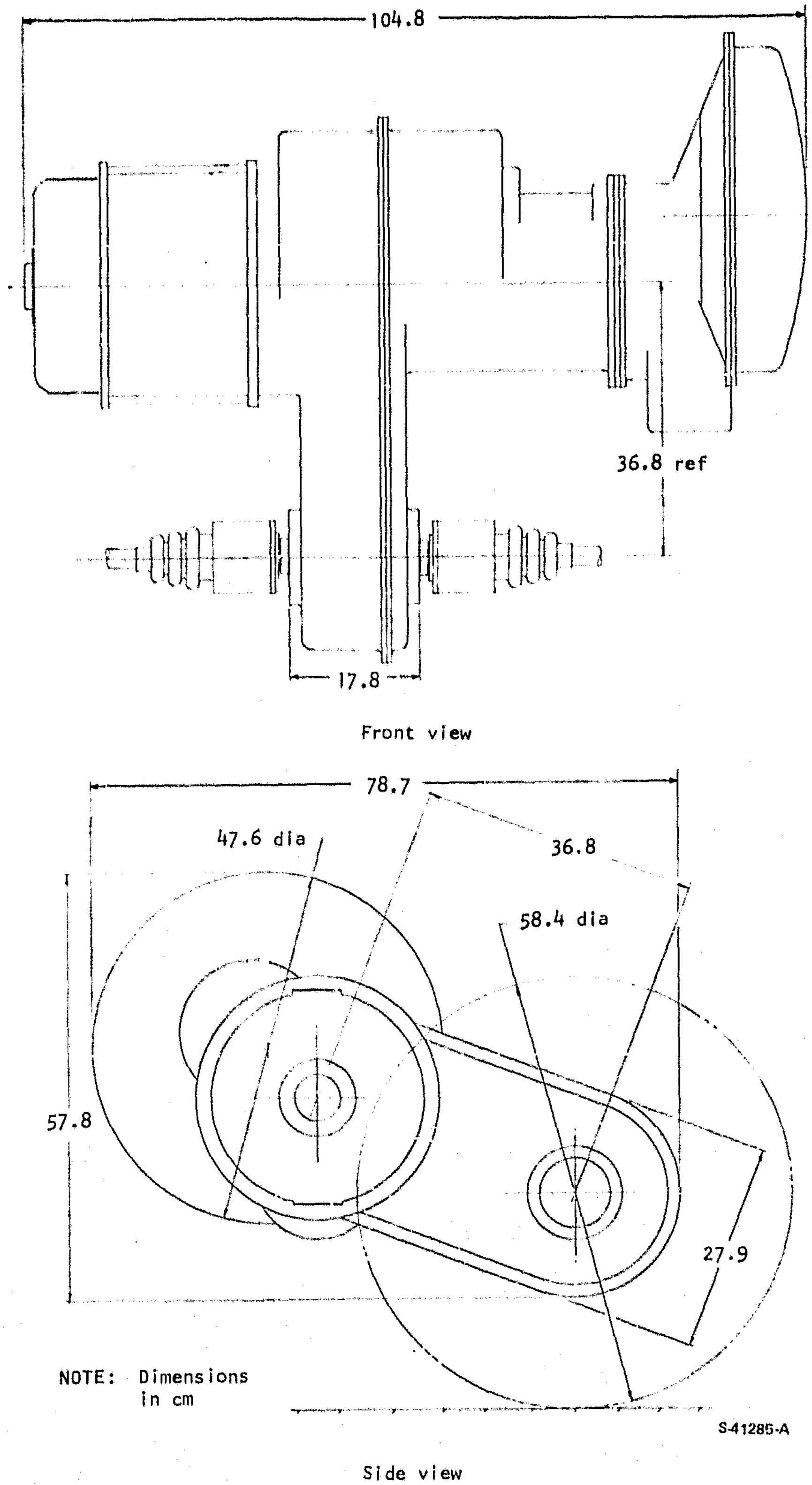

Figure 83.--Flywheel system drive train package.

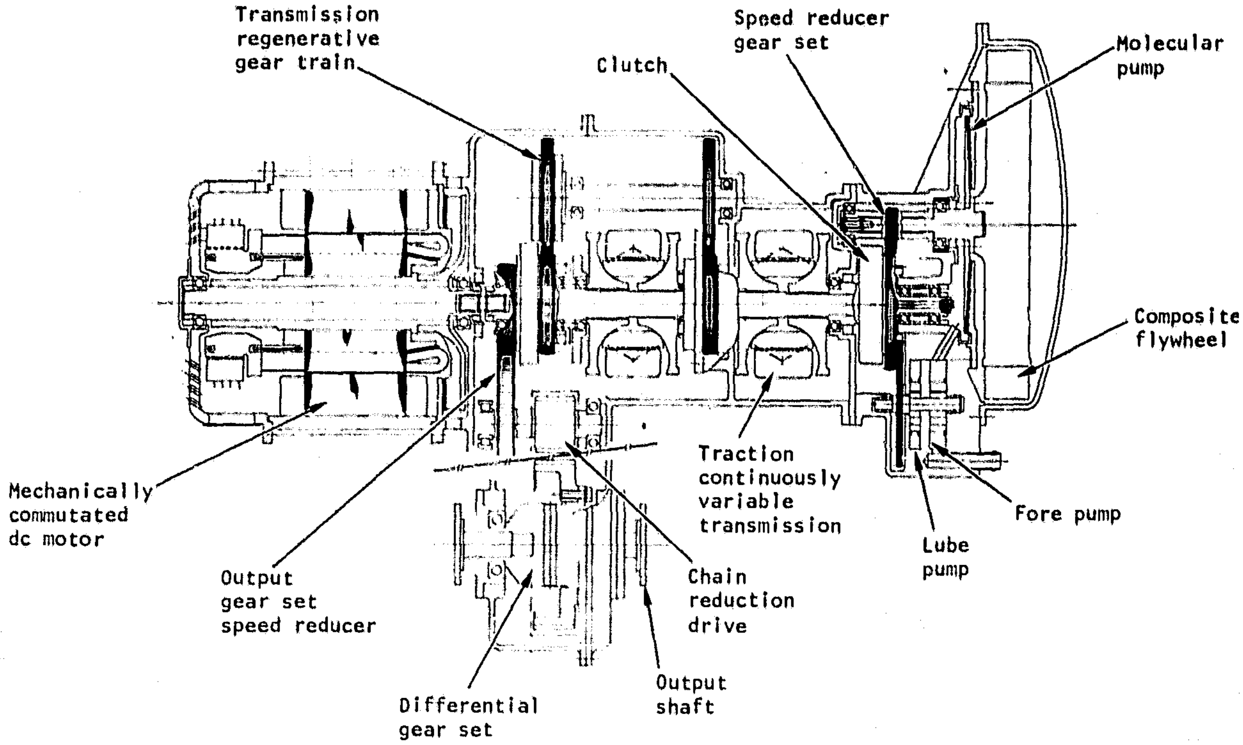

Section view

S-41287

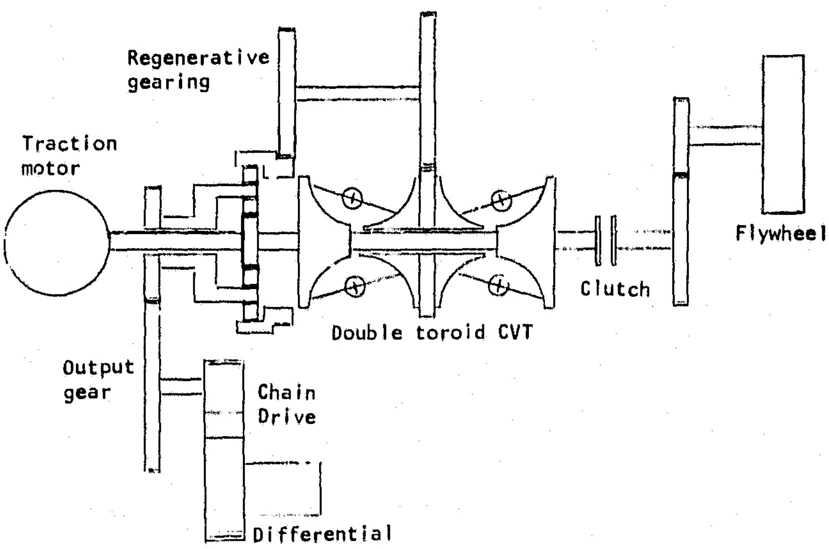

S-44199

Mechanical schematic

Figure 84.--Section view of flywheel system drive train package.

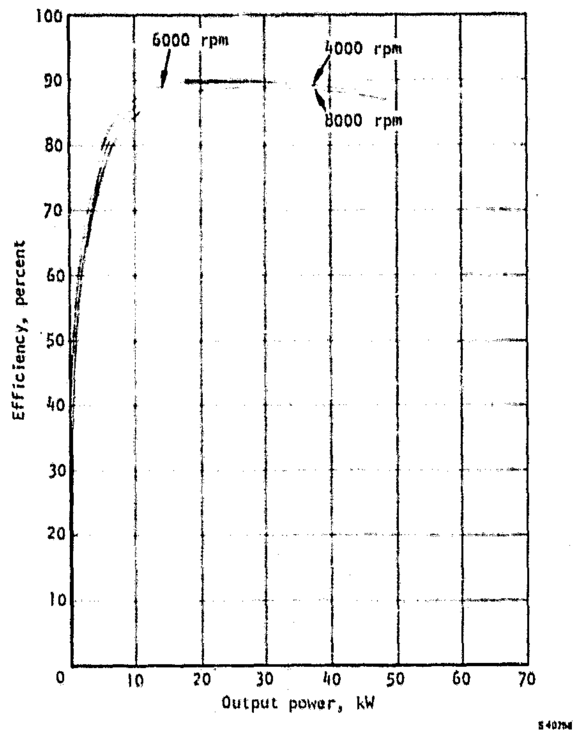

Figure 85.--Dc shunt motor performance

The magnetic portion of the frame consists of a rolled steel ring welded at the seam. The main poles are made of electrical steel secured by rivets. The air gap of the main poles is uneven, with a larger gap at the leading edge to minimize the effects of uneven magnetization. The interpoles incorporated to aid commutation and minimize armature reaction are of solid steel with welded pole shoes. The main pole coils are wound from round copper wire with varnish insulation of IEEE class F (155°C). The interpole coils are wound from rectangular wire with tape insulation.

The endbells are of cast aluminum with steel inserts for bearing supports. The bearings are sealed ball bearings. The end bells are held to the frame by common studs through the endbell flanges. The brushholders are mounted to the rear endbell, with brushes of an electrographitic type selected for durability.

The motor is air cooled by a fan mounted on the shaft. The fan is molded of high-strength plastic with inclined blades shaped for efficiency and quietness. The air enters through louvers on the endbell, cooling first the commutator and brushes to maximize commutator life.

The designs of the uneven air gaps, the brushes, and fan blades are made for optimum performance in the forward direction. The backup mode, with the motor in reverse rotation, is done infrequently and at low power levels, and a lower performance is acceptable under these conditions.

Flywheel energy storage unit.--The flywheel energy storage unit operates in an evacuated housing at a maximum speed of 35 000 rpm. The shaft speed is reduced by a 4.4:1 gear set to match the highest main shaft speed of 8000 rpm. A clutch is used to disengage the flywheel when the vehicle is stopped or moving in reverse.

The flywheel consists of a rim of several rings of filament-wound composite material mounted on a metal star-shaped hub, sized for an energy content of 250 W-hr at a speed of 35 000 rpm. In the composite rings the filaments are joined by a low-strength interlaminate epoxy that gives the ring integrity. The principal filament material is Kevlar-49, and the rim is mounted on a four-spoke aluminum hub.

The flywheel rotor cavity is maintained at a vacuum level below 1.5 microns to minimize windage and frictional heating of the composite material of the flywheel rim. The flywheel chamber is maintained at its designated low level by use of a molecular pump located between the flywheel and the bearing. The molecular pump consists of a disc rotating at flywheel speed and a stator mounted on the housing, separated from the disc by a gap of a few thousandths of a centimeter. The stator has grooves in the form of an Archimedes spiral that guide the passage of air molecules from the periphery to the center outlet. The molecular pump cannot work efficiently against an atmospheric discharge pressure; therefore, a forepump is used to provide an intermediary vacuum level.

On the same shaft as the forepump, a lubrication pump is also included to provide positive bearing lubrication. The flywheel lubrication system is sealed, and separate from the CVT system.

Transmission.--The continuously variable transmission used in the flywheel system differs from the simpler version used in the basic system in the use of a regenerative gear train. The regenerative gear train enables the CVT to obtain reduction ratios as great as 24:1 (an output/input ratio of 0.042). When the unit is operating in extreme reduction, a large percentage of the total power is being recirculated through the regenerative gear train, and efficiency is lower than for the simpler CVT. There is also some loss in maximum efficiency due to the regenerative effect; however, the normal operating point at 72 km/hr in the SAE J227a (D) cycle is at nearly unity ratio and low power, where the CVT efficiency is above 90 percent. The calculated performance of the CVT is shown in fig. 86.

This broad range of CVT operation is needed in a flywheel system, since flywheel speed is usually highest when vehicle speed is lowest. When starting the vehicle, maximum transmission reduction is used so that the motor can accelerate up to flywheel speed while the vehicle speed is very low. The flywheel clutch is then engaged so that the flywheel supplies the primary acceleration power. During acceleration the CVT input speed is dropping while the output (vehicle) speed is rising.

The variable action of the CVT is achieved in the double-cavity toroidal drive as was described for the basic system CVT. The main shaft of the transmission has a drive disc attached to each end, and two similar discs are located inboard of the outer discs, forming the two cavities. Rollers, mounted on swivel

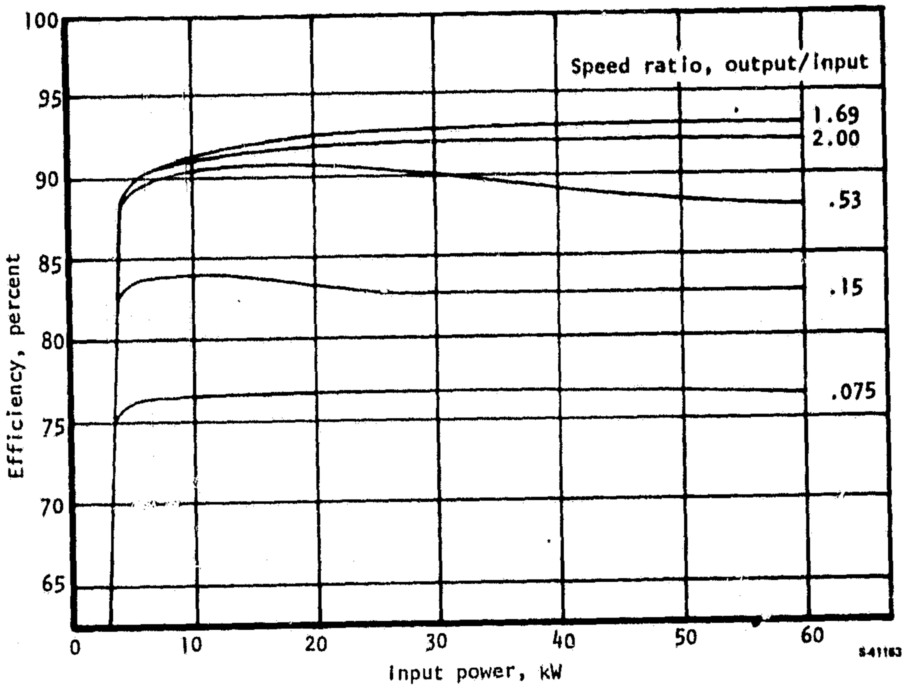

Figure 86.--Traction regenerative continuously variable transmission.

shafts, contact each set of inboard and outboard discs, and the drive ratio is changed by swiveling the contact rollers. The contact force is adjusted by a loading cam located beween the two central discs that provides a separating force, thereby generating equal forces for the two cavities. The contact forces are balanced within the end discs, and no heavy thrust bearings are required for the rotating assembly.

The output from the inboard discs is taken through a gear train to a final planetary gear set with the sun on the main shaft and the output taken from the planet carrier. This final CVT output then goes to the output drive and differential.

Output drive and differential.--The output drive consists of an initial gear reduction and a subsequent chain drive to the differential. This arrangement is nearly identical to that used in the basic system; however, an oil pump is located on the chain sprocket shaft to provide pressure for the CVT hydraulic control pistons and circulation of lubrication. Control of the pistons, which position the traction rollers, is accomplished by an electrohydraulic valve, which establishes the CVT ratio in response to an electrical control signal.

Electronic control unit.--The electronic control unit consists of the electrical control devices for start and run control of the propulsion system. The system controller (a microprocessor) controls system operation in response to drive commands. Motor speed is controlled by varying the current to the field windings, and only low power devices are required. Although the starting components carry high current, these components are not large. The entire unit has an estimated weight of 6.5 kg and occupies a volume of 6000 cm^3.

A schematic diagram of the power control unit, used to control motor power, is shown in fig. 87. The field chopper and controller are small electronic devices, individually packaged. The contactor is a switching device with arc suppression, typical of devices for automotive service. Although not shown, a separate set of contacts would be incorporated for motor reversal. The starting resistor is a current limiting device used only for a few seconds during motor starting, then bypassed during normal operation. The bypass is closed by the controller in response to the motor speed and current signals.

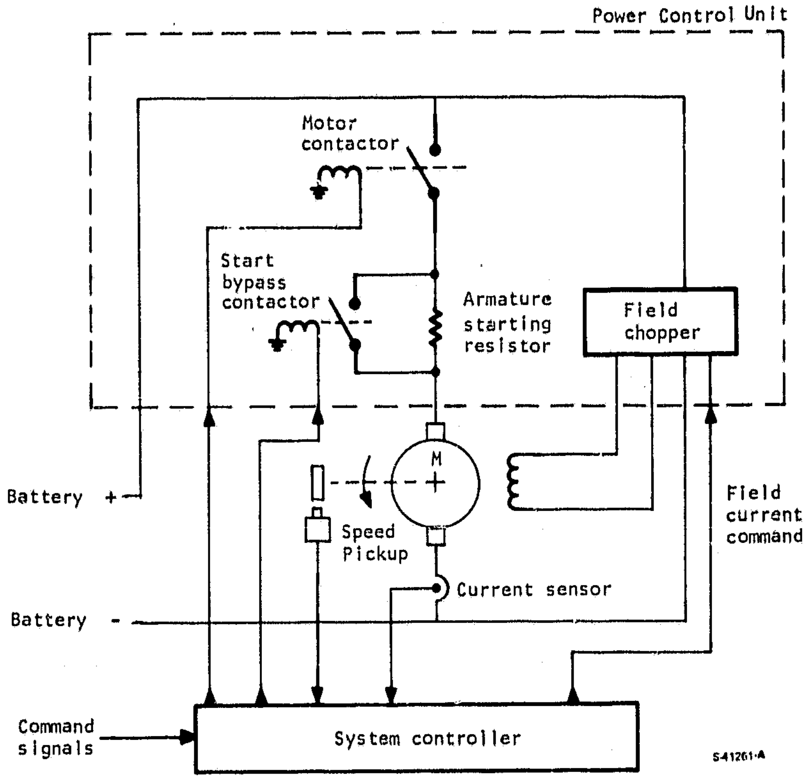

Figure 87.--Power control circuit

The principal operating device of the power control unit is the field chopper, used to control motor speed by varying the current in the field windings. The circuit diagram of the field chopper is shown in fig. 88.

The input command to the field chopper is shown on the schematic as "field current command," and the voltage level of this signal is proportional to the desired current at the output, indicated by "field coil." The command signal sets the pulse period for which the battery voltage is switched off and on, as shown in fig. 89. The pulse rate is constant, but the width, or duration, of the on and off periods can be varied by the command signal.

The current will flow through the windings when the circuit is on, but the inductance of the windings prevents instantaneous changes. The current will increase and decay about some average value, which gives a basic dc current with an ac ripple. A change in the pulse width will cause a corresponding shift in the average current.

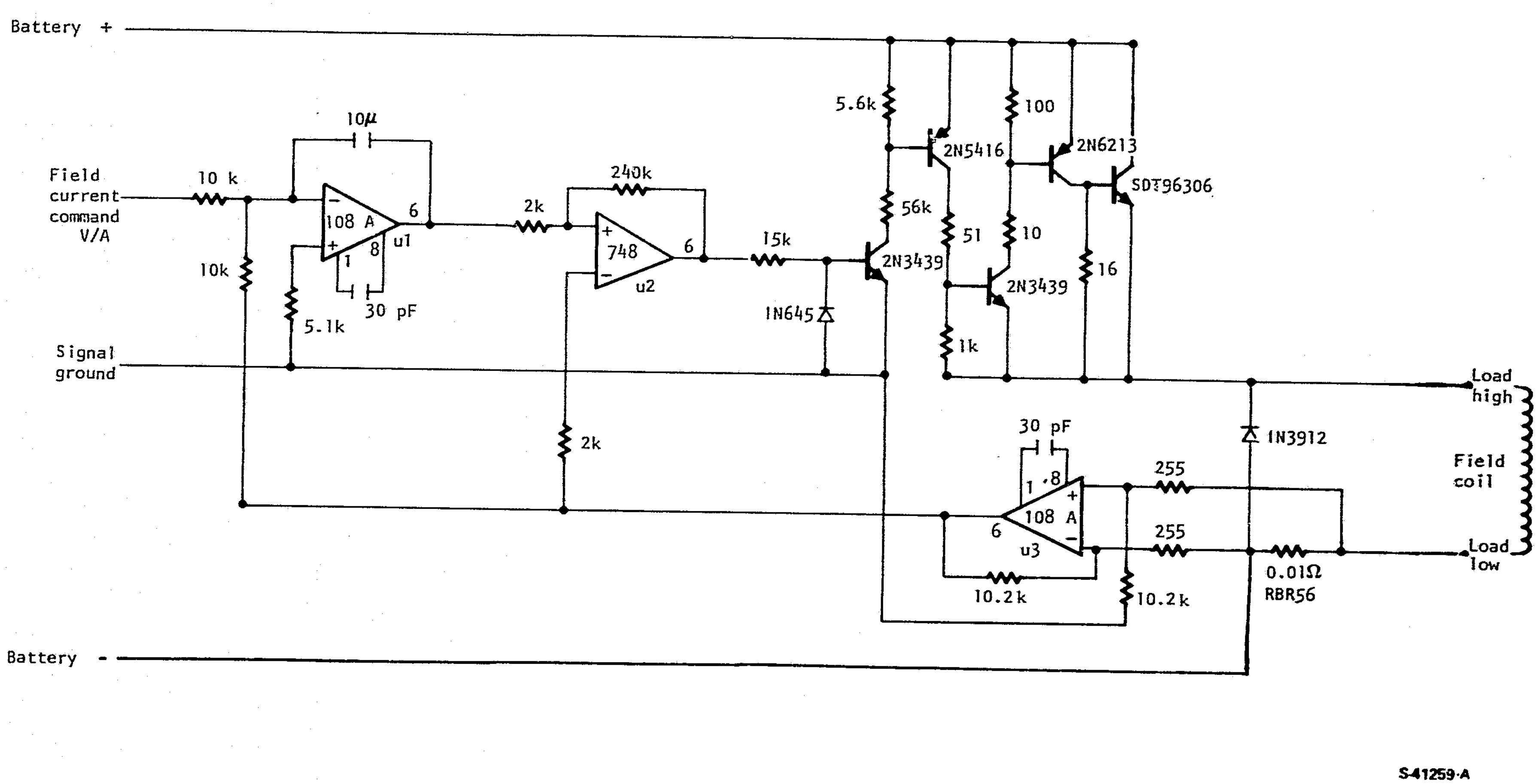

Figure 88.--Field chopper circuit.

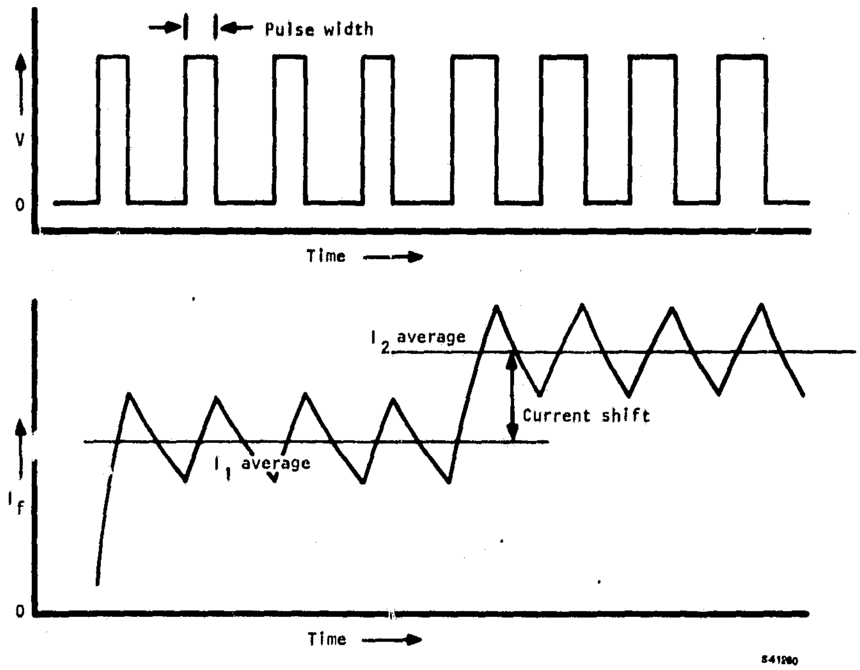

Figure 89.--Typical voltage and current trace from field chopper.

Performance Summary

The two conceptual designs were analyzed to determine significant variations in performance caused by subsequent design changes in the final design effort. Most variations were minor, and the most significant effect was due to the maximum acceleration requirement. This requirement is particularly difficult for the basic configuration, and the final battery selection was determined by this acceleration requirement.

Driving range.--Both designs can achieve the range requirements of 161 km with the J227a schedule D cycle and 209 km when the vehicle is driven at a constant 72 km/hr. The basic system is sized for the 161-km range, and it exceeds the 209-km range at constant speed. The flywheel system has higher operating losses at steady speed than the basic system, and the battery must be sized to achieve the 209-km range. The range with the driving cycle then greatly exceeds the required 161 km. The characteristics of the two systems are presented in table 11.

The flywheel system with nickel-zinc batteries will exceed all the range requirements, because this battery has twice the specific energy of the lead-acid battery but only 50 percent better specific power. The battery size is selected for the required power, and, consequently, demonstrates more energy capacity than is necessary.

Acceleration.--The acceleration schedule, as previously described, achieves 89 km/hr in 15 s, and also establishes 40 km/hr to 89 km/hr in 10 s, as required for merging. The passing speed of 105 km/hr is reached by accelerating from 89 km/hr to 105 km/hr in 8 s.

TABLE 11.--PROPULSION SYSTEM PERFORMANCE

Propulsion systems with lead-acid batteries	Basic system	Flywheel system
Vehicle test weight	1660 kg	1713 kg
Battery weight	671 kg	667 kg
Propulsion system weight	111 kg	159 kg
Range with J227a (D) cycle	161 km	186 km
Range at constant 72 km/hr	240 km	209 km
Maximum acceleration 0 to 72 km/hr	15 s	15 s
Maximum passing speed	105 km/hr	105 km/hr
Flywheel system with nickel-zinc batteries (reference)		
Vehicle test weight		1327 kg
Battery weight		370 kg
Range with J227a(D) cycle		203.9 km
Range at constant 72 km/hr		229.6 km

The maximum power requirement is in the interval 40 km/hr to 89 km/hr, and the schedule is constructed to maintain this power at a constant level. The required power at the axle for both propulsion systems, which have nearly equal weight using lead-acid batteries, is shown in fig. 90.

The basic system must supply this power from the battery, and the battery drain, reflecting motor and controller losses, is shown in fig. 91. The power level of approximately 64 kW exceeds the capability of the EP200AH battery for a battery pack of 671 kg, but can be met with the EV2-13 battery. The EV2-13 battery meets the ISOA goals for specific power, and thus represents system performance with an ISOA battery. The main difference between the EV2-13 and the ISOA goals is in cycle life, as was shown in fig. 25, and this characterstic primarily affects life-cycle cost.

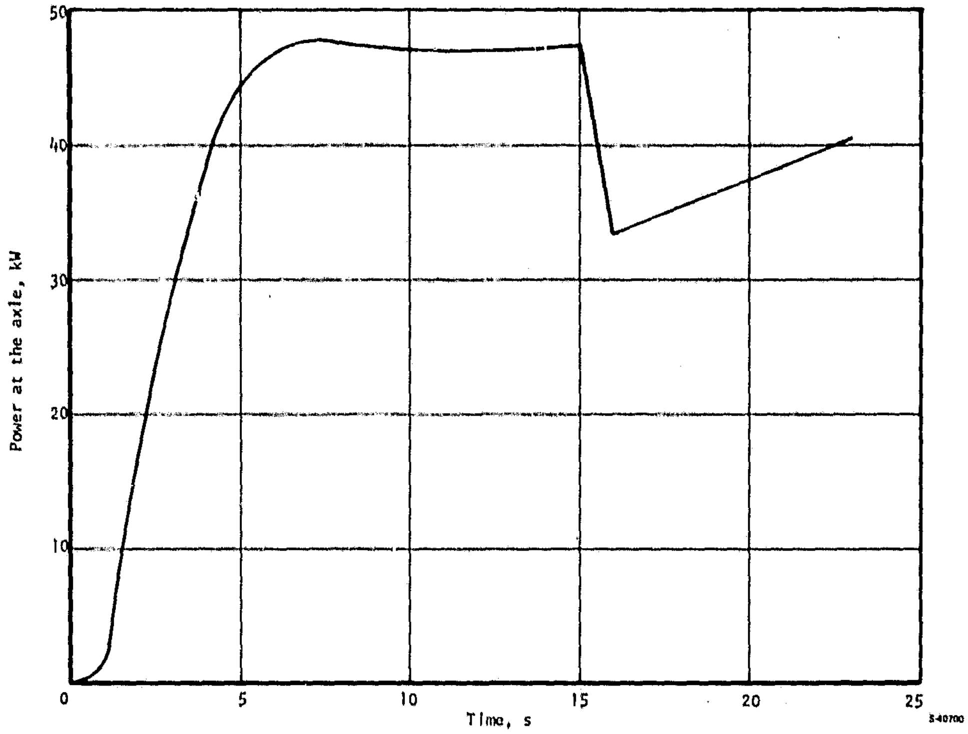

Figure 90.--Power at the axle during acceleration for a 1660-kg vehicle.

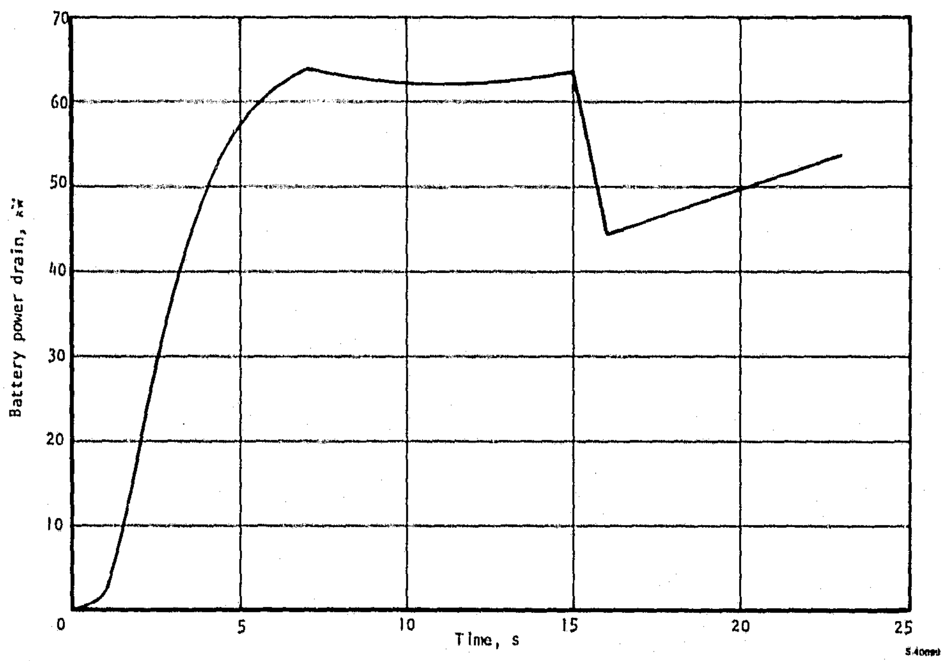

Figure 91.--Battery power for acceleration, basic system.

A vehicle that uses the EV2-13 battery pack and starts with a fully charged battery can achieve four successive accelerations from 0 to 89 km/hr in 15 s, if there is no regeneration between runs. The system would not actually be operated in such a manner, but this procedure permits calculation of the point at which the battery depletion limits the acceleration capability. The most significant fact is that the last acceleration run started at 22 percent depth of discharge. Therefore, it appears that the system would retain full acceleration capability in normal operation until battery depletion falls below 22 percent depth of discharge. Below this point acceleration to top speed is still possible, but the elapsed time would be greater.

The flywheel system derives most of the power for acceleration from the flywheel, and the electrical power requirements are quite small. Motor input power for an acceleration run is shown in fig. 92. Even this power is not actually required, but is dictated, to a considerable extent, by the energy management schedule. Therefore, maximum acceleration capability is retained throughout the vehicle mission. Performance was calculated on the basis of the EP200AH battery, since this battery meets both the energy density goals and the cycle life goals of the ISOA battery (fig. 25). Since the flywheel system does not need the ISOA power limits, the performance is equal to the performance achievable with an ISOA battery.

Effects of acceleration on range.--Some supplementary calculations were made to determine the effects of modifying the J227a(D) driving cycle to use a higher acceleration from 0 to 72 km/hr. Several rates were selected, of which the highest rate is acceleration of 0 to 72 km/hr in 12.3 s. This highest rate is representative of rates used in the Federal Urban Driving Schedule (ref. 26). The results, presented in fig. 93, show that the basic system has a considerable sensitivity to acceleration, with a range decrease of over 50 percent at the highest acceleration. The flywheel system is not affected. The basic system with nickel-zinc batteries is not affected as much as when lead acid batteries are used.

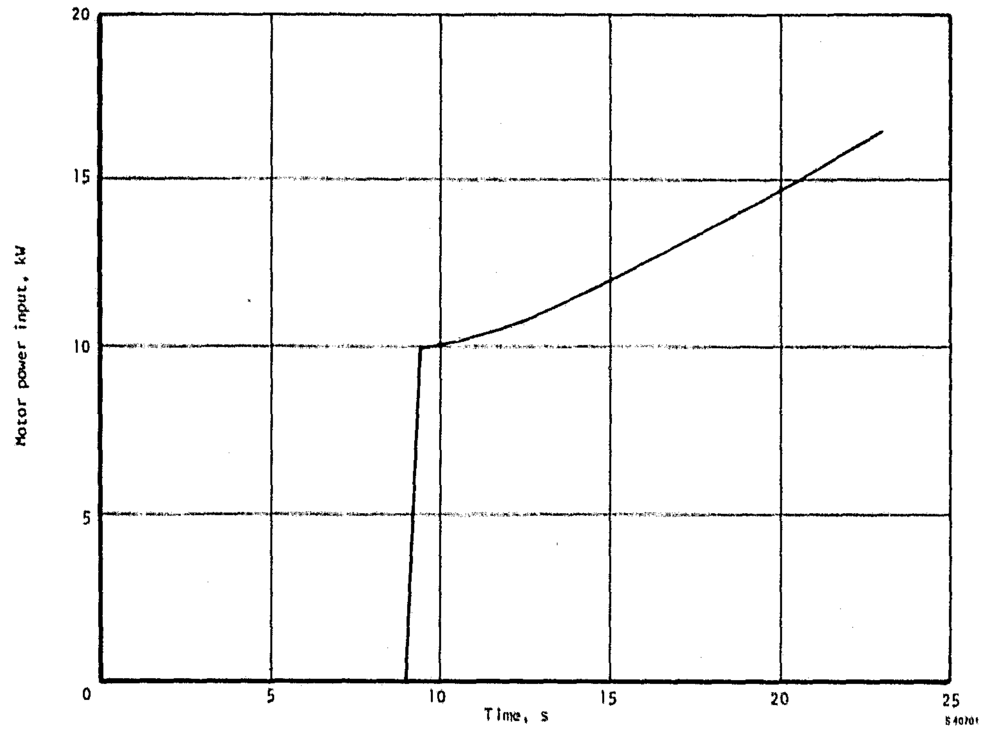

Figure 92.--Supplementary motor power during acceleration for a flywheel system.

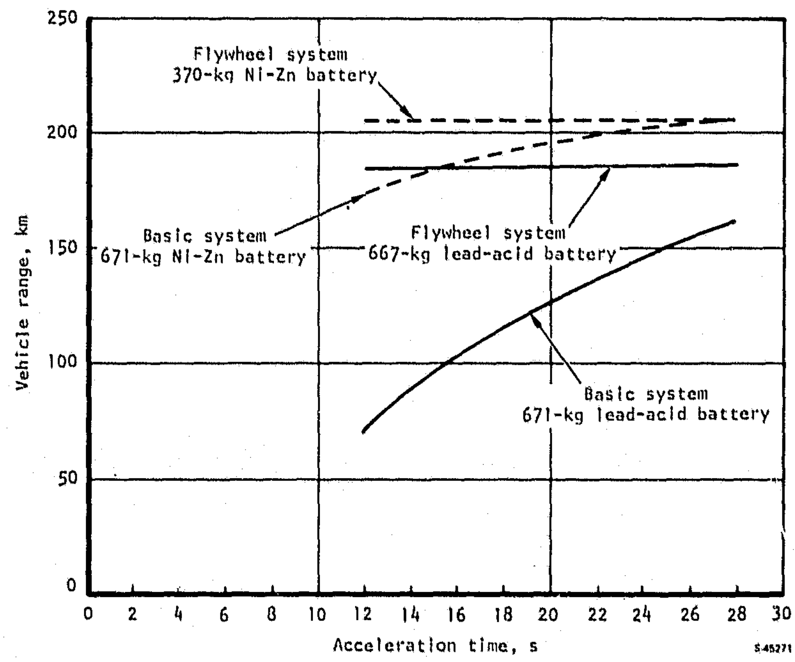

Figure 93.--Range comparisons with driving cycle using varying acceleration rates.

LIFE-CYCLE COST ANALYSIS

The life-cycle cost analysis was done on the two propulsion systems selected for conceptual design studies with the battery pack as described in the preceding section. The analysis included the cost of both the propulsion system and the batteries, and it was found that the battery has a predominant effect: the cost of the battery pack, using the stipulated battery costs, is the major element in the acquisition cost, and battery replacement costs during the vehicle life far outweigh any other operating costs. The most significant cost tradeoffs, therefore, are those affecting battery cost and battery life.

Guidelines For Life-Cycle Cost Calculations

The following guidelines were established by the statement of work for use in the life-cycle cost calculations:

(1) Costs are calculated only for the propulsion system plus the battery; therefore, other vehicle costs, insurance, and taxes are not included.

(2) Costs are expressed in 1976 dollars.

(3) Acquisition cost is the sum of the OEM cost (manufacturing cost plus corporate level costs such as general and administrative, required return on investments of facilities and tooling, cost of sales,...) of components plus the cost of assembling the components plus the dealer markup, given as 17 percent. For the battery, total markup is 30 percent. Sales tax is not added to purchase price.

(4) Annual production is 100 000 units.

(5) Operating cost is the sum of maintenance costs plus repair costs plus electricity cost plus battery replacement costs.

(6) Electricity cost is 4 cents/kW-hr from the wall plug.

(7) Vehicle lifetime is 10 years and 160 900 km.

(8) A constant noninflating dollar is used. No inflation factor is included in the discount rate since it is assumed that personal disposable income tracks inflation. A two percent discount rate for personal cars is used as it represents only time preference (opportunity cost).

(9) Cost of finance is not included in this procedure since it is assumed that the discounted present value of the sequence of total payments would approximately equal the original purchase price.

(10) All expenses are assumed to be costed at the end of each year. Year "Zero" is reserved for those costs that must be incurred before the vehicle is operated.

(11) Propulsion system salvage value is given as 2 percent of the purchase price, depleted battery salvage value is 10 percent of the purchase price, and used battery salvage is 50 percent of the purchase price prorated over the remaining life of the battery.

(12) In determining battery life it is assumed the vehicle is driven 16 090 km per year. For convenience in calculation, the distance is accumulated through successive SAE J227a schedule D driving cycles as follows: 400 trips per year of 16.1 km each, 150 trips of 48.3 km each, and 30 trips of 80.5 km each, charging after each trip. The battery cycle life is based on these trip profiles, field environmental effects, and the degradation due to the actual conditions imposed on the battery by the propulsion system and vehicle.

(13) The calculation of life-cycle cost follows the format on the required worksheets.

Purchase Price

The purchase price of each propulsion system may be found from the manufacturing costs previously presented in table 9, to which are added the appropriate business costs. The design changes in the conceptual design phase were not significant enough to change the cost estimates. The battery is treated as a separately acquired item for which the purchase price is the acquisition cost plus a 30 percent markup. The costs are tabulated in table 12 for the basic system with lead-acid batteries, the flywheel system with lead-acid batteries, and the flywheel system with nickel-zinc batteries. Costs are for the systems as described in table 11.

The business costs are considered representative; in any case, these do not have a large effect on the life-cycle costs. The battery purchase price is also the replacement price of the battery required for periodic replacements, and the price is assumed to include installation.

Maintenance and Repair Costs

Maintenance is defined as scheduled action to maintain equipment in good operating condition. Repair is unscheduled action to correct some malfunction. The propulsion system components will require very little maintenance in comparison with such other vehicle components as tires and brakes. The battery will require periodic water level maintenance, and cleaning of terminals. Repair action is difficult to predict, but it appears from reliability considerations that the most probable repair actions will be for the electronic package.

For maintenance or repair actions, a labor rate of $16/hour is assumed. Repair costs also include the cost of replacement parts.

TABLE 12.--PURCHASE PRICE OF PROPULSION SYSTEMS WITH BATTERY PACK (1976 DOLLARS)

Cost item	System		
	Basic system with lead-acid battery	Flywheel system with lead-acid battery	Flywheel system with nickel-zinc battery
Manufacturing cost of propulsion system	1046	755	755
Manufacturing overhead (22%)	230	166	166
Cost of sales	1276	921	921
General and administrative (25%)	319	230	230
Cost of propulsion system	1595	1151	1151
Return on investment (10%)	160	115	115
Wholesale price	1755	1266	1266
Dealer markup (17%)	298	215	215
Purchase price of propulsion system	2053	1481	1481
Battery cost	1342	1334	2238
Battery markup (30%)	403	400	672
Battery purchase price	1745	1734	2910
Total purchase price	3798	3215	4391

Maintenance items.--For the flywheel system there are two items for equipment for which maintenance is anticipated: the brushes on the dc motor, and the pumps and bearings of the flywheel assembly. The basic system has no scheduled maintenance.

Motor brush replacement for the dc motor is estimated to require one-half hour of labor ($8) and parts costing $10. The total expenses are thus $18, and these are estimated to be required every 2.5 years. Costs will thus appear for the third, fifth, and eighth years.

The flywheel system will require maintenance at the mid-term point during the fifth year. Costs are estimated at $40 for labor and $80 for parts, for a total of $120.

Battery maintenance is estimated to require 2 hours of labor for cleaning and watering, costing $32, for those years during which the battery is not replaced. No parts are required.

Repair Items.--The principal repair anticipated is for the electronic components. It is assumed that at least five times in the life of the vehicle a repair action will be necessary that will require 2 hours of labor ($32) and parts costing $100. The total cost over the life of the car is thus $660. Since this repair is assumed to be due to random failure, the cost is amortized over the life of the system at $66/year.

Battery Use and Replacement

Battery usage was determined through the computer programs previously described. Energy consumption for a single J227a schedule D cycle was found from the vehicle simulation program. Battery depletion for each successive cycle was found from the full mission range dynamic program. Battery depletion is thus established for the various designated trip lengths, as shown in table 13.

The percent of battery life consumed for each trip is based on the battery cycle-life curves previously presented in fig. 25. A battery that is capable of 1000 cycles to a depth of discharge of 70 percent, for example, is assumed to have expended 0.1 percent of its life for each trip that takes it to 70 percent depth of discharge. The battery is replaced when battery life is fully exhausted, based upon the designated driving trip schedule, as given in the guidelines (item 12).

Battery charging is based on the calculated ratio of energy consumption per cycle and the corresponding distance covered. Total energy consumption for a designated trip is the product of energy consumption per kilometer and the required trip length in kilometers. This energy is replaced by the battery charger, which is assumed to operate with an overall efficiency of 75 percent. This efficiency takes account of battery losses and inefficiency during topping-off at a low charge level. Energy cost is 4 cents/kW-hr.

Cost Calculations

The cost calculations are structured by the worksheets in figs. 94 to 99. The life-cycle costs as given on the worksheets are:

(1) Basic system with lead-acid batteries $0.0599/km

(2) Flywheel system with lead-acid batteries $0.0404/km

(3) Flywheel system with nickel-zinc batteries $0.0758/km

TABLE 13.--BATTERY CONSUMPTION AND CHARGING

Battery use	System		
	Basic system with lead-acid battery	Flywheel system with lead-acid battery	Flywheel system with nickel-zinc battery
Energy consumption for J227a (D) cycle, W-hr	210.7	232.2	208.1
Distance traveled in a J227a (D) cycle, km	1.65	1.64	1.64
Rate of energy consumption, W-hr/km	127.7	141.6	126.9
Battery depletion for a 16.1-km trip (depth of discharge), percent	7.29	7.66	7.96
Battery depletion for a 48.3-km trip (depth of discharge), percent	20.7	23.5	23.9
Battery depletion for a 80.5-km trip (depth of discharge), percent	33.8	39.3	39.0
Battery life consumed per year, percent	40.1	19.8	32.1
Cost of battery charging per year, dollars	109.62	121.26	108.69

The flywheel system with lead-acid batteries meets the cost goal of \$0.05/km, and the basic system exceeds the goal by 20 percent. The flywheel system with nickel-zinc batteries exceeds the goal by 52 percent, but might still be considered to be worth the cost because of its much lighter weight.

The basic system would have considerably lower cost if a full-performance ISOA battery were available. Such a battery would provide the specific power, specific energy, and cycle life meeting the ISOA goals, and neither of the specific batteries used in this study met this performance. If ISOA performance could be achieved, life-cycle costs would be \$0.0426/km for the basic system.

YEAR	1	2	3	4	5	6	7	8	9	10
Distance Dependent Costs										
COSTS IN CENTS PER KILOMETER										
Maintenance										
Electric	0	0	0	0	0	0	0	0	0	0
Battery	0.199	0.199	0	0.199	0	0.199	0.199	0	0.199	0.199
Flywheel System	0	0	0	0	0	0	0	0	0	0
A TOTAL	0.199	0.199	0	0.199	0	0.199	0.199	0	0.199	0.199
Repair										
Electric	0	0	0	0	0	0	0	0	0	0
Auxiliaries	0.410	0.410	0.410	0.410	0.410	0.410	0.410	0.410	0.410	0.410
Transmission	0	0	0	0	0	0	0	0	0	0
D TOTAL	0.410	0.410	0.410	0.410	0.410	0.410	0.410	0.410	0.410	0.410
Electricity										
E TOTAL	0.681	0.681	0.681	0.681	0.681	0.681	0.681	0.681	0.681	0.681
F TOTALS A+D+E	1.290	1.290	1.091	1.290	1.091	1.290	1.290	1.091	1.290	1.290
G DISTANCE EACH YEAR	16 090	16 090	16 090	16 090	16 090	16 090	16 090	16 090	16 090	16 090
H TOTAL DOLLARS (F/100) x G	207.62	207.62	175.62	207.62	175.62	207.62	207.62	175.62	207.62	207.62
Battery Replacement	0	0	1570.50	0	1570.50	0	0	1570.50	0	0
YEAR TOTALS	207.62	207.62	1746.12	207.62	1746.12	207.62	207.62	1746.12	207.62	207.62

TOTAL OPERATING COST = 6691.70 OPERATING COST PER KILOMETER = 0.0416

S-40787-A

Figure 94.--Operating cost for basic system with lead-acid batteries.

YEAR	"O"	1	2	3	4	5	6	7	8	9	10
1 PURCHASE PRICE	3798.00										
2 ELECTRICITY		109.62	109.62	109.62	109.62	109.62	109.62	109.62	109.62	109.62	109.62
3 REPAIR + MAINTENANCE		98.00	98.00	66.00	98.00	66.00	98.00	98.00	66.00	98.00	98.00
4 BATTERY REPLACEMENT			0	1745.00	0	1745.00	0	0	1745.00	0	0
5 PROPULSION SYSTEM (MINUS)											-41.06
6 BATTERY SALVAGE (MINUS)			0	-174.50	0	-174.50	0	0	-174.50	0	-174.50
7 TOTAL	3798.00	207.62	207.62	1746.12	207.62	1746.12	207.62	207.62	1746.12	207.62	-7.94
8 DISCOUNT FACTOR	1.0	0.980	0.961	0.942	0.924	0.906	0.888	0.871	0.853	0.837	0.820
9 PRESENT VALUE (7 x 8)	3798.00	203.47	199.52	1644.85	191.84	1581.98	184.37	180.84	1489.44	173.78	-6.51

10 PRESENT VALUE OF LIFE CYCLE COST (SUM OF 9) = 9641.58

11 PRESENT VALUE OF LIFE CYCLE PER KILOMETER DRIVEN (10/TOTAL KM) = 0.0599

S-40796-A

Figure 95.--Life cycle cost for basic system with lead-acid batteries.

COSTS IN CENTS PER KILOMETER

YEAR	1	2	3	4	5	6	7	8	9	10
Distance Dependent Costs										
Maintenance										
Electric	0	0	0.112	0	0.112	0	0	0.112	0	0
Battery	0.199	0.199	0.199	0.199	0.199	0	0.199	0.199	0.199	0.199
Flywheel System	0	0	0	0	0.746	0	0	0	0	0
A TOTAL	0.199	0.199	0.311	0.199	1.057	0	0.199	0.311	0.199	0.199
Repair										
Electric	0	0	0	0	0	0	0	0	0	0
Auxiliaries	0.410	0.410	0.410	0.410	0.410	0.410	0.410	0.410	0.410	0.410
Transmission	0	0	0	0	0	0	0	0	0	0
D TOTAL	0.410	0.410	0.410	0.410	0.410	0.410	0.410	0.410	0.410	0.410
Electricity										
E TOTAL	0.754	0.754	0.754	0.754	0.754	0.754	0.754	0.754	0.754	0.754
F TOTALS A+D+E	1.363	1.363	1.475	1.363	2.221	1.164	1.363	1.475	1.363	1.363
G DISTANCE EACH YEAR	16 090	16 090	16 090	16 090	16 090	16 090	16 090	16 090	16 090	16 090
H TOTAL DOLLARS (F/100) × G	219.26	219.26	237.26	219.26	357.26	187.26	219.26	237.26	219.26	219.26
Battery Replacement	0	0	0	0	0	1560.60	0	0	0	0
YEAR TOTALS	219.26	219.26	237.26	219.26	357.26	1747.86	219.26	237.26	219.26	219.26

TOTAL OPERATING COST = 3895.20

OPERATING COST PER KILOMETER = 0.0242

S-40797-A

Figure 96.--Operating cost for flywheel system with lead-acid batteries.

YEAR	"O"	1	2	3	4	5	6	7	8	9	10
1 PURCHASE PRICE	3215.00										
2 ELECTRICITY		121.26	121.26	121.26	121.26	121.26	121.26	121.26	121.25	121.26	121.26
3 REPAIR + MAINTENANCE		98.00	98.00	116.00	98.00	236.00	66.00	98.00	116.00	98.00	98.00
4 BATTERY REPLACEMENT			0	0	0	0	1734.00	0	0	0	0
5 PROPULSION SYSTEM (MINUS)											-29.62
6 BATTERY SALVAGE (MINUS)			0	0	0	0	-173.40	0	0	0	-173.40
7 TOTAL	3215.00	219.26	219.26	237.26	219.26	357.26	1747.86	219.26	237.26	219.26	16.24
8 DISCOUNT FACTOR	1.0	0.980	0.961	0.942	0.924	0.906	0.888	0.871	0.853	0.837	0.820
9 PRESENT VALUE (7 x 8)	3215.00	214.87	210.71	223.50	202.60	323.68	1552.10	190.98	202.38	183.52	13.32

10 PRESENT VALUE OF LIFE CYCLE COST (SUM OF 9) = 6532.66

11 PRESENT VALUE OF LIFE CYCLE PER KILOMETER DRIVEN (10/TOTAL KM) = 0.0406

S-40786-A

Figure 97.--Life cycle cost for flywheel system with lead-acid batteries.

YEAR	1	2	3	4	5	6	7	8	9	10
Distance Dependent Costs										
COSTS IN CENTS PER KILOMETER										
Maintenance										
Electric	0	0	0.112	0	0.112	0	0	0.112	0	0
Battery	0.199	0.199	0.199	0	0.199	0.199	0	0.199	0.199	0
Flywheel System	0	0	0	0	0.746	0	0	0	0	0
A TOTAL	0.199	0.199	0.311	0	1.057	0.199	0	0.311	0.199	0
Repair										
Electric	0	0	0	0	0	0	0	0	0	0
Auxiliaries	0.410	0.410	0.410	0.410	0.410	0.410	0.410	0.410	0.410	0.410
Transmission	0	0	0	0	0	0	0	0	0	0
D TOTAL	0.410	0.410	0.410	0.410	0.410	0.410	0.410	0.410	0.410	0.410
Electricity										
E TOTAL	0.676	0.676	0.676	0.676	0.676	0.676	0.676	0.676	0.676	0.676
F TOTALS A+D+E	1.285	1.285	1.397	1.086	2.143	1.285	1.086	1.397	1.285	1.086
G DISTANCE EACH YEAR	16 090	16 090	16 090	16 090	16 090	16 090	16 090	16 090	16 090	16 090
H TOTAL DOLLARS (F/100) x G	206.69	206.69	224.69	174.69	344.69	206.69	174.69	224.69	206.69	174.69
Battery Replacement	0	0	0	2619.00	0	0	2619.00	0	0	2619.00
YEAR TOTALS	206.69	206.69	224.69	2793.69	344.69	206.69	2793.69	224.69	206.69	2793.69

TOTAL OPERATING COST = 10 001.90 OPERATING COST PER KILOMETER = 0.0622

S-40797-A

Figure 98.--Operating cost for flywheel system with nickel-zinc batteries.

YEAR	"O"	1	2	3	4	5	6	7	8	9	10
1 PURCHASE PRICE	4391.00										
2 ELECTRICITY		108.69	108.69	108.69	108.69	108.69	108.69	108.69	108.69	108.69	108.69
3 REPAIR + MAINTENANCE		98.00	98.00	116.00	66.00	236.00	98.00	66.00	116.00	98.00	66.00
4 BATTERY REPLACEMENT			0	0	2910.00	0	0	2910.00	0	0	2910.00
5 PROPULSION SYSTEM (MINUS)											-29.62
6 BATTERY SALVAGE (MINUS)			0	0	-291.00	0	0	-291.00	0	0	-1455.00
7 TOTAL	4391.00	206.69	206.69	224.69	2793.69	344.69	206.69	2793.69	224.69	206.69	1600.07
8 DISCOUNT FACTOR	1.0	0.980	0.961	0.942	0.924	0.906	0.888	0.871	0.853	0.837	0.820
9 PRESENT VALUE (7 x 8)	4391.00	202.56	108.63	211.66	2581.37	312.29	183.54	2433.30	191.66	173.00	1312.06

10 PRESENT VALUE OF LIFE CYCLE COST (SUM OF 9) = 12 191.07

11 PRESENT VALUE OF LIFE CYCLE PER KILOMETER DRIVEN (10/TOTAL KM) = 0.0758

S-40796-A

Figure 99.--Life cycle cost for flywheel system with nickel-zinc batteries.

COMPONENT SPECIFICATIONS

The propulsion system conceptual designs have been presented in the form of layout drawings that show internal designs of the principal components; however, many of these design details are subject to variation in any system as it goes through design tradeoffs and development. Therefore, the specifications and performance maps that designate the essential features of the various components are only preliminary.

General Specification

A general specification has been prepared covering the universal requirements that pertain to all components, such as environmental conditions and service life. Some of these general conditions have not yet been established by all concerned agencies and such items are noted in the specification as "to be determined" (TBD).

To avoid excessive duplication, the general specification is written to include both types of propulsion system, the basic system and the flywheel system. Although most conditions are common to both systems, some of the goals are different, as noted.

The general specification is included in this report in the appendix.

Individual Component Specifications

Individual component specifications will be required for the principal system components of the configuration ultimately selected for development. These specifications will present the performance requirements determined for the individual components in the system as determined by the conceptual design. Further tradeoffs of individual components may be required in the development of a hardware system; in this case specification changes would have to be coordinated.

DISCUSSION OF RESULTS

This report has presented a study of various propulsion system configurations considered suitable to power an electric vehicle. The established goals were intended to be representative of acceptable performance for a four-passenger commuter vehicle. The study indicates that these goals can be met with equipment designed for the application, using components that can be fully developed by 1983. Although the component designs require development, they do not require new technology, since they are based on similar devices that have been built and tested. The principal design requirement for the propulsion system is that it be designed specifically for electric vehicle service.

This study also demonstrates that the battery pack characteristics are a major factor in electric vehicle system performance, and the overwhelming factor in life-cycle cost. For this reason results are presented based on two actual battery designs that meet some of the ISOA battery goals. A battery that meets all ISOA performance, life, and cost goals may not be available as scheduled, thus system performance is presented in terms of currently attainable standards; however, all the battery performance models that are available are subject to some uncertainty, and this can only be resolved by additional battery research and testing. The greatest uncertainty is in the effects of high power drains and high regeneration rates on battery capacity and life.

The high power drain characteristics particularly affect the performance of a basic system during maximum acceleration. The maximum acceleration goals in this study are comparable to those of current conventional automobiles, and are generally considered necessary to achieve maneuverability in typical urban traffic. If a driver depends on such acceleration capability, then the system should retain the capability over a representative driving mission. Premature loss of acceleration capability can be a safety hazard, where the driver misjudges the limits of his system. At present, it appears that the maximum acceleration capability of a system without an energy storage device cannot be maintained beyond 20 or 30 percent of battery depletion.

There is some question whether the driving range goals established for the study are sufficiently representative of ultimate consumer needs. The SAE J227a schedule D driving cycle is a convenient vehicle test cycle, but there is considerable evidence (ref. 27) that it is not representative of actual public driving conditions. The Federal Urban Driving Schedule (FUDS) was originally established as an environmental test schedule (ref. 26), and it is based on an actual measured profile of city driving demands, with both stop-and-start segments and freeway driving. The acceleration demands of the Federal Urban Driving Schedule are greater than the SAE J227a schedule D cycle, and consequently, affect the range of a basic propulsion system more than that of a flywheel system.

CONCLUSIONS AND RECOMMENDATIONS

Based on the results of the study, an advanced electric propulsion system for electric vehicles can be developed by 1983. Such a system would have performance comparable to current conventional automobiles and range capabilities adequate for commuter service.

The greatest area of concern is the performance achieveable from a battery pack. It is recommended that battery research and testing be intensified to accumulate knowledge on battery performance, particularly at high power rates, and that battery performance models be improved. The effect of battery pack voltage on propulsion system performance should be investigated, particularly with regard to battery power density, energy density, and cost.

It is recommended that the propulsion system with a flywheel energy storage unit be considered for further development, since it gives promise of best meeting the needs of a propulsion system for an urban commuter vehicle.

APPENDIX

ELECTRIC VEHICLE PROPULSION SYSTEM GENERAL SPECIFICATION

PRECEDING PAGE BLANK NOT FILMED

TABLE OF CONTENTS

PRECEDING PAGE BLANK NOT FILMED

1.0 SCOPE

This specification describes and identifies the requirements of a propulsion system for a near term electric powered vehicle. As defined in this specification, the propulsion system consists of an electric motor and all of the power train components from this motor to, and including, the drive axle. Also included are the electronic control devices necessary to control power flow to the motor.

2.0 APPLICABLE DOCUMENTS

2.1 Government Documents

The following documents of the exact issue shown form a part of this specification to the extent specified herein. In the event of conflict between the documents referenced herein and the contents of this specification, the contents of this specification shall be considered a superceding document.

Specifications

TBD

Standards

TBD

2.2 Non-Government Documents

The following documents of the exact issue shown form a part of this specification to the extent specified herein. In the event of conflict between the documents referenced herein and the contents of this specification, the contents of this specification shall be considered a superceding document.

Specifications

XXX	Traction Motor Specification, Electric Vehicle Propulsion System
XXX	Continuously Variable Transmission Specification, Electric Vehicle Propulsion System
XXX	Output Drive and Differential, Electric Vehicle Propulsion System
XXX	Flywheel Energy Storage Assembly, Electric Vehicle Propulsion System
XXX	Power control Unit, Electric Vehicle Propulsion System
XXX	Battery, Lead-Acid, Improved-State-of-the-Art (ISOA)
XXX	Interface Specification, Propulsion System, Electric Vehicle

Standards

SAE - Electric Vehicle Test Procedures J227a, February 1976

Drawings

(TBD) List of envelope drawings

Other Publications

TBD

3.0 REQUIREMENTS

3.1 Item Definition

The propulsion system is the aggregation of all components that are assembled in a system to obtain energy from a battery and to provide shaft power at the vehicle axle. The propulsion system is designed to power the test vehicle through the design duty cycle and other requirements such as gradeability and braking.

3.1.1 Block Diagram

The block diagram of the propulsion system is shown in Fig. 1 (TBD).

3.1.2 Interface Definition

The propulsion system interfaces include the body structure, chassis, operator controls and displays, and the propulsion battery. Fig. 2 (TBD) is a schematic diagram which indicates the propulsion system interfaces. Interface requirements are defined by the interface specification (TBD).

3.1.3 Vehicle Definition

The propulsion system, as identified in para. 3.1, shall interface with the frame, body structure, appointments, tires, and payload so that the whole asembly can be identified as an electrically powered vehicle that shall meet the requirement characterisitics of para. 3.2 and the physical characteristics of para. 3.3. This vehicle, excluding the propulsion system, is defined by the following parameters:

- Product of aerodynamic coefficient and frontal area, minimum

$$C_D A = 0.56 \text{ m}^2$$

- Tire rolling resistance coefficient (V = km/hr)

$$C_R = 0.008 + (1 \times 10^{-5} V) + (8 \times 10^{-8} V^2)$$

- Tire rolling radius = 29.2 cm

- Maximum design payload ($W_{PL,\ max}$). — 272 kg
- Fixed weight (W_F) — 326 kg
- Gross vehicle weight (W_G) — $W_G = W_S + W_{PL} + W_B + W_F$
- Curb weight (W_C) — $W_C = W_G - W_{PL,\ max.}$
- Test weight (W_T) — $W_T = W_C + 136$ kg
- Structure and chassis weight (W_S) — $W_S = 0.23\ W_G$
- Propulsion system weight (W_{PS}) — (TBD)
- Battery weight (W_B) — (TBD)

3.1.4 Major Component List

The propulsion system is composed of the following major components:

Major Component	Specification Sheet Identification
Traction Motor Continuously Variable Transmission Output Drive and Differential Flywheel Energy Storage Assembly Power Control Unit	TBD

3.2 Characteristics

3.2.1 Performance

When installed in a vehicle that has the necessary new, fully charged batteries, the propulsion system shall provide the following performance characteristics at an ambient temperature of 27°C (80°F).

3.2.1.1 Range

The vehicle shall meet the two following minimum range requirements:

- 161 km employing the driving cycle range identified by SAE J227a, schedule D
- 209 km at a constant velocity of 72 km/hr

3.2.1.2 Acceleration Time

The maximum time for the vehicle to accelerate from zero to 89 km/hr shall be 15 s.

3.2.1.3 Merging Time

Merging time is the time required to accelerate the vehicle from 40 to 89 km/hr for the purpose of accelerating the vehicle from a merging velocity to through traffic highway velocity. This time shall not exceed 10 s.

3.2.1.4 Passing Velocity

Minimum passing velocity shall be 105 km/hr.

3.2.1.5 Sustained Ramp Velocity

Sustained vehicle velocity on a four-percent grade shall be 89 km/hr minimum.

3.2.1.6 Accelerated Ramp Velocity

The vehicle shall attain a velocity of 65 km/hr from a standstill, up a six percent grade within a distance of 328 m.

3.2.1.7 Endurance

Battery life and propulsion system fatigue life are based upon a vehicle use cycle of 16 090 km per year and the following usage rate wherein distance is accumulated through successive SAE J277a schedule D driving cycles.

• 400 trips per year of 16.1 km	=	6 440 km/year
• 150 trips per year of 48.3 km	=	7 240 km/year
• 30 trips per year of 80.5 km	=	2 410 km/year
		16 090 km/year

3.2.2 Physical Characteristics

The propulsion system physical characteristics are defined by the individual components specifications and envelope drawings. Propulsion system weight shall not exceed (TBD).

3.2.3 Reliability/Safety

The propulsion sytem shall be designed such that no single point failure will cause the loss of vehicle control. The propulsion system shall be designed for a life of 10 years with a mean-time-between-failure goal of (TBD).

3.2.4 Maintainability

The propulsion system shall be designed for tuning and adjusting service in the electric vehicle. If major service is required, the system modules will be removable from the electric vehicle for factory service. The propulsion system shall meet the maintainability requirements specified in table 1.

TABLE 1. PROPULSION SYSTEM MAINTAINABILITY

Maximum propulsion system replacement time, minutes	TBD
Maintenance instrumentation	TBD

3.2.5 Environmental

3.2.5.1 Temperature

The propulsion system shall operate for 10 SAE-J227a schedule D driving cycles or equivalent. The first three cycles shall be conducted at an ambient temperature of -29°C (-20°F) min. and the remaining seven cycles at an ambient temperature of 52°C (125°F) min.

3.2.5.2 Shock

(TBD)

3.2.5.3 Vibration

(TBD)

3.2.5.4 Humidity and Moisture

(TBD)

3.2.5.5 Sand and Dust

(TBD)

3.3 Design and Construction

3.3.1 Materials, Processes, and Parts

The propulsion system will be constructed using materials, processes, and parts that are common in commercial/industrial electronics and electrical equipment and that are compatible with the weight and environmental requirements. Unnecessary use of strategic or critical materials will be avoided. Materials or formulations that would result in toxic products during normal use of the electric drive subsystem shall not be used. Materials used in the construction of the propulsion system will conform to ANSI, ASTM, SAE, or similar associations' published standards. Materials used shall be protected from galvanic action or corrosion by the use of protective coatings or finishes.

3.3.2 EMI/EMC

The EMI/EMC radiation from the propulsion system shall meet the following Federal regulations and guidelines.

The EMI/EMC environment in which the propulsion system shall be able to operate is (TBD).

3.3.3 Workmanship

Propulsion system workmanship will be equivalent to that found in the electronics and automotive industry. All burrs and sharp edges will be dressed so as to avoid injury to operator or maintenance personnel. Solder connections will be in accordance with good electronics practice. Wiring will be neatly routed, wrapped, or tied. Exterior housing surfaces will be primed and painted or otherwise finished for protection from the environment and for professional appearance.

3.3.4 Interchangeability

The propulsion system or its modules shall be interchangeable with any other propulsion sytem supplied under this specification. Modules of the propulsion system will be interchangeable in the field, but components such as those within the power control unit will be changed during factory service.

3.3.5 Human Engineering

The propulsion system mounting and electrical terminations shall be designed for ready accessibility and ease of removal of mounting bolts or electrical connectors when the propulsion system is mounted in the electric vehicle. The following documents are applicable:

(TBD)

4.0 QUALITY ASSURANCE

4.1 General

The inspections specified herein define the examinations and test requirements for the propulsion system.

4.1.1 Responsibility for Inspection

Unless otherwise specified, the contractor will be responsible for the performance of all inspection requirements as specified herein.

4.1.2 Government Verification

All quality assurance operations will be subject to Government verification, which may consist of surveillance to determine that practices, methods, and procedures of the written quality assurance system are being properly applied and to measure quality of the product.

4.1.3 Test Program Documentation

Test plans and test procedures shall be prepared and submitted for approval to NASA by the contractor in accordance with the program plam. Test reports shall be prepared in accordance with the program plan.

4.2 Test Requirements

(TBD)

5.0 NOTES

(Contents of this section will not be binding).

6.0 APPENDIXES

(Appendixes will be included as required).

REFERENCES

1. Mighdol, P., W. F. Hahn: Preliminary Power Train Design for a State-of-the Art Electric Vehicle. Booz, Allen & Hamilton, Report No. DOE/NASA/0595-78/1, September 1978.

2. Ross, J. A., G. A. Wooldridge: Preliminary Power Train Design for a State-of-the-Art Electric Vehicle. Rohr Industries, Report No. DOE/NASA/0592-78/1, September 1978.

3. U. S. Department of Energy: Near-Term Electric Vehicle Program. Report No. SAN/1213-02, SAN/1294-02, August 1978.

4. Rowlette, J., C. Leising: Electric Vehicle Battery Test Report. Jet Propulsion Laboratory Report No. 5030-286, December 1978.

5. Frank, H. A., A. M. Phillips: Evaluation of Battery Models for Prediction of Electric Vehicle Range. Jet Propulsion Laboratory, Publication 77-29, August 1, 1977.

6. U. S. Department of Energy: Electric and Hybrid Vehicle Program. 3rd EHV Program Contractors' Meeting, Presentation Aids, June 25, 1979.

7. Shepherd, C. M.: Design of Primary and Secondary Cells, II An Equation Describing Battery Discharge: Journal of the Electromechanical Society. July 1965.

8. Klein, M., D. Dube: Design and Cost Study of Nickel-Zinc Batteries for Electric Vehicle. Energy Research Corp. Report No. ANL-K-76-3541-1, October 1, 1976.

9. Yardney Electric Corp: Design and Cost Study Zinc/Nickel Oxide Battery for Electric Vehicle Propulsion. Report No. ANL-K-76-3543-1, October 1976.

10. Cataldo, R. L.: Response of Lead-Acid Batteries to Chopper-Controlled Discharge: Preliminary Results. NASA Lewis Research Center, NASA TM-73834, February 1978.

11. Dudley, D. W.: Gear Handbook, McGraw-Hill Book Co., 1962.

12. AiResearch Manufacturing Company: Automobile Gas Turbine Optimization Study for the Environmental Protection Agency, Report AT-6100-R7, July 10, 1972.

13. Hewko, L. O.: Roller Traction Drive for Extremely Quiet Power Transmission: Journal of Hydronautics. Vol. 2. No. 3, July 1968.

14. Morris, R.: Variable-Speed Belt Drives, Automatic Transmission of the Future: Machine Design. Vol. 48, No. 19, August 12, 1976.

PRECEDING PAGE BLANK NOT FILMED

15. Huntley, P.: Design Factors of Hydro-Mechanical Transmissions of Passenger Cars. Proceedings of the Fourth International Symposium on Automotive Propulsion Systems, NATO/CCMS N. 61, Vol. II, April 18, 1977.

16. Klein, E. A., G. A. Norris: Hydrostatics Tackle Tough New Jobs: Machine Design. Vol. 49, No. 19, August 25, 1977.

17. Behrin, E. et al: Energy Storage Systems for Automobile Propulsion. Volumes 1 and 2, Lawrence Livermore Laboratories, Report UCRL-52303, December 15, 1978.

18. U. S. Department of Energy: Proceedings of the 1978 Mechanical and Magnetic Energy Storage Contractors' Review Meeting. CONF-781046, October 24, 1978.

19. Towgood, D. A.: An Advanced Vehicular Flywheel S,. em for the ERDA Electric Powered Passenger Vehicle: DOE Flywheel Technology Symposium Abstracts, October 5-7, 1977.

20. Satchwell, D. L.: An Advanced Energy Storage Unit for a U.S. Postal Service Delivery Vehicle: DOE Flywheel Technology Symposium Abstracts, October 5-7, 1977.

21. Rath and Strong, Inc.: Estimated Weights and Manufacturing Costs of Automobiles: Fuel Economy Goals Beyond 1980. Report to U. S. Department of Transportation, Transportation Systems Center.

22. The Aerospace Corporation: Hybrid Heat Engine/Electric Systems Study. Report No. TOR-059 (6769-01) -2, June 1, 1971.

23. AiResearch Manufacturing Company of California: Study of Heat Engine/Flywheel Hybrid Propulsion Configuration with Electrical Transmission System. ALO-41/1, April 1978.

24. Marello, L: Optimizing the Engine-Transmission System by Means of an Electronically Controlled Gearbox. Proceedings of the Fourth International Symposium on Automative Propulsion Systems, NATO/CCMS N. 61, Vol. II, page 610, April 18, 1977.

25. Loewenthal, S. H. et al: Performance of a Nasvytis Multiroller Traction Drive. NASA Technical Paper 1378, AVRADCOM Technical Report 78-36, November 1978.

26. Kruse, R. E., T. A. Huls: Development of the Federal Urban Driving Schedule: Society of Automotive Engineers, Paper 730553, 1973.

27. Simanaitis, D. J.: Emission Test Cycles Around the World: Automotive Engineering. Vol. 85, No. 8, August 1977.

BIBLIOGRAPHY

AiResearch Manufacturing Company of California: Flywheel Energy Storage Unit Technology Development Program, 1st Quarterly Technical Report. Report No. 78-15345, August 15, 1978.

Bode, H.: Lead Acid Batteries. John Wiley and Sons, Inc., New York, N.Y.

Brennand, J., R. Curtis, H. Fox, W. Hamilton: Electric and Hybrid Vehicle Performance and Design Goal Determination Study. General Research Corporation Report No. SAN/1215-1, August 1977.

Carson, R. W.: New and Better Traction Drives are Here: Machine Design. Vol. 46, No. 10, April 18, 1974.

Chang, M. C.: Computer Simulation of an Advanced Hybrid Electric-Powered Vehicle. Society of Automotive Engineers, Paper No. 780217, February 27, 1978.

Christianson, C. C., R. F. Bourke: A Propulsion System for an Electric Delivery Van. The Fifth International Electric Vehicle Symposium, Paper No. 782202(E), October 1978.

George, J. H. B., L. J. Stratton, R. G. Acton: Prospects for Electric Vehicles. Arthur D. Little, Inc., No. C-69260, May 15, 1968.

Guess, R.: Design of a Current Technology Electric Vehicle. Proceedings of the Fourth International Symposium on Automotive Propulsion Systems, NATO/CCMS N. 61, Vol. II, page 948, April 18, 1977.

Hagen, H., R. Zelinka: The M.A.N Elektrobus Experience Gained in Large-Scale Tests. Fourth International Electric Vehicle Symposium, Dusseldorf, Germany, August 31, 1976.

Herbert, G. F., A. E. Anderson: Power Requirements of Electric Vehicles. Society of Automotive Engineers, Paper No. 710238, January 11, 1971.

Hoxie, E. A.: Some Discharge Characteristics of Lead-Acid Batteries: AIEE Transactions. Vol. 73, Part 2, March 1954.

Kleckner, K. R.: Modeling and Testing of Storage Batteries. Society of Automotive Engineers, Paper No. 730251, January 8, 1973.

Klein, E. A., G. A. Norris: Hydrostatics Tackle Tough New Jobs: Machine Design. Vol. 49, No. 19, August 25, 1977.

Krouse, J. K.: Belt Drives that Shift Themselves: Machine Design. Vol. 49, No. 19, August 25, 1977.

Lawson, L. J., A. K. Smith, G. D. Davis: Study of Flywheel Energy Storage, Final Report. Report No. UMTA-CA-06-0106-77-1, September 1, 1977.

Rowland, E. A.: Evaluation of Battery Performance for an Electric Vehicle with Regenerative Braking. The Fifth International Electric Vehicle Symposium, Paper No. 783106(E), October 1978.

Society of Automotive Engineers, Inc.: Electric Vehicle Test Procedure J227a. February 1976.

Soltis, R. F., E. McBrien, J. M. Bozek, F. Gourash: Baseline Tests of the Volkswagen Transporter Electric Delivery Van. NASA Lewis Research Center, NASA TM-73766, January 1978.

Taylor, D. F., E. G. Siwek: The Dynamic Characterization of Lead-Acid Batteries for Vehicle Applications. Society of Automotive Engineers, Paper No. 730252, January 8, 1973.

Vinal, G. W.: Storage Batteries. 4th Edition, Chapter 5, John Wiley and Sons, Inc., New York, N.Y.

Wallin, A. W.: Efficiency of Synchronous Belts and V-Belts. Uniroyal Inc.